

NOVEL TARGETS OF EIF2 KINASES DETERMINE
CELL FATE DURING THE INTEGRATED STRESS RESPONSE

Thomas David Baird

Submitted to the faculty of the University Graduate School

in partial fulfillment of the requirements

for the degree

Doctor of Philosophy

in the Department of Biochemistry and Molecular Biology,

Indiana University

December 2014

Accepted by the Graduate Faculty, Indiana University, in partial
fulfillment of the requirements for the degree of Doctor of Philosophy.

Ronald C. Wek, Ph.D., Chair

Ryan M. Anderson, Ph.D.

Doctoral Committee

Yunlong Liu, Ph.D.

October 24, 2014

Lawrence A. Quilliam, Ph.D.

John J. Turchi, Ph.D.

© 2014

Thomas David Baird

ACKNOWLEDGEMENTS

I would like to thank the faculty and staff of the Department of Biochemistry for their generous support and guidance. Furthermore, I appreciate the time and dedication of my thesis committee: Dr. Lawrence Quilliam, Dr. John Turchi, Dr. Ryan Anderson, and Dr. Yunlong Liu. Past and current members of the Wek lab were paramount to the work presented in this thesis, particularly Dr. Reddy Palam with the initial microarray analysis and Sara Young with her invaluable contribution to the EPRS project and overall support. And foremost I'm indebted to Dr. Ron Wek for being an extraordinary mentor both in the laboratory and the lecture hall. This work was supported by National Institutes of Health Grants GM049164 to R.C.W. and T32DK064466 to T.D.B.

Thomas David Baird

NOVEL TARGETS OF EIF2 KINASES DETERMINE
CELL FATE DURING THE INTEGRATED STRESS RESPONSE

Eukaryotic cells rapidly modulate protein synthesis in response to environmental cues through the reversible phosphorylation of eukaryotic initiation factor 2 (eIF2 α ~P) by a family of eIF2 α kinases. The eIF2 delivers initiator Met-tRNA_i^{Met} to the translational apparatus, and eIF2 α ~P transforms its function from a translation initiation factor into a competitive inhibitor of the guanine nucleotide exchange factor (GEF) eIF2B, which is responsible for the recycling of eIF2-GDP to the translationally-competent eIF2-GTP state. Reduced eIF2-GTP levels lower general protein synthesis, which allows for the conservation of energy and nutrients, and a restructuring of gene expression. Coincident with global translational control, eIF2 α ~P directs the preferential translation of mRNA encoding ATF4, a transcriptional activator of genes important for stress remediation. The term Integrated Stress Response (ISR) describes this pathway in which multiple stresses converge to phosphorylate eIF2 α and enhance synthesis of ATF4 and its downstream effectors. In this study, we used sucrose gradient ultracentrifugation and a genome-wide microarray approach to measure changes in mRNA translation during ER stress. Our analysis suggests that translational efficiencies vary across a broad range during ER stress, with the majority of transcripts being either repressed or resistant to eIF2 α ~P, while a notable cohort of key regulators are subject to preferential translation. From this latter group, we identify *IBTK α* as being subject to both translational and transcriptional induction during eIF2 α ~P in both cell lines and a mouse model of ER stress. Translational regulation of *IBTK α* mRNA involves the stress-induced relief of two inhibitory uORFs in the 5'-leader of the transcript. Also identified as being subject to

preferential translation is mRNA encoding the bifunctional aminoacyl tRNA synthetase EPRS. During eIF2 α ~P, translational regulation of *EPRS* is suggested to occur through the bypass of a non-canonical upstream ORF encoded by a *CUG* start codon, highlighting the diversity by which upstream translation initiation events can regulate expression of a downstream coding sequence. This body of work provides for a better understanding of how translational control during stress is modulated genome-wide and for the processes by which this mode of gene regulation in the ISR contributes to cell fate.

Ronald C. Wek, Ph.D., Chair

TABLE OF CONTENTS

| | |
|---|-----|
| LIST OF TABLES | ix |
| LIST OF FIGURES | ix |
| ABBREVIATIONS | xii |
| CHAPTER 1. INTRODUCTION | |
| 1.1 Eukaryotic Initiation Factor 2 phosphorylation and translational control | 1 |
| 1.2 Cellular stresses regulate translation initiation | 2 |
| 1.3 eIF2 α kinases: sentinels against cellular stress | 7 |
| 1.4 Preferential translation of <i>ATF4</i> during eIF2 α ~P | 13 |
| 1.5 ATF4 directs transcription of ISR genes | 16 |
| 1.6 Multiple mechanisms regulate gene-specific translation during eIF2 α ~P | 20 |
| 1.7 Discordant induction of eIF2 α ~P and ATF4 | 22 |
| 1.8 Cross-regulation between the ISR and other signaling pathways | 24 |
| 1.9 Role of eIF2 α ~P in diabetes | 27 |
| 1.10 Behavior, memory, and neurological degeneration | 29 |
| 1.11 Nutrient availability, hypoxia, and tumorigenesis | 30 |
| 1.12 Global regulation of mRNA transcripts during PERK activation – new members of the ISR | 31 |
| CHAPTER 2. EXPERIMENTAL METHODS | |
| 2.1 Cell culture and generation of stable cell lines | 33 |
| 2.2 Immunoblot analyses | 33 |
| 2.3 Polysome profiling and sucrose gradient ultracentrifugation | 34 |
| 2.4 Microarray analysis | 35 |
| 2.5 Measurement of mRNA by qPCR | 37 |
| 2.6 Plasmid constructions and luciferase assays | 38 |

| | |
|---|----|
| 2.7 Animal study | 39 |
| 2.8 Cell proliferation and viability assays | 40 |
| CHAPTER 3. RESULTS: <i>IBTKα</i> IS SUBJECT TO PREFERENTIAL TRANSLATION DURING STRESS | |
| 3.1 eIF2 α ~P during ER stress induces a gradient of mRNA translational efficiencies | 41 |
| 3.2 eIF2 α ~P leads to translational expression of <i>IBTKα</i> mRNA | 52 |
| 3.3 Induction of <i>IBTKα</i> gene expression requires PERK in both culture cell and animal models of ER stress..... | 58 |
| 3.4 Loss of <i>IBTKα</i> expression results in lowered cell viability | 61 |
| CHAPTER 4. RESULTS: BYPASS OF A NONCANONICAL uORF REGULATES TRANSLATION OF <i>EPRS</i> mRNA | |
| 4.1 eIF2 α ~P leads to translation expression of <i>EPRS</i> mRNA | 65 |
| 4.2 A noncanonical <i>CUG</i> serves to initiate translation of an inhibitory uORF in the <i>EPRS</i> transcript..... | 67 |
| 4.3 Translation control of <i>EPRS</i> during treatment with the drug Halofuginone | 73 |
| CHAPTER 5. DISCUSSION | |
| 5.1 Selective regulation of the translome during ER stress..... | 78 |
| 5.2 Translation control of <i>IBTKα</i> by eIF2 α ~P..... | 78 |
| 5.3 <i>IBTKα</i> facilitates cell survival..... | 80 |
| 5.4 Translational control of <i>EPRS</i> by eIF2 α ~P | 81 |
| 5.5 HF preconditioning activates ISR gene expression..... | 84 |
| 5.6 Concluding remarks | 86 |

APPENDIX

Appendix 1 The bottom, middle, and top 200 gene transcripts representing the repressed, resistant, and preferentially translated groups during eIF2 α ~P 89

REFERENCES 106

CURRICULUM VITAE

LIST OF TABLES

Table 1 The 5'-leader characteristics for gene transcripts suggested to be preferentially translated, resistant, or repressed during ER stress..... 46

LIST OF FIGURES

Figure 1 Regulation of translation initiation is a rapid means for coupling stress conditions with levels of protein synthesis..... 6

Figure 2 A family of eukaryotic initiation factor 2 α kinases are activated in response to diverse stress conditions 12

Figure 3 Mechanisms of preferential translation during phosphorylation of the α subunit of eukaryotic initiation factor 2 (eIF2 α ~P)..... 15

Figure 4 Transcriptional regulation of *ATF4* enables differential expression of integrated stress response (ISR) genes 19

Figure 5 eIF2 α ~P represses global translation initiation during ER stress 47

| | |
|---|----|
| Figure 6 Genome-wide analyses of gene-specific translation during ER stress | 49 |
| Figure 7 Changes in polysome association of gene transcripts suggest preferential, resistant, or repressed translation during ER stress | 51 |
| Figure 8 The 5'-leader of the <i>IBTKα</i> gene transcript confers preferential translation in response to eIF2 α ~P | 55 |
| Figure 9 Translation of <i>IBTKα</i> mRNA is regulated by a scanning model involving two inhibitory upstream ORFs | 57 |
| Figure 10 Enhanced <i>IBTKα</i> gene expression requires PERK in both cultured cell and animal models of ER stress | 60 |
| Figure 11 Knockdown of <i>IBTKα</i> reduces cell viability and increases caspase 3/7 cleavage..... | 63 |
| Figure 12 Model depicting <i>IBTKα</i> transcriptional and translation regulation during PERK induced eIF2 α ~P | 64 |
| Figure 13 <i>EPRS</i> mRNA associates with large polysomes during ER stress..... | 67 |
| Figure 14 The 5'-leader of <i>EPRS</i> mRNA confers preferential translation during eIF2 α ~P | 70 |

| | |
|--|----|
| Figure 15 An upstream <i>CUG</i> in the <i>EPRS</i> 5'-leader serves as a non-canonical initiation codon for mRNA translation..... | 72 |
| Figure 16 HF treatment reduces large polysomes and induces the 5'-mediated preferential translation of <i>EPRS</i> mRNA..... | 75 |
| Figure 17 GCN2 confers protection against HF-induced toxicity through general and gene-specific translation control..... | 76 |
| Figure 18 Proposed model of <i>EPRS</i> mRNA translation regulation | 84 |

ABBREVIATIONS

| | |
|------------------|---|
| ASNS | Asparagine Synthetase |
| ATF | Activating Transcription Factor |
| bZIP | Basic Leucine Zipper |
| CDS | Coding Sequence |
| CHOP | C/EBP Homologous Protein |
| eIF | Eukaryotic Initiation Factor |
| eIF2 α ~P | Phosphorylation of The α Subunit of Eukaryotic Initiation Factor 2 |
| eIF2-TC | Eukaryotic Initiation Factor 2 Ternary Complex |
| EPRS | Glutamyl-Prolyl-tRNA Synthetase |
| ER | Endoplasmic Reticulum |
| GCN | General Control Nonderepressible |
| GEF | Guanine Nucleotide Exchange Factor |
| HF | Halofuginone |
| IBTK α | α Isoform of Inhibitor of Bruton's Tyrosine Kinase |
| IRES | Internal Ribosome Entry Site |
| ISR | Integrated Stress Response |
| MEF | Mouse Embryonic Fibroblast |
| mTOR | Mammalian Target of Rapamycin |
| ORF | Open Reading Frame |
| 43S PIC | 43S Preinitiation Complex |
| PERK | PKR-like Endoplasmic Reticulum Kinase |
| TG | Thapsigargin |
| tRNA | Transfer RNA |

| | |
|------|--|
| TSC | Tuberous Sclerosis Complex |
| uORF | Upstream Open Reading Frame |
| UPR | Unfolded Protein Reponse |
| WRS | Wolcott-Rallison Syndrome |
| MEF | Mouse Embryonic Fibroblast |
| PCR | Polymerase Chain Reaction |
| PKR | double-stranded RNA-activated Protein Kinase |
| PEK | Pancreatic eIF2 kinase |
| PERK | PKR-Like Endoplasmic Reticulum Kinase |
| qPCR | Quantitative PCR |
| TC | Ternary Complex |
| UPR | Unfolded Protein Response |
| UTR | Untranslated Region |
| uORF | upstream Open Reading Frame |
| WT | wild-type |
| WRS | Wolcott-Rallison Syndrome |

CHAPTER 1. INTRODUCTION

1.1 Eukaryotic Initiation Factor 2 Phosphorylation and Translational Control

The process of mRNA translation is dynamic and a primary level of control of protein abundance in mammalian cells (1). As such, regulation at the level of translation is a rapid and effective means for the cell to respond to many different stresses, including those affecting nutrition, such as deficiencies for amino acids or glucose, and high fat diets. A central mechanism for translational control involves phosphorylation of the α subunit of eukaryotic Initiation Factor 2 (eIF2), which represses the initiation phase of protein synthesis, allowing cells to conserve resources while a new gene expression program is adopted to prevent stress damage. Accompanying this global translational control, phosphorylation of eIF2 α (eIF2 α ~P) selectively enhances the translation of *ATF4*, a transcriptional activator of genes involved in metabolism and nutrient uptake, the redox status of cells, and the regulation of apoptosis (2-5). The idea that ATF4 is a common downstream target that integrates signaling from multiple eIF2 α kinases has led to the eIF2 α ~P/ATF4 pathway being referred to as the Integrated Stress Response (ISR) (5). The ISR shares many features with induced eIF2 α ~P and *GCN4* translational control in the General Amino Acid Control pathway in yeast, highlighting its evolutionary conserved role in ameliorating nutritional deficiencies (6,7).

The introduction of this thesis will begin with a brief overview of translation initiation and the processes controlled by nutrition, with an emphasis on the events triggered by eIF2 α ~P. Additionally, I will describe the family of eIF2 α kinases. Each serves as a sensor for different stress arrangements, standing guard for disturbances in cellular homeostasis. Enhanced eIF2 α ~P initiates a gradient of translational control of preexisting mRNAs, in which most mRNAs are translationally repressed, while a cadre of stress-related mRNAs are preferentially translated. In this introductory section, we will

then focus on three key topics concerning translational control elicited by eIF2 α ~P. First, we will highlight the mechanisms by which eIF2 α ~P confers preferential translation on select mRNAs and its consequence on the gene expression programs induced by the ISR. One mechanism described for *ATF4* involves delayed translation reinitiation, which allows for scanning ribosomes to selectively enhance *ATF4* expression in response to eIF2 α ~P. In addition to *ATF4*, many other mRNAs are suggested to be subject to preferential translation during eIF2 α ~P, some via alternative mechanisms (8-11). Our second topic concerns the molecular processes by which stress signals can differentially activate eIF2 α ~P and *ATF4* expression. *ATF4* expression is controlled by both transcriptional and translational mechanisms, and certain stresses can repress *ATF4* transcription, reducing the levels of *ATF4* mRNA available for translation despite robust eIF2 α ~P (12). In this situation, eIF2 α ~P and translational control is invoked without activating *ATF4* and its downstream targets. The third topic addresses the cross-regulation of the ISR with other stress response pathways, such as the Unfolded Protein Response (UPR) and mTOR, and the role that these regulatory networks can play in health and disease, with a focus on diabetes and related metabolic disorders. This thesis will highlight recent advances in these areas of research, emphasizing an understanding of how eIF2 α ~P and key metabolic processes are intricately linked.

1.2 Cellular Stresses Regulate Translation Initiation

The regulation of eukaryotic protein synthesis occurs predominately during translation initiation, and multiple associated proteins, termed eukaryotic Initiation Factors (eIFs), are required to assemble a translationally-competent 80S ribosome. While many eIFs are indispensable for initiation, the nutritional status primarily regulates translation initiation at two steps involving the eIF4F cap-binding complex and eIF2 carrying an initiator methionyl tRNA (eIF2-GTP-Met-tRNA^{Met}_i). Translational control

facilitated by eIF2 α -P will be a primary focus of this thesis (Figure 1). For in depth reviews of the mechanisms underlying protein synthesis and additional regulatory schemes see the following references (7,13,14).

All eukaryotic mRNAs have 5'-leader structures proximal to the primary coding sequence that are required for recruiting the translation initiation machinery. It is important to note that the distal 3'-noncoding portion of the mRNA can also contribute to enhanced translation efficiency, and in some cases repress protein synthesis, via the closed loop model of ribosome recycling (13). The mechanisms involving the 3'-noncoding portion of the mRNA will not be discussed in detail here, but are highlighted in depth in recent reviews (15-17). Individual 5'-leaders vary in length, and can regulate expression of the downstream coding sequence via complex secondary structures and upstream Open Reading Frames (uORFs) located 5' to the primary coding sequence of mRNAs. In a sense, these 5'-leaders serve as bar codes by which ribosomes will identify which transcripts are to be repressed or preferentially translated upon enhanced eIF2 α -P.

Once in the cytoplasm, the 7-methyl guanosine (7mG) 5'-cap structure of the mRNA to be translated is bound by eIF4F, consisting of the eIF4E subunit that binds to the cap, the helicase eIF4A, and scaffolding protein eIF4G, which facilitates the closed-loop between the 5' and 3'-ends of the mRNA (Figure 1). With the eIF4F complex effectively bound to the 5'-cap, the next step of translation involves the recruitment of a 43S preinitiation complex (PIC) comprised of the 40S ribosomal subunit bound to eIF3, eIF1, eIF1A, eIF5 and the eIF2-GTP-Met-tRNA^{Met}_i ternary complex (eIF2-TC). The 43S PIC scans the 5'-leader in a processive 5' to 3' manner until it encounters an initiation codon, at which point P_i is released from the hydrolyzed GTP associated with eIF2, and the anticodon loop of the initiator methionyl tRNA base-pairs with the initiation codon in

the P site of the 40S subunit (13,18). Following the recognition of the start codon and the joining of the 40S and 60S ribosomal subunits, the 80S ribosome is primed for translation elongation and subsequent polypeptide synthesis.

The recycling of eIF2-GDP to its translationally-active eIF2-GTP form by the guanine nucleotide exchange factor (GEF) eIF2B is a key regulatory switch in the modulation of protein synthesis (Figure 1). eIF2B is a complex GEF consisting of five different subunits, two participating in catalytic function and the other three facilitating regulation (6,19-22). During nutrient deprivation and other stress conditions, eIF2 α is phosphorylated at serine 51, which then directly engages with the regulatory subcomplex of eIF2B, transforming eIF2 from a member of the 43S PIC into a competitive inhibitor of the GEF. As a consequence, there is reduced eIF2-GTP levels and lowered global protein synthesis.

During conditions of low nutrient availability, eIF4E can also be sequestered by the eIF4E-binding proteins (4E-BP), thus limiting assembly of the eIF4F complex (Figure 1) (23-25). Once nutrient availability returns to optimal levels, mTORC1, consisting of mTOR complexed with Raptor and Lst8 (G β L), signals for increased protein synthesis by phosphorylating 4E-BP1 and 4E-BP2, preventing their binding to eIF4E and effectively promoting cap-dependent translation. A recent ribosome profiling study in cells treated with the mTORC1 inhibitor Torin 1 described a model in which mTORC1 specifically regulates transcripts with 5' terminal oligopyrimidine (TOP) motifs (26). While the study found no evidence for 5'-UTR length or overall RNA complexity affecting mTORC1-dependent translation control, the specific mechanism by which TOP mRNA regulation occurs remains unknown. Additionally, mTORC1 can phosphorylate and activate the S6 kinases, which in turn phosphorylate eIF4B, thus enhancing the affinity of eIF4B for the helicase eIF4A (23,24,27,28). As a consequence, eIF4A has enhanced binding to ATP and increased processivity of the helicase, which promotes ribosome scanning of

mRNAs. Therefore, mTORC1 enhances cap-dependent translation by multiple mechanisms involving eIF4F.

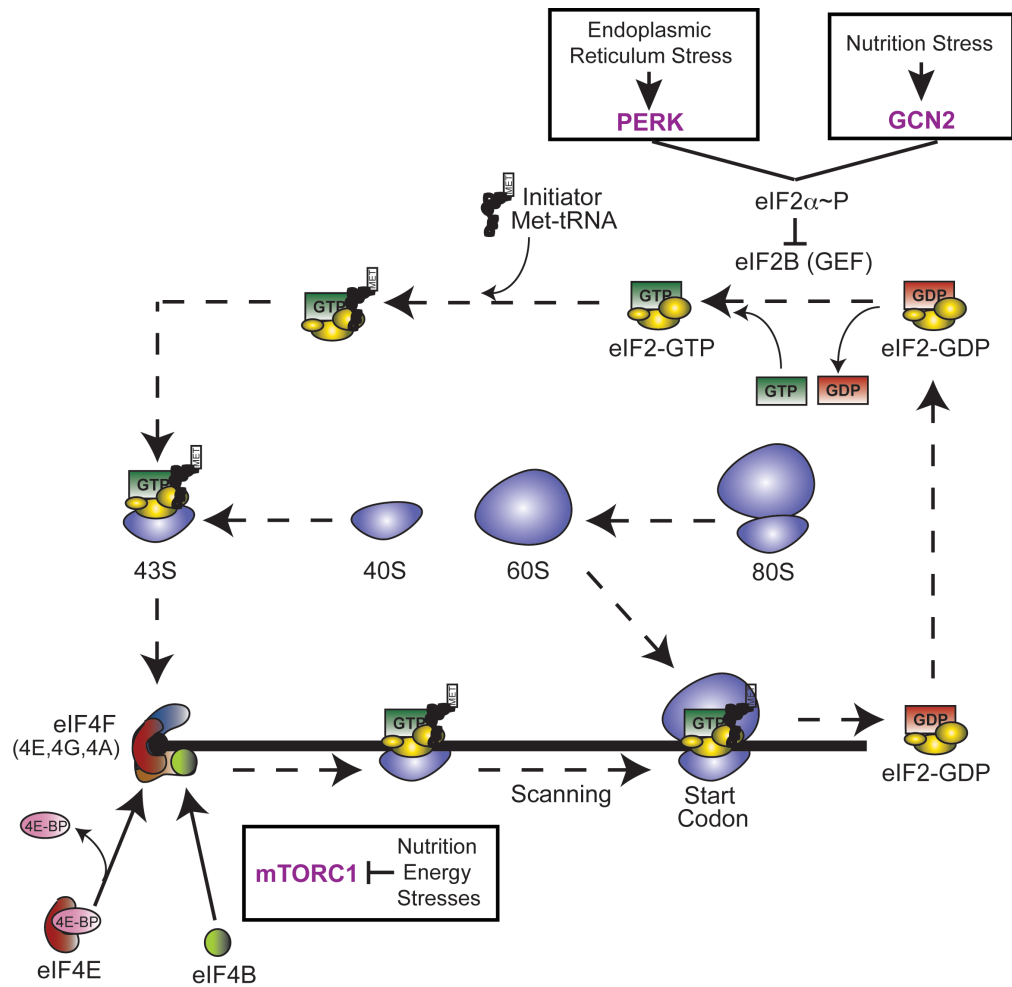


Figure 1. Regulation of translation initiation is a rapid means for coupling nutrient deprivation and other stress conditions with levels of protein synthesis. This illustration shows the dissociation of the 80S ribosome complex into the individual 40S and 60S ribosomal subunits, which participate in translation initiation in conjunction with additional translation factors to initiate protein synthesis. Cap-dependent initiation of translation can be divided into two key events: the binding of the eIF4F complex to the 7mG 5'-cap, and the subsequent recruitment and scanning of the 43S complex, comprised of eIF2-GTP-Met-tRNA^{Met}_i and other eIFs attached to the 40S ribosomal subunit. Following recognition of the start codon by the scanning 43S PIC, a 60S subunit joins to form an actively translating 80S ribosome. During conditions of low stress and high nutrient availability, an abundance of active eIF4F and eIF2-TC complexes

promotes high levels of cap-dependent translation. Nutritional stresses, such as amino acid or glucose deprivation, signal for a rapid reduction in global translation through phosphorylation of eIF2 α (eIF2 α ~P) and repression of mTORC1. Enhanced eIF2 α ~P leads to inhibition of eIF2B and lowered exchange of eIF2-GDP to eIF2-GTP. mTORC1 can enhance cap-dependent translation by two mechanisms. First, mTORC1 enhances phosphorylation of 4E-BP1 and 4E-BP2, leading to release of this inhibitory protein from eIF4E, the cap-binding subunit of eIF4F. Second, mTORC1 triggers S6 kinase phosphorylation of eIF4B, which then associates with the eIF4A subunit of eIF4F, enhancing eIF4A helicase function that expedites ribosome scanning during translation. In addition to nutritional stresses, perturbations in ER function activates PERK-induced eIF2 α ~P, effectively reducing the influx of nascent peptides to the overloaded protein folding machinery.

1.3 eIF2 α Kinases: Sentinels Against Cellular Stress

Mammals express four different eIF2 α kinases, each serving as a cellular sentry that monitors for different exogenous and endogenous stresses. Family members and their respective stress signals include GCN2 (EIF2AK4), an eIF2 α kinase induced in response to nutritional stresses (6,29), PERK (EIF2AK3/PEK), which responds to perturbations in the endoplasmic reticulum (ER stress) (30,31), HRI (EIF2AK1) that is activated by heme deprivation in erythroid cells (32,33), and PKR (EIF2AK2), which participates in an antiviral defense pathway involving interferon (Figure 2) (34-37). Dysfunctions in each of these eIF2 α kinases are linked with pathologies in multiple organs, emphasizing their critical roles in the recognition and alleviation of environmental stress.

GCN2 is the primary responder to nutritional deprivation and is the only eIF2 α kinase conserved among virtually all eukaryotes. The mechanism of activation during

amino acid depletion involves the binding of accumulating uncharged tRNAs in the cytoplasm to a region of GCN2 homologous with histidyl-tRNA synthetases (6,38-40) (HisRS) (Figure 2). GCN2 binding to uncharged tRNA ultimately triggers a conformational change that relieves inhibitory interactions within the protein kinase domain, resulting in autophosphorylation in the activation loop of the enzyme (6,41-43). Activation of GCN2 involves not only histidine starvation, but limitations for other essential amino acids, as well as some non-essential (6,29,38,44-46). Furthermore this eIF2 α kinase was reported to be activated by genetic disruptions of aminoacyl-tRNA synthetases or amino acid transporters, and drugs that diminish the uptake or synthesis of amino acids, or charging of tRNAs (45,47-52). These findings suggest that the aminoacylation levels of many different tRNAs, including tRNA^{His}, can be used by GCN2 to measure the availability of amino acids. Loss of *GCN2* in mice subject to leucine starvation diminishes eIF2 α -P in the liver, which can occur in wild-type mice within 1 hour of a leucine-deprived diet (46). However, protein synthesis was reduced to the same extent in both the wild-type and *GCN2*^{-/-} mice during short term administration of the leucine-deficient diet. Conversely, after 6 days of leucine deprivation there were significant differences in the levels of translation between the wild-type and *GCN2*^{-/-} mice. In wild-type mice, eIF2 α -P continued to be high, accompanied by significant lowering of protein synthesis in the liver and shrinkage of this organ. By contrast, in *GCN2*-deficient mice, there were high levels of liver protein synthesis despite deficiencies for the essential amino acids (46). As a consequence, there was extensive muscle breakdown in *GCN2*^{-/-} mice in a futile attempt to replenish amino acids and quench the liver translation system. Furthermore, whereas lipid synthesis is repressed in livers of wild-type mice during longer periods of leucine starvation, the production of lipids occurs unabated in *GCN2*-deficient mice, ultimately contributing to liver steatosis

(53). An underlying rationale for the dysregulated lipid metabolism in the livers of *GCN2*^{-/-} mice was suggested to be persistent activation of SREBP-1c and its target genes involved in the production and transport of fatty acids. A recent study using whole-exome sequencing in human patients with pulmonary veno-occlusive disease (PVOD) identified recessive mutations in *GCN2* in PVOD families, further highlighting the importance of *GCN2* gene function in proper tissue development and maintenance (54).

GCN2 can also be activated by glucose deprivation and exposure to high salt, and stresses not directly related to nutrients, such as UV irradiation and anti-cancer drugs that inhibit proteasomes or histone deacetylases (12,55-62). Currently it is unclear whether uncharged tRNAs are the activating ligand for *GCN2* during these diverse stresses. In the yeast model system, mutations that disrupt *GCN2* binding to uncharged tRNAs block induced eIF2 α -P in response to stresses involving amino acid starvation, as well as those not directly linked to nutrients (38,39,63,64). This finding suggests that changes in tRNA charging may be a common activating signal for *GCN2* in response to many different stresses. To directly test this idea, tRNA charging was measured genome-wide in yeast using a microarray-based approach (65). In response to starvation for histidine, leucine, or tryptophan, there was a decrease in the charging of the cognate tRNAs. Interestingly, tRNA deacylation was not only limited to those tRNAs for which the cognate amino acid was depleted, as many tRNAs charged with replete amino acids were also rapidly deacylated (65). Additionally, high salinity stress also triggered transient changes in the charging of several different tRNAs. These studies suggest that *GCN2* can be activated by many different tRNA species, and that changes in the charging of tRNAs can serve as a broad sensor of metabolic homeostasis in cells.

In addition to uncharged tRNAs, regulatory proteins can alter the activity of *GCN2*. For example, *GCN1* is a ribosome-associated protein that directly binds to the amino-terminal RWD segment of *GCN2* (66-70). *GCN1* is suggested to facilitate

passage and binding of uncharged tRNAs to the HisRS-related domain of GCN2, thus enhancing eIF2 α ~P during nutrient stress (6,71). Interestingly, IMPACT (yeast YIH1) is a protein that also contains a RWD that can compete with GCN2 for binding to the activator GCN1, thus blocking activation of the eIF2 α kinase (72-74). IMPACT is variably expressed among cell types, with highest abundance in the central nervous system, suggesting that IMPACT can differentially repress GCN2 in selected tissues during dietary limitations for essential amino acids. Finally, stress signaling pathways are suggested to regulate GCN2 and eIF2 α ~P. For example, the DNA damage checkpoint protein kinase, DNA-PKc, was reported to directly or indirectly phosphorylate GCN2 in response to UV irradiation, facilitating translational control and cell survival (11).

The other eIF2 α kinase that has a major role in nutrient stress and metabolism is PERK. PERK is an ER transmembrane protein that contains a regulatory region that resides in the lumen of the ER and a cytosolic eIF2 α kinase domain (30,31,75-78). Calcium dysregulation, oxidative damage, and increased secretory loads or perturbations in post-translational modification of proteins can lead to accumulation of misfolded protein that can cause ER stress (30). Regarding nutritional stresses, fluctuations in glucose levels and high fat diets are linked with ER stress. In addition to PERK and the ISR, ER stress activates two additional transmembrane proteins IRE1 (ERN1) and ATF6, which collectively induce the UPR. The UPR features translational control by PERK phosphorylation of eIF2 α , which reduces the influx of nascent proteins into the ER, along with activating a program of gene expression designed to expand the processing capacity of the ER and enhance ER-associated protein degradation (ERAD), a mechanism for the clearance and degradation of misfolded proteins from the secretory pathway. The UPR is linked to the progression and treatment of many diseases, including diabetes and related metabolic disorders, renal disorders, neuropathologies,

and cancers (31,79-83). The importance of PERK in diabetes is highlighted by the discovery that mutations disrupting this eIF2 α kinase result in Wolcott-Rallison Syndrome (WRS), which is characterized by neonatal diabetes, atrophy of the exocrine pancreas, skeletal dysplasia, growth retardation, and hepatic complications resulting in morbidity (84-87).

Activation of PERK during ER stress is thought to occur in parallel with the other UPR sensors, but the timing or duration of each may differ. Although the mechanistic details are not yet resolved, it has been proposed that the ER luminal portion of PERK can be bound and repressed by the ER chaperone BiP/GRP78 (77,78). Misfolded proteins that accumulate in the ER lumen during stress are suggested to compete with PERK for BiP binding, triggering the release of the ER chaperone, thus leading to PERK oligomerization which facilitates PERK autophosphorylation and enhanced eIF2 α -P. It has been suggested that because of the abundance of BiP in the ER, this regulatory scheme would be too coarse to trigger a rapid titration of BiP from UPR sensors such as PERK (88,89). This concern assumes that PERK and BiP are distributed equally across the ER, as opposed to being localized in some form of regulatory hub. An alternative mechanism proposed for the activation of the ER sensor IRE1 suggests that unfolded proteins can directly interact with the luminal regulatory region of IRE1, triggering its oligomerization and activation (89-92). This direct unfolded protein binding model is supported by genetic, biochemical and structural studies, and addresses the rapidity in which the UPR is activated upon disruptions of the ER (89,90). Because PERK and IRE1 share sequence homology in their luminal regulatory domains, features of the latter model are also germane to the regulation of PERK. Note that these models are not necessarily mutually exclusive, but rather may represent activation mechanisms invoked at different stages of the UPR.

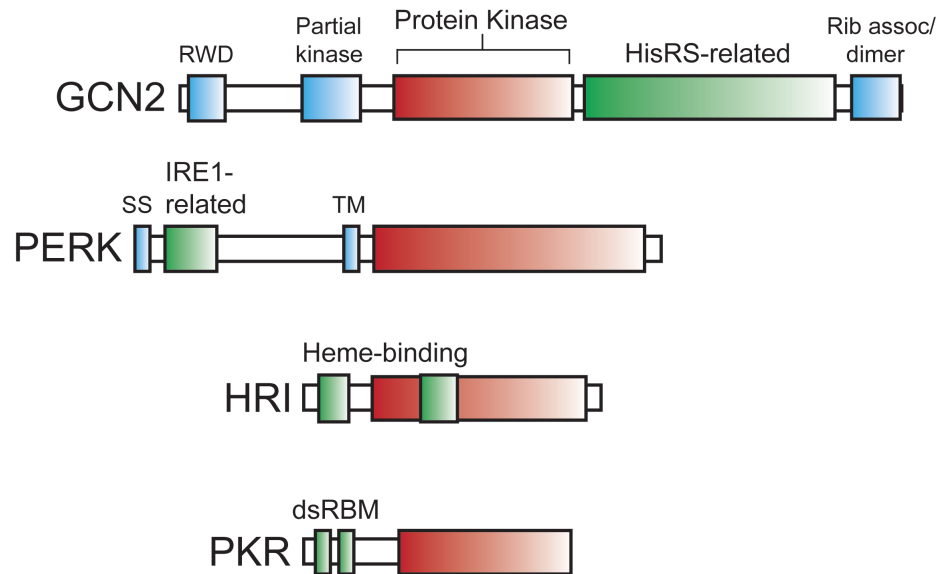


Figure 2. A family of eIF2 α kinases are activated in response to diverse stress

conditions. The eIF2 α kinases possess a related protein kinase domain (red box) that

is flanked by distinct regulatory sequences, which facilitate induction of eIF2 α -P in

response to different stress conditions. Due to differences in the length of the

characteristic insert sequences shared among eIF2 α kinases, the size of the protein

kinase domain differs among family members. The eIF2 α kinase GCN2 contains a RWD

sequence that associates with the activator protein GCN1, a partial kinase domain

required for GCN2 activation, HisRS-related sequences that directly bind uncharged

tRNAs which accumulate during nutritional stress, and a carboxy terminal region that

facilitates GCN2 dimerization and its ribosome association. Note many of the functional

features of these domains are based on studies for yeast GCN2, which shares the same domain arrangement. PERK contains an ER transmembrane domain which divides this

eIF2 α kinase into two. The carboxy terminal protein kinase domain catalyzes eIF2 α -P.

The amino terminal portion features a signal sequence (SS), facilitating translocation of

this portion of PERK into the lumen of the ER, and sequences related to the UPR sensor

IRE1, which are suggested to monitor accumulation of unfolded protein in this organelle.

HRI contains two regions that bind to heme, one at the amino-terminal portion of HRI and the second in the insert region of the protein kinase domain, which can repress this eIF2 α kinase. Low levels of iron lead to reduced amounts of heme in erythroid cells, which triggers a release from this repressing mechanism and enhanced eIF2 α -P. As a consequence, the availability of heme is tightly coupled to globin synthesis, the predominant translation product in erythroid tissues. PKR participates in an anti-viral defense mechanism triggered by interferon. Two double-stranded RNA binding motifs (dsRBM) associate with double-stranded RNA that can accumulate in cells infected by viruses, leading to PKR autophosphorylation and enhanced eIF2 α -P. Lowered protein synthesis would reduce viral replication and proliferation.

1.4 Preferential Translation of ATF4 During eIF2 α -P

ATF4 is a basic leucine zipper (bZIP) transcription factor that is preferentially translated in response to eIF2 α -P. The 5'-leader of *ATF4* mRNA contains two uORFs that orchestrate a mechanism by which *ATF4* expression is paradoxically enhanced during eIF2 α -P (Figure 3) (2-4,13). Increased ATF4 synthesis can subsequently activate the transcription of target genes in the ISR that can collectively alleviate the nutritional stress. Preferential translation of *ATF4* begins with the joining of the 43S PIC to the 5'-cap complex of the *ATF4* mRNA. The 43S PIC then scans along the transcript in a 5' to 3' manner, and translation initiation occurs at the start codon of the 5'-proximal uORF1 of *ATF4*. Following termination of translation at uORF1, the small ribosomal subunit is not disengaged from the *ATF4* mRNA, but rather resumes scanning processively along the leader of the *ATF4* transcript. To initiate translation once again, the 40S ribosomal subunit must reacquire the eIF2-TC. Under non-stressed conditions and high levels of eIF2-GTP, reinitiation occurs rapidly at the next available initiation codon, which corresponds to that of the inhibitory uORF2 (Figure 3). The uORF2 overlaps out-of-

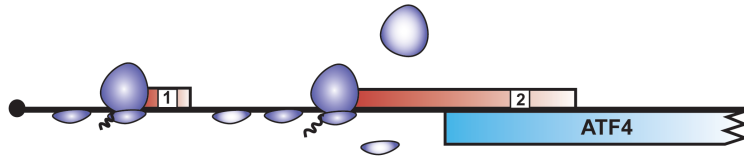
frame with the primary *ATF4* coding region, and following translation of uORF2, ribosomes dissociate from the *ATF4* mRNA, and therefore ATF4 synthesis is diminished.

Upon amino acid depletion and enhanced eIF2 α -P, there is reduced eIF2-GTP recycling, and therefore the levels of the eIF2-TC are lowered. Consequently, following termination of translation at the positive-acting uORF1, the scanning 40S ribosomal subunit is unable to attain a new eIF2-TC in sufficient time to recognize the start codon of the inhibitory uORF2. Instead, as the small ribosomal subunit scans the interval between the initiation codons of uORF2 and the *ATF4* coding region, the eIF2-TC is reacquired and the ribosome initiates translation at the *ATF4* ORF (Figure 3) (4). This mechanism, deemed 'delayed translation reinitiation,' thus relies on a sparsity of eIF2-TC during eIF2 α -P for preferential translation of *ATF4* mRNA and subsequent enhanced expression of ATF4 protein (4).

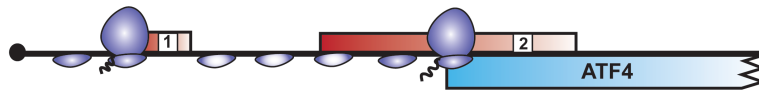
The key features of the model for preferential translation of *ATF4* are shared with those elegantly studied by Hinnebusch (6) and colleagues for yeast *GCN4* translation control. In the *GCN4* transcript there are three inhibitory uORFs that the reinitiating ribosomes bypass during the delayed reacquisition of eIF2-TC. Therefore, this mode of translational control induced by eIF2 α -P can accommodate two or more uORFs and is shared among diverse eukaryotes. Furthermore, recent studies on yeast *GCN4* have begun to provide mechanistic insight as to how ribosomes can reinitiate after translation of uORF1. The multi-subunit initiation factor eIF3 is suggested to be retained on ribosomes for the duration of the translation of uORF1. Upon termination of translation of uORF1, eIF3 can stabilize mRNA association with small ribosomal subunits and facilitate resumption of ribosomal scanning for subsequent recruitment of the eIF2-TC and reinitiation of translation at a downstream ORF (93,94).

A Delayed Reinitiation Model

No Stress: Low eIF2 α -P; High eIF2-GTP levels



Stress: High eIF2 α -P; Low eIF2-GTP levels



B Bypass Model

No Stress: Low eIF2 α -P; High eIF2-GTP levels



Stress: High eIF2 α -P; Low eIF2-GTP levels

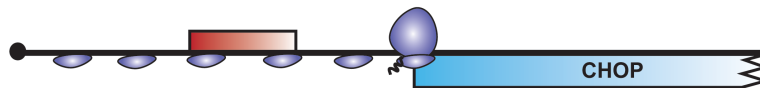


Figure 3. Mechanisms of preferential translation during eIF2 α -P. (A) In the delayed translation reinitiation model, two uORFs (red boxes) in the 5'-leader of the *ATF4* mRNA direct preferential translation. The 5'-proximal uORF1 is a positive-acting element that facilitates retention of the scanning 40S subunit and resumption of scanning 5' to 3', leading inevitably to reinitiation at a downstream start codon. During non-stressed conditions, when eIF2 α -P is low and eIF2-GTP levels are abundant, the scanning ribosome readily acquires the eIF2-TC and reinitiates translation at the next available uORF, i.e., uORF2. Reacquisition of eIF2-TC is indicated by the darker shading in the scanning 40S ribosome. The uORF2 overlaps out-of-frame with the coding sequence (blue box), and when translated prevents synthesis of ATF4, as depicted by the

dissociation of the small and large subunits following termination of uORF2 translation. During nutrient deprivation, and other stressful events, there is an increase in eIF2 α ~P, which lowers levels of eIF2-GTP. As a consequence the 40S ribosome, which continues scanning following the translation of uORF1, needs additional time to reacquire the limiting eIF2-TC. This delay in reinitiation of translation allows for the 40S ribosome to scan through the uORF2 initiation codon. During the interval between the initiation codons of the uORF2 and the ATF4 coding region, the 40S ribosome obtains the limiting eIF2-TC (dark shading) and translates the *ATF4* ORF. (B) Translation of *CHOP* mRNA is inhibited during non-stress conditions by the presence of a single inhibitory uORF, which when translated functions to block translation elongation or termination, as illustrated by the “T” symbol. This inhibitory uORF encodes a 34 amino acid residue sequence that is well-conserved among vertebrates. In the bypass model of translational control, stress induced eIF2 α ~P facilitates leaky ribosome scanning through the inhibitory uORF, which is suggested to result from the poor Kozak context of the start codons in the uORF. Consequently, the scanning ribosome initiates translation at the *CHOP* coding region, which features an initiation codon containing a strong Kozak consensus sequence.

1.5 ATF4 Directs Transcription of ISR Genes

Elevated synthesis of ATF4 during eIF2 α ~P facilitates transcriptional regulation of genes subject to the ISR. In this process, ATF4 can form homodimers or heterodimers with several other bZIP transcription factors, including the C/EBP isoforms, FOS, JUN, NRF2, and CHOP (DDIT3/GADD153). ATF4 can then bind to the ISR-targeted promoters via CARE elements, which contain a half-site for members of the C/EBP family and a half-site for ATF transcription factors (95,96). Microarray analyses and other functional studies of *ATF4*-dependent gene expression identified target genes involved

in diverse cellular functions, including the synthesis and import of amino acids, maturation and degradation of proteins, glutathione synthesis and the control of the cellular redox status, autophagy, mitochondrial function, control of apoptosis, signaling and expression of additional transcription factors, and feedback regulation of the ISR (5,97-100). While ATF4 triggers the transcription of many common target genes during diverse stresses, activation of many other genes can be specific to a given stress condition or to a selected tissue.

One of the best characterized promoters activated by ATF4 is asparagine synthetase (*ASNS*), which catalyzes the conversion of aspartate to asparagine (95,101,102). During limitations for essential amino acids, ATF4 complexed with C/EBP β binds to an element in the *ASNS* promoter, leading to localized histone acetylation. The resulting chromatin remodeling recruits general transcription factors and RNA polymerase II, leading to increased *ASNS* mRNA synthesis. Following several hours of amino acid deprivation, ATF4 can be displaced at the *ASNS* promoter by another transcription factor induced by the ISR, ATF3, coinciding with diminished *ASNS* transcription (102). This illustrates the dynamic regulation of ATF4-targeted genes during dietary stress, and highlights the importance of feedback systems in the control of gene expression of the ISR. In addition to the displacement of ATF4 at target promoters, eIF2 α -P itself is subject to feedback control. ATF4 and the ISR activates the transcription of *GADD34* (*Ppp1r15a*), encoding a regulatory subunit of the Type 1 serine/threonine protein phosphatase that dephosphorylates eIF2 α -P. Therefore, protein synthesis can be restored once a new transcriptome is implemented by the ISR (Figure 4) (83,103-108).

Mice homozygous for an *ATF4* knock-out exhibit defects in ocular, skeletal, pancreatic, and hematopoietic development, as well as significant changes in glucose

and insulin homeostasis (109,110). The hallmark feature of the *ATF4*^{-/-} mice is microphthalmia due to the absence of the lens of the eye (110,111). ER stress accompanies eye development, and loss of *ATF4*, which is required for full implementation of the UPR, was reported to lead to massive and synchronous apoptosis of cells of the epithelial lens. Furthermore, mice deleted for *ATF4* exhibit bone deformities due to decreased synthesis and secretion of Type 1 collagen (112). Given the important role of ATF4 for amino acid synthesis and uptake, it was proposed that low levels of amino acids in *ATF4*-deficient osteoblasts would decrease translation, thus reducing the major biosynthetic product, collagen. Consistent with this idea, providing *ATF4*^{-/-} mice a high protein diet helped to alleviate developmental defects and low bone mass (113). Finally, *ATF4*-deficient mice were reported to have enhanced energy expenditure and decreased diet-induced diabetes, along with lowered hyperlipidemia and hepatosteatosis (114). These findings reflect the changes that the ISR can elicit in lipid and glucose metabolism, which are a consequence of differences in nutrient utilization, changes in protein synthesis, and direct and indirect modulation of key transcription factors, such as PPAR γ , PGC1 α , SREBP1, and CHOP, which can regulate expression of metabolic genes (53,115-118).

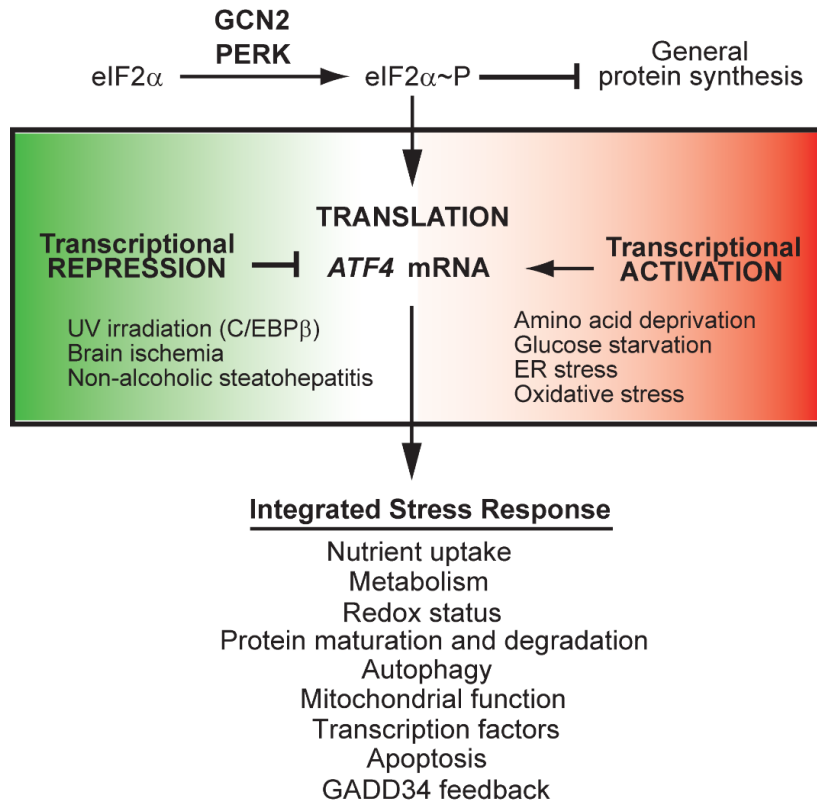


Figure 4. Transcriptional regulation of *ATF4* enables differential expression of ISR genes. In response to nutritional deprivation and other diverse stress conditions, phosphorylation of *eIF2 α* by GCN2 or PERK represses global translation. Additionally, *eIF2 α ~P* preferentially enhances the translation of *ATF4*. Increased levels of the ATF4 transcription factor triggers the transcription of a gene expression program collectively referred to as the Integrated Stress Response (ISR). Expression of *ATF4* is also subject to transcriptional regulation. Transcriptional activation in response to the indicated stress conditions serve to provide high levels of mRNA available for preferential translation during *eIF2 α ~P*, thus enhancing the ISR. Alternatively, transcriptional repression reduces the levels of *ATF4* mRNA available for translation. In this case, there is discordant induction of the ISR, with *eIF2 α ~P* reducing global protein synthesis, but low expression levels of ATF4 and its target genes.

1.6 Multiple Mechanisms Regulate Gene-Specific Translation During eIF2 α ~P

It was reported that there are hundreds of different mRNAs, approximately 3% of protein-coding genes, which are subject to preferential translation in response to GCN2 phosphorylation of eIF2 α (8). In this study, livers from wild-type and *GCN2*^{-/-} mice were perfused with medium lacking methionine, and then lysates were subjected to sucrose gradient centrifugation to identify mRNAs that show enhanced association with large polysomes specifically in wild-type mice upon the nutrient limitation. The mRNA association with large polysomes is a predictor of preferential translation. Transcripts participating in metabolism and energy production were prevalent among those genes suggested to be preferentially translated. This indicates that enhanced translation is central to not only *ATF4* expression, but also to many other genes in the ISR. Included among those genes that were preferentially translated was *ATF5*, a bZIP transcription factor most closely related to ATF4 (119). The *ATF5* mRNA contains two uORFs and is induced by eIF2 α ~P by the mechanism of delayed translation reinitiation described earlier for ATF4 (120,121). *ATF5* expression is enhanced by multiple stress conditions, and ATF5 has been reported to be important for both neural differentiation and the formation of gliomas (120,122,123).

Other members of the ISR are also subject to preferential translation during eIF2 α ~P, albeit by alternative mechanisms. CHOP is a bZIP transcription factor and an ATF4-targeted gene that is important for triggering apoptosis during chronic stress (5,96,124,125). *CHOP* mRNA is poorly translated under basal conditions as the result of a single uORF (10,126-128). Translation of the uORF during non-stressed conditions serves as a barrier that prevents translation of the downstream *CHOP* coding region. However, upon stress eIF2 α ~P facilitates the 43S PIC bypass of the uORF and instead the scanning ribosome translates *CHOP* (Figure 3) (10).

We still do not fully understand the nature by which eIF2 α ~P mediates the bypass of the inhibitory uORF. This uORF has two AUG codons at codon positions 1 and 4 in the uORF. The second initiation codon is dominant, although both are suggested to be able to serve as the initiator of translation of the uORF (10,126). The frequency of initiation during scanning of the 43S PIC is influenced by the nucleotide sequence surrounding the start AUG codon. Kozak (129) first described the importance of this consensus sequence (termed the 'Kozak context') in the late 1980s, where an optimal context in mammalian mRNAs is considered 5'-GCC(A/G)CCAUG(G)-3' (7). Deviations from this context, particularly at the -3 and +4 positions, can reduce the efficiency of translation initiation. In the 'Bypass' mechanism of *CHOP* translation control, both of the initiation codons in the inhibitory uORF are in poor context whereas the start codon of the *CHOP* coding region is optimal. Under non-stressed conditions and low eIF2 α ~P, translation initiation at the uORF leads to a block in translation elongation or termination, preventing further ribosome scanning and translation at the downstream *CHOP* ORF. Critical to this inhibitory function of the uORF is the synthesis of the carboxy terminal portion of the 34 residue uORF. However, as a consequence of the poor Kozak context of the uORF, stress-induced eIF2 α ~P is suggested to facilitate leaky scanning through the inhibitory uORF and instead initiation occurs downstream at the optimal context of the *CHOP* coding sequence. In support of this idea, substitution of an optimal Kozak context for the initiation codon of the uORF substantially reduces *CHOP* expression even during induced eIF2 α ~P (10). The Bypass model for *CHOP* translational control helps explain how expression of *CHOP* and the fate of cells are tightly linked to the levels of eIF2 α ~P and stress damage (Figure 3)(10).

Another mRNA in the ISR that is subject to preferential translation in response to eIF2 α ~P, is *GADD34* (130). As noted earlier, *GADD34* is a stress-inducible factor

responsible for facilitating the dephosphorylation of eIF2 α -P (130). The *GADD34* mRNA contains two uORFs, and it is currently unclear whether the delayed reinitiation or bypass models underlie *GADD34* translational control. Nonetheless, the preferential translation of *GADD34* provides an explanation for how the accompanying feedback mechanism is induced during a global repression of protein synthesis.

Another means by which mRNAs can be preferentially translated during a global decrease in eIF2-GTP levels is through cap-independent processes. While the overwhelming majority of cellular mRNAs rely on the scanning mechanism for translation initiation, non-canonical cap-independent initiation via Internal Ribosome Entry Sites (IRESs) is suggested to be important for the expression of several cellular proteins including HIF1 α , Bcl2, CAT-1 and XIAP (131-134). First described in viral mRNAs, IRESs are RNA elements which can directly recruit components of the translational machinery to the mRNA independent of eIF4E cap binding, and many are suggested to be resistant to reductions in eIF2-TC levels as a result of eIF2 α -P (9,135). The delayed reinitiation, ribosomal bypass, and IRES-mediated mechanisms of translational control each provide a means by which protein expression for an individual gene is enhanced during a global reduction in mRNA translation. Given that only a handful of mRNAs have thus far been characterized among the hundreds of genes suggested to be subject to preferential translation during eIF2 α -P, there are likely additional translational control mechanisms that contribute to the ISR.

1.7 Discordant Induction Of eIF2 α -P and ATF4

While eIF2 α -P elicits translational control in response to many different stresses, there are selected stresses, such as exposure to UV irradiation, that do not increase *ATF4* expression despite robust eIF2 α -P (55,56,136). The molecular basis for this discordant induction of *ATF4* expression and eIF2 α -P is that *ATF4* is subject to both

translational and transcriptional regulation (Figure 4). In response to UV irradiation, transcription of *ATF4* is repressed, and therefore *ATF4* mRNA is not readily available for preferential translation (136).

Transcriptional regulation of *ATF4* provides an important regulatory hub for the cellular implementation of the ISR. The half-life of *ATF4* mRNA and protein are short, from 2 to 4 hours (136,137); therefore, the activity of ATF4 is tightly linked to its synthesis, namely the transcription of *ATF4* and its translation, which is dictated by the status of eIF2 α -P. Activation of *ATF4* transcription leads to more mRNA available for preferential translation induced by eIF2 α -P (Figure 4) (136). Alternatively, repression of *ATF4* leads to lower mRNA, thus diminishing synthesis of ATF4. Elevated eIF2 α -P and accompanying translational control enhance the resistance of cultured cells to UV treatment, whereas forced expression of *ATF4* with the UV insult substantially reduces survival(136). In the case of UV stress, eIF2 α -P was reported to lead to preferential translation of alternative mRNAs, those encoding key members of the nucleotide excision repair pathway, thus facilitating the repair of DNA damage (11). In addition to UV irradiation, brain ischemia (138) and non-alcoholic steatohepatitis (139) were reported to trigger eIF2 α -P but not increased *ATF4* expression. Therefore, transcription repression and the discordant induction of *ATF4* and eIF2 α -P is suggested to occur during diverse stress conditions.

We are only beginning to understand the full mechanistic features for transcriptional regulation of *ATF4*. The transcription factor C/EBP β is suggested to be a potent repressor of *ATF4* transcription in response to UV irradiation (140). Expression of different isoforms of C/EBP β are controlled by a range of developmental and differentiation processes, along with environmental stresses, providing these cellular processes a vehicle for controlling a key step in the ISR. Stresses shown to enhance

ATF4 mRNA levels include ER stress (3,141,142), starvation for amino acids (143), oxidative stress (144-146) and resistance to anticancer agents (146,147). During oxidative stress, the transcription factor NRF2 can bind to the *ATF4* promoter and enhance its transcription, which serves to alleviate oxidative damage and facilitate angiogenesis (Figure 4) (144,145). The transcription factor CLOCK can also associate with the *ATF4* promoter, leading to increased *ATF4* expression which facilitates resistance to the anti-cancer drugs cisplatin and etoposide (148). Similarly PDX1, a pancreas-specific transcription factor was reported to regulate ER stress responses in islet β -cells by binding to the *ATF4* promoter and increasing its expression (149). These studies suggest that many different transcription factors can bind to the *ATF4* promoter and modulate the levels of *ATF4* mRNA. Some of these transcription factors are repressors, triggering discordant induction of $eIF2\alpha\sim P$ and *ATF4* expression upon selected environmental stresses, while others are activators, accentuating *ATF4* levels in the ISR. As a consequence, multiple stress pathways can control the induction *ATF4* by $eIF2\alpha\sim P$, insuring that the expression of *ATF4* and its ISR-target genes are tailored for a given stress condition.

1.8 Cross-Regulation Between the ISR and Other Signaling Pathways

Translational and transcriptional control induced by the ISR can be integrated with additional stress signal pathways to direct gene expression dedicated for specific stresses and control cell fate. An example of this integration can be seen in cells responding to ER stress, where PERK functions in conjunction with the two other stress sensors, ATF6 and IRE1, to induce the UPR. Upon ER stress, ATF6 transports from the ER to the Golgi apparatus, where ATF6 is subject to intramembrane proteolysis, allowing for the release of the amino-terminal cytoplasmic portion of ATF6 (150,151). This portion of ATF6 functions as a bZIP transcription factor that enters the nucleus and

targets UPR genes involved in protein folding and the ERAD pathway for clearance of unfolded protein from the ER. IRE1 is a riboendonuclease that cleaves *XBP1* mRNA in the cytoplasm, leading to translation of another active bZIP transcription factor of the UPR (152,153).

While activation of the three UPR sensors by ER stress can be viewed as occurring in parallel, PERK-mediated eIF2 α -P was shown to trigger not only translational control, but was only central to the transcriptional phase of the UPR (97). In mice subjected to tunicamycin, a potent inducer of ER stress, PERK was shown to be required for 74% of the UPR genes induced in livers by 2-fold or greater. Furthermore, PERK-deficiency in the livers of these mice led to increased triglycerides and apoptosis within 24 hours of the onset of ER stress. The rationale for the broad impact of PERK on the UPR transcriptome is that ATF4 facilitates activation of ATF6 during ER stress by at least two mechanisms. First, ATF4 enhances the transcription of *ATF6*, ensuring that newly synthesized ATF6 is available for continued processing and activation (97). Second, ATF4 contributes to the trafficking of ATF6 from the ER to the Golgi for subsequent proteolysis and activation (97). ATF4 enhances the expression of numerous genes that facilitate protein passage from the ER to Golgi, and it was proposed that one or more of these genes are critical for ATF6 processing and activation. Therefore, the PERK/eIF2 α -P/ATF4 pathway is integrated with additional ER stress sensors to activate a collection of UPR genes critical for alleviating the accumulation of unfolded protein in the secretory pathway.

The function of the ISR can also be integrated with mTOR. Central to the signaling pathways controlling mTOR is the tuberous sclerosis complex (TSC), which consists of TSC1 and TSC2 subunits that inhibit RHEB, a small GTPase which binds and activates mTORC1 (23). Loss of TSC triggers constitutive activation of mTORC1,

leading to neoplasms that are characterized by high levels of protein synthesis. Interestingly, it was reported that disruption of TSC also causes ER stress, activating PERK and the UPR (154). Induction of the UPR with loss of TSC was observed in cell culture and mouse models, as well as in cortical tubers, the most common kind of tumors arising in tuberous sclerosis patients. It was proposed that elevated protein synthesis resulting from hyperactivation of mTORC1 in the TSC-deficient cells can increase the influx of nascent proteins entering the secretory system and as a consequence overload the ER. Supporting this idea, treatment of *TSC*-deficient cells with cycloheximide, an inhibitor of translation elongation, prevents activation of the UPR (154). Additional targets altered by hyperactivation of mTORC1 have also been shown to be important in ISR signaling, as mTORC-1 activity is required for the efficient translation of c-MYC, which can then bind to the promoter of *ATF4* regulating its transcriptional activation (155).

Dysregulated activation of mTORC1 can interfere with insulin signaling, and the induced UPR in *TSC*-deficient cells plays a critical role in the inhibitory process. IRE1 signaling via recruitment of TRAF2 and subsequent activation of JNK can lead to inhibitory phosphorylation and degradation of IRS1 (156,157). Therefore, the key signaling events that stem from the UPR help explain the insulin resistance associated with *TSC*. From a protein synthesis perspective, the UPR diminishment of insulin activity would make sense, in that insulin signaling would enhance translation, which would further exacerbate the ER stress. Finally, loss of *TSC* renders cells sensitive to drugs that can elicit ER stress, such as the proteasome inhibitor bortezomib, which is currently approved for the treatment of multiple myeloma (154,158,159). While the UPR is generally viewed as cytoprotective, accentuated ER stress can alter this stress response pathway to become one that is pro-apoptotic (82,160,161). Therefore, drugs that can trigger ER stress may provide a potent treatment strategy for treating tuberous sclerosis.

The ISR is also suggested to direct gene expression that can control mTORC1 function. For example, in response to ER and oxidative stress, ATF4 can reduce mTORC1 activity by enhancing expression of *REDD1*, which interfaces with TSC to inhibit mTOR signaling (162-164). ATF4 was also reported to directly increase the expression of a downstream effector of mTORC1, 4E-BP1, in islet β -cells. Loss of 4E-BP1 leads to deregulated translational control, contributing to loss of β -cells and exacerbating hyperglycemia in mouse models (165).

1.9 Role of eIF2 α ~P in Diabetes

As the acronym UPR implies, it is suggested that accumulation of unfolded or misfolded protein is the critical signal that activates the ER stress sensors. However, it is important to emphasize that measuring ER stress directly is problematic, and most studies infer ER stress by assaying for activation of the UPR sensors, such as PERK. There may be many different ER signals directly triggering the UPR, some effecting other cellular compartments. Tissues specialized for secretion, such as the pancreas and liver, are suggested to encounter fluctuating ER stress under normal physiological conditions, and the UPR allows cells to adapt to these physiological stresses, as well as to overcome stress caused by disease or environmental perturbations. These ideas can be illustrated in islet β -cells exposed to transient high blood glucose, leading to an increase in proinsulin mRNA translation and the protein processing workload of the ER, thereby activating the UPR. Furthermore in the obese state, chronic elevated levels of free fatty acids and glucose, along with inflammatory cytokines, can trigger ER stress in many different tissues.

Our understanding of the stresses activating the UPR and the role this pathway plays in alleviating these cellular insults is largely based on the characterization of gene mutations disrupting key steps in the UPR. As noted earlier in this review, mutations have been identified in patients that disrupt *PERK* resulting in WRS, and alterations in

upstream regulators and downstream effectors have also been shown to have a major impact on the UPR and cell fate. Importantly, mouse models containing these precise mutations result in pathologies that closely mirror the human condition.

Missense or truncation mutations in *PERK* (*EIF2AK3*) lead to WRS, which features neonatal diabetes due to loss of β -cells. *PERK*-deficient mice also display hyperglycemia due to loss of these islet cells (166,167). It was suggested that β -cell death is a consequence of unresolvable ER stress that can occur as a result of unregulated translation and excessive proinsulin targeting to the ER. Conditional mutations in *PERK* suggest that this eIF2 α kinase is also required for the development of the pancreas, including β -cells (168). Loss of *PERK*, or its downstream target ATF4, also leads to atrophy of the acinar cells of the pancreas, which is associated with inflammatory responses and pancreatitis (169). Given the earlier discussion of the role of *PERK*/eIF2 α -P/ATF4 in the activation of ATF6, it is likely that the absence of *PERK* also broadly compromises the UPR transcriptome, preventing the appropriate expansion of the ER processing capacity.

The Akita mouse strain features a dominant missense mutation, C96Y, in the insulin 2 gene which eliminates a disulfide linkage and impairs protein folding (170,171). As a consequence, there is dysfunction and death of β -cells, and accompanying diabetes. The same mutation in the insulin gene was recently identified in patients with early onset diabetes (172). The dysfunctional insulin folding would result in an unresolvable ER stress that would lead to constant activation of the UPR sensors. Significant levels of ER stress in β -cells can also be the consequence of continued exposure to free fatty acids and cytokines (173-176). While the UPR is important for resolution of ER stress, chronic induction of *PERK* is suggested to trigger maladaptive responses and cell death. Consistent with this idea, deletion of *CHOP* in the Akita

mouse, as well as in mouse obesity models, delayed the onset of hyperglycemia and β -cell death (118,177). CHOP is suggested to elicit apoptosis through repression of *BCL2*, and the induction of pro-apoptotic genes, such as *BIM*, *DR5*, *TRB3*, and those tied to autophagy (96,98,118,126,178-182). Additionally, continued induction of *CHOP* can lead to oxidative stress and promotion of protein synthesis by feedback regulation of *GADD34*, which would further exacerbate preexisting ER stress.

WFS1 is a target gene of the UPR, whose disruption leads to Wolfram syndrome, characterized by juvenile-onset diabetes, optic atrophy, and later onset of neurodegeneration ultimately leading to patient death (183,184). *WFS1* protein is localized to the ER and is highly expressed in β -cells. *WFS1* is predicted to be a multi-pass transmembrane protein that may function as an ion channel to facilitate calcium mobilization and ER homeostasis (185,186). Another function attributed to *WFS1* is feedback control of ATF6, facilitating ATF6 ubiquitination and degradation by the proteasome (187). In mouse β -cells and lymphocytes derived from Wolfram syndrome patients, loss of *WFS1* leads to hyperactivation of ATF6. Therefore, disruption of a downstream effector of the UPR can also lead to its dysfunction, triggering maladaptive responses.

1.10 Behavior, Memory, and Neurological Degeneration

GCN2 and tRNA charging also have a role in animal behavior. Animals have an innate ability to detect imbalanced diets lacking essential amino acids, and upon doing so reject the deficient diet to forage for a balanced food source. This 'food aversion' response is not regulated by peripheral sensations like taste or smell, but rather is modulated by tRNA charging in the anterior piriform cortex, an area of the cerebral cortex responsible for detecting amino acid homeostasis (188). When levels of an essential amino acid are low, uncharged cognate tRNAs accumulate and subsequently activate the GCN2/eIF2 α -P pathway (188-190). GCN2 is central to this regulated

behavior, as *GCN2*-deficient mice have an impaired ability to both avoid imbalanced diets and phosphorylate eIF2 α in brain tissues when deprived of essential amino acids. Thus *GCN2* triggers a mechanism shared among metazoans in which amino acid availability is coupled to foraging behavior to insure the maintenance of amino acid homeostasis. *GCN2* and ATF4 signaling in the hippocampus have also been shown to regulate memory and learning. *GCN2*^{-/-} mice were reported to have aberrant induction of long-term potentiation and impaired spatial memory patterns when compared with wild-type littermates (191).

Disruptions in the ISR can also lead to neural degeneration. Missense mutations in any of the five subunits of the GEF eIF2B reduce eIF2-GTP recycling independent of stress and result in an inherited neurodegenerative disorder termed Vanishing White Matter Leukoencephalopathy (VWM, also known as Childhood Ataxia with Central Nervous System Hypomyelination) (192-197). These genetic alterations cause reduced eIF2B activity and lowered eIF2-TC levels independent of eIF2 α ~P. In the event of a provoking stress, such as head trauma or fever, there is induced eIF2 α ~P, which combined with underlying eIF2B lesions is suggested to lead to hyperactivation of the ISR. The net result is that the ISR, which typically serves to alleviate stress damage, is altered to one that becomes maladaptive. Consequently, astrocytes and oligodendrocytes in the brain of the VWM patients perish, ultimately resulting in rapid neurologic deterioration and death.

1.11 Nutrient Availability, Hypoxia, and Tumorigenesis

Recent studies have emphasized the importance of the eIF2 α ~P/ATF4 axis in tumor proliferation. The tumor microenvironment is often characterized by hypoxic regions limited for nutrients due to vasculature restrictions. An important means by which solid tumors survive and proliferate in these stressful conditions is the induction of

eIF2 α -P and *ATF4* expression. Knockdown of *ATF4* mRNA causes reduced cell survival and increased G₁/S arrest in human fibrosarcoma and colorectal adenocarcinoma cells, and nude mice injected with K-RasV12-transformed *GCN2*^{-/-} MEF cells develop substantially smaller tumors than those injected with the transformed wild-type (61). The mechanistic basis for this reliance on elevated levels of ATF4 involves a dependency on the aforementioned ATF4 downstream target *ASNS*, encoding asparagine synthetase. The reliance of multiple cancer types on asparagine and its synthesis is already being targeted in the clinic as a means for treating hematological neoplasms. L-asparaginase depletes asparagine from the blood stream, effectively inhibiting tumorigenesis and malignancy in patients with acute lymphoblastic leukemia (198).

In addition to nutrient limitation, tumor cells must also cope with both acute and chronic episodes of extreme hypoxia. One mechanism by which transformed cells survive the hypoxic microenvironment is through PERK activation, which allows for the conservation of resources via the global reduction in protein synthesis and preferential translation of *ATF4* that is important in combating oxidative stress. Constitutive activation of the ISR in the tumor microenvironment provides a selective advantage in transformed cancer cells, therefore eIF2 α kinases and downstream target genes offer attractive new targets for cancer therapies (199).

1.12 Global Regulation of mRNA Transcripts During PERK Activation -- New Members of the ISR

Prevailing views of translational control in the UPR suggest there are a few select gene transcripts that are preferentially translated coincident with repression predominant among the remaining mRNAs. We propose that the UPR translational control network may be more expansive than the models described above, including many additional key regulatory genes subject to preferential translation. To address this hypothesis, we

carried out a genome-wide study using sucrose gradient ultracentrifugation to separate translating mRNAs on large polysomes from those associated with fewer ribosomes. Gene transcripts in these gradient fractions were then measured globally to address how translational efficiencies for mRNAs changed in response to ER stress. Our study suggests a gradient model of translational control in which many mRNAs are repressed or resistant to eIF2 α -P, whereas a significant subset are preferentially translated. From this latter group, we identified *IBTK α* as being subject to both preferential translation and increased transcriptional expression in response to PERK-induced eIF2 α -P. *IBTK α* is a multidomain protein suggested to associate with the ubiquitin ligase CUL3 and serve as a substrate adaptor for protein ubiquitylation (200,201). We show that knockdown of *IBTK α* increased caspase activation and lowered cell survival, suggesting *IBTK α* is central for the efficacy of the UPR. We also identified mRNA encoding the bifunctional Glutamyl-Prolyl tRNA synthetase (*EPRS*) as being subject to preferential translation during both PERK and GCN2 activation. The *EPRS* model of translation control involves the stress-induced bypass of a non-canonical *CUG* in the 5'-leader. The mechanisms regulating *IBTK α* and *EPRS* expression highlight the diversity by which uORFs can modulate downstream coding sequence expression.

CHAPTER 2. EXPERIMENTAL METHODS

2.1 Cell culture and generation of stable cell lines

Wild-type, eIF2 α -S51A, *PERK*^{-/-}, *GCN2*^{-/-} and *ATF4*^{-/-} mouse embryonic fibroblast (MEF) cells were previously described (100). The MEF cells were grown in Dulbecco's modified Eagle's medium (DMEM) (Corning) supplemented with 1 mM non-essential amino acids, 10% (v/v) fetal bovine serum, 100 units/mL penicillin, and 100 μ g/mL streptomycin at 37°C. The *ATF4*^{-/-} cells, and its wild-type counterpart, were supplemented with additional amino acids and 55 μ M β -mercaptoethanol due to a predisposed sensitivity of ATF4-depleted cells to oxidative stress (5). For Halifuginone treatments, both control and treatment groups were cultured in DMEM supplemented with 10% (v/v) dialyzed fetal bovine serum (Gibco). HepG2 cells were cultured in Minimum Essential Media (Gibco) supplemented with 1 mM non-essential amino acids, 1 mM sodium pyruvate, 2 mM glutamax, and 10% (v/v) fetal bovine serum at 37°C. Cells were cultured to 60-70% confluence and treated with TG for the indicated times.

Stable *IBTK α* knockdown and scramble control cells were produced by transducing wild-type MEF cells with lentivirus encoding shRNA against *IBTK α* from validated mission shRNA TRC clones TRCN0000088505 and TRCN0000088503 (Sigma-Aldrich, St. Louis, MO), or control SHC007, or in HepG2 cells TRC clones TRC0000082575 and TRC0000082577, or control SHC007. Transduced cells were selected for shRNA expression with 5 μ g/ml puromycin and maintained in DMEM or MEM. Cell culture maintenance and all assays were performed in the absence of puromycin.

2.2 Immunoblot analyses

MEF cells were treated with 1 μ M TG for 6 hours, or without treatment, and protein lysates were prepared, and proteins were measured by the Bradford assay.

Proteins were separated by SDS-PAGE and immunoblot analyses were carried out in three independent experiments using horseradish peroxidase-tagged secondary antibody as previously described (202). Antibodies used in the immunoblot analysis are as follows: eIF2 α ~P antibody from Cell Signaling Technologies (catalog number 9721), monoclonal antibody for total eIF2 α from Dr. Scott Kimball (Pennsylvania State University College of Medicine, Hershey, PA), CHOP from Santa Cruz Biotechnology (catalog number sc-7351), ATF4 prepared against recombinant protein (120), β -actin from Sigma (catalog number A5441), ATF6 against recombinant protein (97), IBTK α from Abnova (catalog number H00025998-B01P) and EPRS from Abcam (catalog number ab31531).

2.3 Polysome profiling and sucrose gradient ultracentrifugation

Sucrose gradients ranging from 10% to 50% in a solution containing 20 mM Tris-HCl (pH 7.5), 100 mM NaCl, 5 mM MgCl₂, and 50 μ g/ml cycloheximide were used for polysome analysis as previously described using a tilted tube rotation method on a gradient station equipped with a Piston Gradient Fractionator™ and a Gradient Master™ from BioComp (NB, Canada) (203). MEF cells were cultured in DMEM in the presence or absence of 1 μ M TG or HF for 6 hours. Prior to harvesting, cells were incubated in culture media containing 50 μ g/ml cycloheximide for 10 min at 37°C. Cells were rinsed twice with chilled PBS containing 50 μ g/ml cycloheximide, and then lysed with 500 μ l of cold lysis buffer consisting of 20 mM Tris (pH 7.5), 100 mM NaCl, 10 mM MgCl₂, 0.4% nonident P-40, 50 μ g/ml cycloheximide, and EDTA-free protease inhibitor cocktail tablet (Roche). The lysates were sheared with a sterile syringe with a 23 gauge needle, incubated on ice for 10 min, and clarified at 8000 \times g for 10 min. 400 μ l of supernatant was layered atop the sucrose gradients, which were subjected to centrifugation in a Beckman SW41Ti rotor at 40,000 rpm for 2 h at 4°C. Sucrose fractions and the resulting

polysome profiles for each sample were then collected using a Piston Gradient Fractionator and a 254-nm UV monitor with Data Quest software.

To investigate specific mRNA transcript shifts during stress, 10 ng/ml firefly luciferase control RNA (Promega) was added to each pooled sample prior to RNA isolation, allowing for measurements of the relative amounts of the transcript of interest to be normalized to an exogenous RNA control (10,203). Samples were then immediately mixed with 750 μ l of TRIzol Reagent LS, and RNA isolation and cDNA generation performed as described below. To calculate “% total gene transcript” for the 7 fractions, $2^{(-\Delta\Delta CT)}$ were summed for each treatment group, and the $2^{(-\Delta\Delta CT)}$ value for each fraction was considered as a percentage of the total. This calculation serves to omit for changes in the levels of transcript abundance between treatment groups. All polysome profiles and mRNA shifts depicted are representative of three independent biological replicates. The percent shift was calculated as [% total mRNA in fractions 5,6,7 during ER stress] – [% total mRNA in fractions 5,6,7 during no stress].

2.4 Microarray analysis

The MEF cells were cultured in DMEM treated with 5 μ M TG for 6 hours or no stress. We have observed variations in the ER stress response between different preparations of TG and this concentration of this drug lot was optimal for induced eIF2 α ~P and downstream translational control. 6 hours of stress treatment was used as this was optimal for expression of downstream targets of PERK, such as *CHOP*, which require elevated mRNA expression for subsequent preferential translation by eIF2 α ~P. Prior to harvesting, the MEF cells were treated with 50 μ g/ml cycloheximide and incubated at 37°C for 10 minutes. Cell lysates were subjected to sucrose gradient centrifugation and the polysome fractionation. A total of 7 fractions were collected from the top of the gradients into cold microfuge tubes and immediately placed on ice. Each

fraction was adjusted to 0.5% SDS, and fractions were combined to form three pools as follows: fractions 1–2, 3–4, 5–7 were combined as pools 1, 2, and 3, respectively. In parallel, total RNA was isolated from unfractionated lysates for analysis of total gene transcript levels. Synthetic Poly(A) luciferase RNA (10 ng/ml) (Promega), along with a bacterial spike-in control RNA (Affymetrix), were added to each gradient fraction pool. Synthetic luciferase RNA served as a control for the efficiency of RNA isolation. The bacterial spike-in RNA has different concentrations of each of the four exogenous, premixed, polyadenylated prokaryotic RNA controls. These prokaryotic genes have limited cross-hybridization with mammalian sequences, but have target sequences on the Affymetrix arrays. These spike-ins normally serve as quality controls for the labeling step so are added after RNA extraction as the first step of the Affymetrix labeling protocol. Here they are being used to normalize the arrays from the different fractions because the amount of RNA in each fraction may not be equivalent. RNA was precipitated at -70°C with 2.5 volumes 100% ethanol and purified using QIAGEN RNeasy midi-columns. For total unfractionated RNA, samples were subjected to ethanol precipitation. Total RNA was isolated, analyzed, and stored the same way as the RNA from polysomal fractions. The quality of RNA was measured by using an Agilent Bioanalyzer. RINs (RNA integrity number) for the unfractionated total RNA were ≥ 9.9 .

RNA preparations were then labeled using the standard Affymetrix protocol for 3'-IVT arrays (GeneChip® Expression Analysis Technical Manual, Rev. 5, Affymetrix, Santa Clara, CA) starting with 2 μ g of total RNA for all samples. Labeled cRNA was hybridized for 17 hours to the Affymetrix Mouse Genome 430 2.0 Array. The signal values and detection calls were derived using the MAS5 algorithm in Affymetrix GeneChip Operating Software. Affymetrix arrays were hybridized and scanned at the Center for Medical Genomics at IUSM following standard protocols. Scaling was not

used to normalize the arrays. Raw intensity values for the spike-in control RNA probesets were used to normalize gene expression values across all arrays. Transformations by using the spike-in control probeset values were performed as previously described (204). Probe sets were retained for analysis if a probe set was called present in at least 66.6% of the samples in either the control and treated unfractionated samples. The same probe sets were retained in the fractioned polysomal RNA samples and considered for further analysis.

Differentially translated genes were identified using the data generated from the three pools following a modification of the procedure employed for the unfractionated RNA analysis. This analysis is based upon the fact that the majority of mRNA bound to multiple ribosomes were in pool 3, while pools 1 and 2 contain mRNAs bound to no ribosomes and 1–3 ribosomes, respectively. Consequently, the percentage of a transcript that resides in pool 3 is a measure of increased mRNA binding to translating ribosomes -- a suggested measure of translational efficiency. For each replicate control and treated sample, the fraction of normalized \log_2 transformed mRNA intensity in pool 3 was divided by the total mRNA intensity (pool 3 / [pool 1+2+3]). Statistical analyses on the biological replicates were performed using student's t-test to derive p-values for each probe set. Microarray data are deposited in Gene Expression Omnibus (www.ncbi.nlm.nih.gov/geo/) under the series number GSE54581. The following link was created to allow review of microarray data:

<http://www.ncbi.nlm.nih.gov/geo/query/acc.cgi?token=inchsgsonnobrcd&acc=GSE54581>

.2.5 Measurement of mRNA by qPCR

RNA was isolated from cultured cells using TRIzol reagent (Invitrogen). Single-strand cDNA synthesis was carried out using the TaqMan reverse transcriptase kit (Applied Biosystems) following the manufacturer's instructions. Total RNA was extracted from frozen liver preparations as described (97). Levels of mRNA were measured by

qPCR using the SYBR Green (Applied Biosystems) method on a Realplex² Master Cyclor (Eppendorf). To measure the levels of target mRNAs, transcripts were normalized to either β -actin or luciferase control RNA (Promega) for changes in polysome fraction distribution. The primers used for measuring mRNA levels were as follows: *IBTK α* : forward primer, 5'-CCACCGTCTGCAGGATTATT-3'; reverse primer, 5'-CTCGACCTTATCCGAATGGA-3'; *ATF5*: forward primer, 5'-GGCTGGCTCGTAGACTATGG-3'; reverse primer, 5'-CCAGAGGAAGGAGAGCTGTG-3'; *ATF4*: forward primer, 5'-GCCGGTTTAAGTTGTGTGCT-3'; reverse primer, 5'-CTGGATTCGAGGAATGTGCT-3'; *β -actin*: forward primer, 5'-TGTTACCAACTGGGACGACA-3'; reverse primer, 5'-GGGGTGTGTAAGGTCTCAA-3'; *eIF4e*: forward primer, 5'-CAGGAGGTTGCTAACCAG-3'; reverse primer, 5'-ATAGGCTCAATCCCGTCCTT-3'; *CReP*: forward primer, 5'-GGCTACAGTGGCCTTCTCTG-3'; reverse primer, 5'-CATCCATCCCTTGCAAATTC-3'; *firefly luciferase*: forward primer, 5'-CCAGGGATTCAGTCGATGT-3'; reverse primer, 5'-AATCTCACGCAGGCAGTTCT-3'; and *EPRS*: forward primer, 5'-TGTGGGGAAATTGACTGTGA-3'; reverse primer, 5'-AACTCCGACCAAACAAGGTG-3'.

2.6 Plasmid constructions and luciferase assays

A 5'-Rapid Amplification of cDNA Ends (RACE; FirstChoice® Ambion) was performed following the manufacturer's protocol using RNA samples extracted from wild-type MEF cells treated with 1 μ M TG for 6 hours, or no stress agent, to determine the transcriptional start site for *IBTK α* and *EPRS*. The cDNA fragments encoding the 5'-leaders of *IBTK α* mRNA and *EPRS* mRNA were inserted between HindIII and NcoI restriction sites in a derivative of a pGL3 basic luciferase vector (4,10). The resulting *P_{TK}-IBTK α -Luc* and *P_{TK}-EPRS-Luc* reporter plasmids contain the 5'-leader of mouse *IBTK α* mRNA and 5'-leader of mouse *EPRS* mRNA fused to a luciferase reporter

downstream of a constitutive TK promoter, respectively. ATG start codons were mutated to AGG codons individually for all permutations reported in figure 9 by site-directed mutagenesis (Stratagene) following the manufacturer's instructions. Conversely, CTG codons were mutated to AAA codons individually for all permutations in figure 15 following the same protocol. For the stem-loop construct impeding cap-dependent scanning, a previously described stem-loop structure ($\Delta G = -41$ kcal/mol) was inserted 30-bp downstream of the encoded transcription start site (4). All plasmid constructs were sequenced to verify nucleotide substitutions. *P_{TK}-IBTK α -Luc* and *P_{TK}-EPRS-Luc* constructs were transiently co-transfected with a Renilla reporter plasmid into wild-type or eIF2 α -S51A MEF cells for 24 hours. Transfected cells were treated with 0.1 μ M TG for 12 hours, and cells were collected and firefly and Renilla luciferase activities measured as previously described. Relative values of firefly luciferase activities, normalized for *Renilla* luciferase control, were determined in triplicate for each of at least three different biological samples.

2.7 Animal study

The animal study protocol was approved by the Institutional Care and Use Committee at the Indiana University School of Medicine. LsPERK-KO mice were derived by deletion of floxed *PERK*^{f/f} using *cre* expression driven by the liver-specific albumin promoter, as described previously (47,97). Mice were genotyped to ensure efficient *PERK* gene deletion. Mice received intraperitoneal injections of tunicamycin at a dose of 1 mg/kg body weight or an equivalent volume of excipient (0.3% dimethyl sulfoxide in phosphate-buffered saline) as described. Mice were killed by decapitation 6 hours after injection, and dissected livers were rinsed in chilled PBS, weighed, and snap-frozen in liquid nitrogen. Preparations of RNA and protein, qPCR measurements of the *ATF4* and

IBTK α mRNAs, and the indicated protein measurements by immunoblot were prepared as described above.

2.8 Cell proliferation and viability assays

Scramble and *IBTK α* KD MEF cells were seeded at either 2 or 5 x10⁵ cells in 10 cm dishes and harvested using TrypLE™ (Life Technologies) for up to 72 hours.

Harvested cell suspensions were counted for viability by trypan exclusion using a Vi-Cell Cell Viability Analyzer (Beckman Coulter). For cell proliferation assays, knockdown MEF cells and their scramble counterparts were seeded at 2.5 x10⁵ cells/well in 96-well plates and allowed to set overnight. Prior to fixation with 3.7% formalin, 20 μ M EdU was added to cells for 2 hours at 37°C. Cells were permeabilized with Triton-X100 and labeled using Click-iT EdU reaction mixture (Invitrogen). Data were normalized to day zero for each respective cell line. Images for microscopy depict total nuclear staining (10 μ g/mL Hoechst) and cells actively in S-phase (10 μ M EdU). For Caspase 3/7 cleavage assays, cells were plated at 10,000 cells/well in a 96 well plate, allowed to grow for 24 hours, and then measured using the ApoLive-Glo™ Multiplex assay (Promega) on a Synergy H1 Microplate reader (BioTek®). For MTT assays describing cell viability during Halofuginone and treatment, wild-type and GCN2^{-/-} MEF cells were seeded in 96-well culture plates at 5,000 cells/well 24 hours prior to treatment. Both control and treatment groups were plated in DMEM supplemented with 10% dialyzed FBS. Cells were treated with 25 nM HF for 0, 3, 6 or 9 hours, and viability measured according to the CellTiter 96® Non-Radioactive Cell Proliferation Assay kit protocol (Promega, Catalog Number G4001). Treatment values were normalized to untreated groups for each respective cell line.

CHAPTER 3. RESULTS: *IBTK α* IS SUBJECT TO PREFERENTIAL TRANSLATION DURING STRESS

3.1 eIF2 α ~P during ER stress induces a gradient of mRNA translational efficiencies

Thapsigargin (TG) is a potent inducer of ER stress by inhibiting the SERCA family of Ca²⁺ ATPases, effectively reducing levels of calcium in the lumen of the ER and activating the UPR. As a result, eIF2 α ~P by PERK and the accompanying reduction in eIF2-GTP leads to an overall reduction in translation initiation (Figure 5A). This decrease of global translation initiation during ER stress in MEF cells is visualized by a reduction in large polysomes, accompanied by increased monosomes. By comparison, MEF cells expressing an eIF2 α mutant for which the phosphorylated serine 51 was replaced with an alanine residue (eIF2 α -S51A) displayed wild-type levels of polysomes independent of treatment with TG (Figure 5B). In addition to reducing genome-wide translation, eIF2 α ~P also enhanced expression of ATF4 and CHOP proteins, key downstream targets of PERK (Figure 5C).

To address gene-specific changes in the translome following ER stress, wild-type MEF cells were exposed to TG for 6 hours, a time point that potently increases known PERK targets, such as CHOP, or left untreated. Following treatment, cycloheximide was used on both treatment groups to arrest elongating ribosomes on mRNAs. Lysates were then subjected to sucrose gradient ultracentrifugation, and sample fractions were pooled into three groups: free ribosomal subunits (fractions 1-2); monosomes and small polysomes (fractions 3-4); and large polysomes (fractions 5-7). RNA was purified from each pooled group, and expression microarray analyses were conducted for the pools from ER stress and non-treatment groups. To further investigate mRNA changes during ER stress, microarray analyses were also performed on whole

cell lysate RNA. In response to stress, there was a global decrease in the number of mRNAs associated with large polysomes, indicative of an overall decrease in translating ribosomes (Figure 6A). By comparison, a smaller collection of gene transcripts showed significantly greater association ($\geq 15\%$) with large polysomes upon ER stress, suggesting preferential translation (Figure 6B).

We selected the bottom, middle and top 200 genes as the repressed, resistant, and preferentially translated groups during $eIF2\alpha\sim P$, respectively (Appendix 1). Included among the top 200 genes, which corresponded to $\sim 15\%$ or greater increased association with ribosomes during stress, are *ATF4*, *ATF5* and *CHOP*, each of which were previously shown to be preferentially translated (4,10,120). To investigate categories of gene function, we performed an Ingenuity Pathway Analysis (IPA) on those members suggested to be preferentially translated during ER stress. The results indicate that this group encodes a diverse class of proteins, with the majority involved in gene expression, cellular assembly and organization, and molecular transport (Figure 6C).

By performing expression microarray analyses on both polysome fractions and whole cell RNA lysates, we were able to address the dynamic nature between transcriptional and translational regulation during ER stress. As mentioned previously, key regulators of the UPR are regulated both transcriptionally and translationally. For example, *ATF5* mRNA was shown to increase 3-fold, while increasing 33% towards higher polysomes (Figure 6D). Likewise, the levels of *CHOP* mRNA were increased 20-fold, and shifted 20% towards large polysomes. Interestingly, of the top 200 genes suggested to be preferentially translated during ER stress, only 36 (18%) also showed significant increases in mRNA levels ($p < 0.05$; Figure 6E), which is comparable to the 18% (4007/22862) of gene transcripts that were significantly increased in response to ER stress in our genome-wide analysis. This finding suggests the PERK pathway relies largely on translational control for regulation of many of its critical target genes.

The information encoded in the 5'-leaders of gene transcripts is suggested to be critical for their preferential translation in response to eIF2 α ~P. The composition of the 5'-leader sequences and the placement of uORFs for the top 200 gene transcripts shows enhanced association with large polysomes in response to ER stress, as illustrated in Appendix 1. The median value for leader length in nucleotides for preferentially translated mRNAs was 226 (+/- 10.6 SEM); resistant was 260 (+/- 14.8 SEM); and repressed was 199 (+/- 13.0 SEM), with a significant difference in the length of the 5'-leaders identified between the resistant and repressed groups (one-way ANOVA, $p = 0.004$) (Figure 6F).

As previously noted, uORFs have been shown to be critical for translational regulation and we hypothesized there may be an enrichment of uORFs in the preferentially translated cohort. However, an analysis of uORF frequency among groups failed to show a significant difference in the presence, number, or length of uORFs among the groups (Table 1). Of the 600 total transcripts analyzed, 271 (45%) possessed uORFs. This percentage is representative of previous studies reporting 35-50% of mouse and human transcripts contain uORFs (205,206). Furthermore, there was no significance difference in the GC composition among the predicted 5'-leaders of the mRNAs in the repressed, resistant, and preferentially translated groups (Table 1). The initiation codon context can be important for ribosome selection of a CDS (7,129), with the optimized sequence *gcc*(**A/G**)*cc*ATG(**G**), with the initiation codon (underlined) and purine residues at -3 and +4 (bold) being most critical. An alteration at either purine is suggested to reduce a strong initiation codon to adequate, and loss of both purines is suggested to render an initiation codon to a weak context. Among mRNAs suggested to be preferentially translated that contain a single uORF, 58% of the transcripts showed a stronger start codon context for the CDS as compared to the uORF (Table 1). By comparison those in the repressed group were significantly different with only 31% of

transcripts adopting this configuration (Chi-squared, $p = 0.01$). This suggests the initiation context of uORFs can be important for translational control during ER stress.

To validate the results of the translational microarray analysis, we performed qPCR analyses using RNA prepared from sucrose gradient fractions to measure specific examples of key regulatory genes that fell into each of the three categories. *ATF4* and *ATF5* mRNAs, both shown to be preferentially translated during ER stress, shifted 55 and 51% towards large polysomes, respectively (Figure 7A). The left side of the figure illustrates the levels of gene transcripts present in each sucrose gradient fraction, relative to an exogenous, polyadenylated *Luciferase* spike-in control mRNA. There were increased levels of *ATF4* and *ATF5* mRNAs in response to ER stress, along with a shift of the gene transcripts to the large polysome fractions. The right panels depict the percent of the *ATF4* and *ATF5* gene transcripts among the gradient fractions for each of the two conditions, therefore highlighting changes in ribosome association with these mRNAs independent of changes in total transcript levels (Figure 7A). After *ATF5*, the second largest shift towards polysomes during ER stress in our microarray analysis was *IBTK α* (Figure 6D, Appendix 1), which was confirmed by qPCR analysis (Figure 7A). *IBTK α* will be a focus of this chapter.

Among the resistant cohort, we verified minimal changes in large polysome association between the stressed and non-stressed conditions for *PPP1R15b* (*CReP*), a gene encoding the protein phosphatase regulatory subunit which constitutively targets PP1c to dephosphorylate eIF2 α ~P (Figure 7B). We found the mRNA encoding the 5'-cap-binding protein, eIF4e, to be shifted 23% away from large polysomes during ER stress (Figure 7C). Furthermore, the total levels of *eIF4e* mRNA was sharply reduced in the stress lysates (Figure 7C, left panel). This finding illustrates a dynamic coordination

between transcription and translation that can serve to dampen gene expression during ER stress.

Table 1. The 5'-leader characteristics for gene transcripts suggested to be preferentially translated, resistant, or repressed during ER stress.

| Characteristic | Preferential (top 200) | Resistant (middle 200) | Repressed (bottom 200) |
|--|-----------------------------------|-----------------------------------|-----------------------------------|
| 5'-Leader length (mean nts) | 225.7 | 260.2 | 199.8 |
| 5'-Leader length (median nts) | 201.5 | 212.5 | 143 |
| uORF frequency (%) | 38.5 | 48.5 | 48.5 |
| uORF length (mean nts) | 120.5 | 112.8 | 93.9 |
| CG content of 5'-leader (%) | 61 | 62 | 64 |
| Transcripts with optimal Kozak context for CDS (%) | 52 | 53 | 40 |
| Transcripts with uORF in poor Kozak context (%) | 58 | 61 | 31 |

For 5'-leader length, a One-way ANOVA reported a significant difference between groups ($p = 0.004$), with a Tukey's HSD *post hoc* test indicating a difference in leader length between the 'repressed' and 'resistant' groups. For uORF length, when multiple uORFs were present, the longest uORF was used in the analysis. A One-way ANOVA indicated no significant difference between groups ($p = 0.155$).

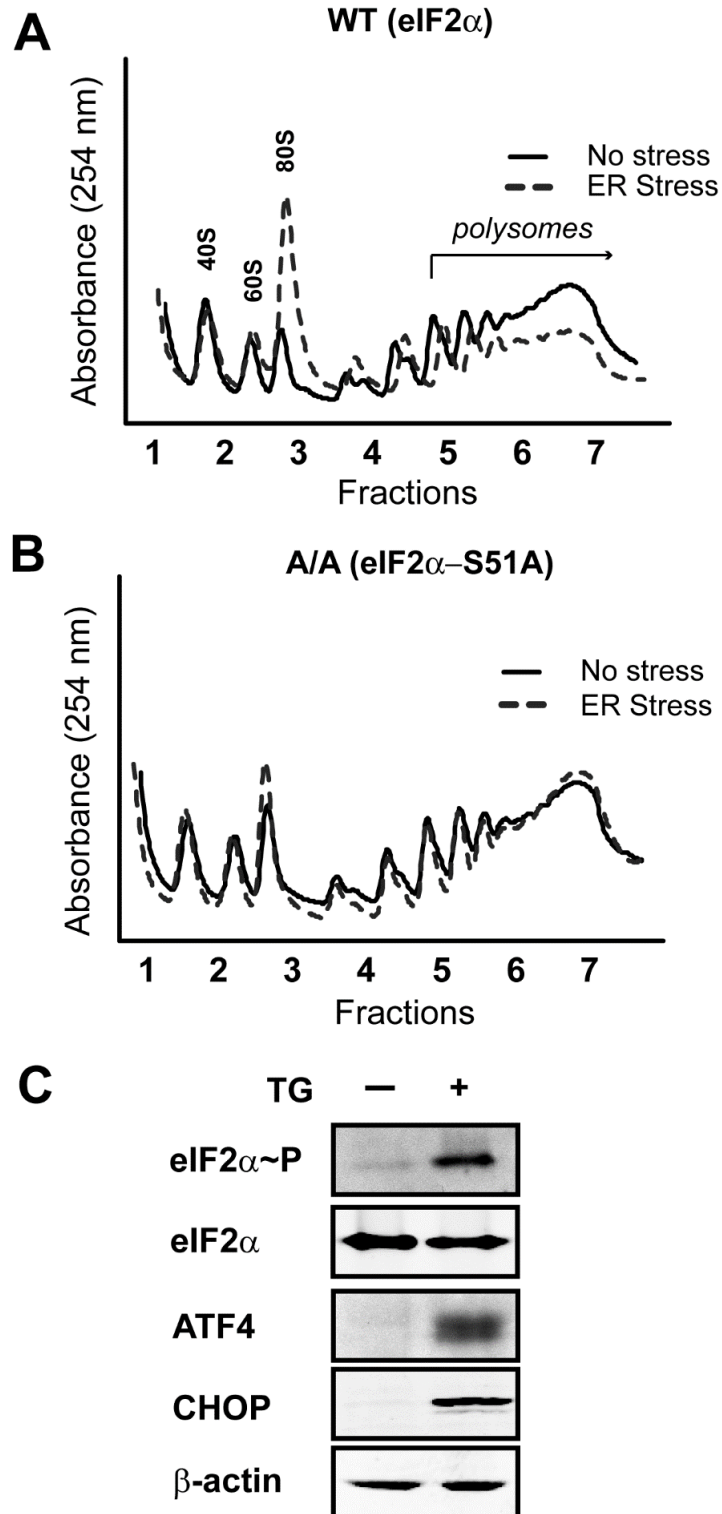


Figure 5. eIF2 α -P represses global translation initiation during ER stress.

Polysome profiling was carried out using wild-type (A) or eIF2 α -S51A (B) knock-in MEF cells treated with TG (ER stress) for 6 hours or no stress treatment. (C) Immunoblot

analysis of lysates prepared from wild-type MEF cells treated with TG for 6 hours (+), or no stress. The indicated proteins were measured using antibodies specific to each.

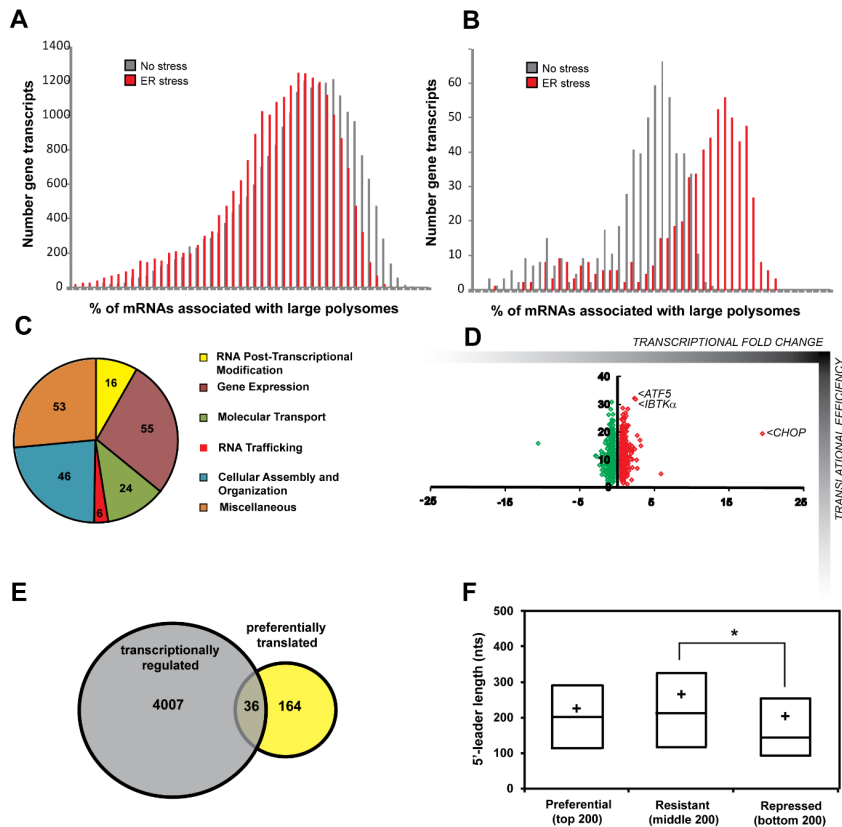


Figure 6. Genome-wide analyses of gene-specific translation during ER stress. (A)

Number of gene transcripts as defined by analysis of the 22,862 probe sets that are associated with the indicated percentage of large polysomes in wild-type MEF cells treated with TG for 6 hours or no stress. (B) Percentage association with large polysomes of the top 200 gene transcripts suggested to be preferentially translated in response to ER stress. (C) Pie chart representing the categories of molecular and cellular functions as determined by Ingenuity Pathway Analysis (IPA) of the top 200 genes suggested to be subjected to preferential translation. (D) Scatterplot illustrating the percent shift towards large polysomes during stress suggestive of translational control (y-axis) versus their relative mRNA fold changes in response to stress (x-axis, transcriptional control). (E) Venn diagram of the overlap between the total 4007 genes encoding mRNAs that were significantly increased in response to ER stress ($p < 0.05$) and the top 200 genes suggested to be preferentially translated during ER stress. (F)

Repressed genes encode mRNAs with significantly shorter 5'-UTRs than the stress-resistant cohort (one-way ANOVA with Tukey's HSD *post hoc* test, $p = 0.0042$). Lines of box-plot diagram illustrate 75th, 50th, and 25th percentile values, while the + symbol indicates the arithmetic mean.

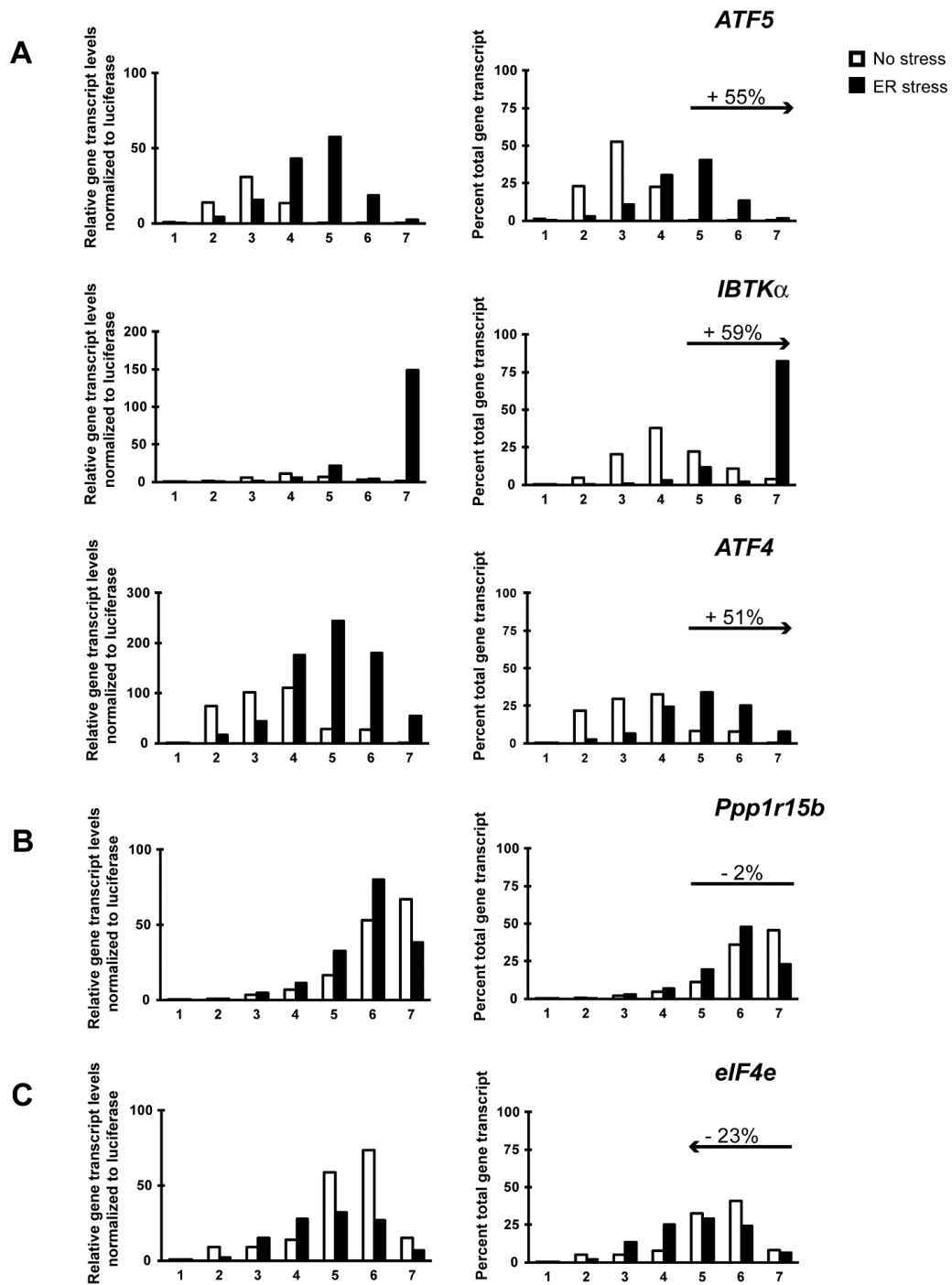


Figure 7. Changes in polysome association of gene transcripts suggest preferential, resistant, or repressed translation during ER stress.

Fractions were collected by sucrose gradient analyses of lysates prepared from wild-type MEF cells treated with TG for 6 hours (ER stress) or no stress. Relative levels

of the indicated gene transcripts were then determined by qPCR for each fraction (left column), with preferentially translated gene transcripts in response to ER stress (A), resistant (B), and repressed (C). For these values, gene expression was normalized to an exogenous polyadenylated *Luciferase* spike-in mRNA control. The right column represents the percentage of the total gene transcripts in each of the seven fractions prepared from the TG-treated and non-stressed cells. The percent changes in association with large polysomes (fractions 5-7) in response to ER stress is indicated for each gene transcript panel. For example, *ATF5* showed a 55% increase in transcripts levels into fractions 5-7 during ER stress compared to no-stress.

3.2 eIF2 α -P leads to translational expression of *IBTK α* mRNA.

Two transcripts can be generated from the mouse *IBTK* gene, designated α and γ , by a mechanism suggested to involve transcription from different promoters (207). The transcript that we measured in the microarray and qPCR analyses is the longer version, *IBTK α* , which is 5679-nucleotides in length with an encoded protein of 150 kDa suggested to be widely expressed among tissues (207). To define the 5'-leader of the *IBTK α* transcript, we performed a 5'-RACE to determine the transcription start site using RNA that was isolated from wild-type MEF cells in the absence and presence of ER stress. The 5'-leader of *IBTK α* is 588 nucleotides in length and encodes four uORFs. A phylogenetic analysis among mammals illustrates a high level of conservation for both leader length and placement of the uORFs, with uORFs 1 and 2 being conserved among each of the orthologues.

To determine whether the 5'-leader of *IBTK α* confers preferential translation in response to eIF2 α -P, the cDNA segment encoding the 5'-leader of the mouse *IBTK α* mRNA was inserted between a constitutive *TK* promoter and a firefly luciferase reporter gene. The resulting *P_{TK}-IBTK α -Luc* plasmid was transfected into wild-type MEF cells,

and these cells were exposed to TG or left untreated. In response to ER stress, there was a ~2.5 fold induction of luciferase activity despite minimal changes in mRNA levels (Figure 8C). Importantly, when this same reporter construct was analyzed in MEF cells expressing eIF2 α -S51A, which cannot be phosphorylated by PERK, this induction of luciferase expression was abolished (Figure 8C). As expected, there were no significant changes in the levels of the reporter transcripts in these MEF cells and treatment conditions. Moreover, 5'-RACE assays were performed on the *IBTK α -Luc* construct to rule out the possibility of truncation or alternative splicing events in the 5'-leader. These results suggest that *IBTK α* mRNA is preferentially translated in response to eIF2 α ~P and ER stress. To address the mechanism underlying preferential translation of *IBTK α* in response to eIF2 α ~P, we generated multiple mutant constructs of the wild-type *P_{TK}-IBTK α -Luc* reporter. An illustration of these constructs, along with their luciferase activity and mRNA levels in response to TG or no stress treatment, are depicted in Figure 9. To address whether translation of *IBTK α* occurs by cap-dependent scanning, we generated a stem-loop construct in which a highly-structured palindromic sequence with a high free energy ($\Delta G = -41$ kcal/mol) was inserted 30 nucleotides downstream of the cap structure (construct 2). This highly structured stem-loop sequence, which was shown previously to impede ribosome scanning (4), caused a significant reduction in basal luciferase expression and a loss of stress induction. There were no significant changes in the mRNA levels among these reporter constructs and those that followed.

To further dissect the mechanism of regulation, *AUG* start codons for the uORFs, both individually and in combination, were mutated to non-initiating *AGG* codons. Mutating the start codons for each of the four uORFs led to a 15-fold increase in luciferase activity independent of stress conditions (Figure 9, construct 3). Interestingly, the same level of enhanced reporter activity was observed when only the start codon for

uORF1 was altered (construct 4), indicating that uORF1 is a major repressive element for translation of the *IBTK α* downstream CDS. Conversely, mutating the start codon of uORF2 resulted in a modest 5-fold increase in basal levels of luciferase expression (construct 5), whereas uORFs 3 and 4 were wholly dispensable (constructs 6 and 7). We further showed that uORFs 1 and 2 alone were sufficient to facilitate the 3-fold stress induction observed in the wild-type construct (construct 7).

Previous genome-wide ribosome footprinting studies in human and murine cell lines reported initiating ribosomes in *IBTK α* at uORFs 1, 2, and a non-canonical *uCUG* start codon at position -468 nucleotides upstream of the CDS start codon (208,209). We addressed whether this latter *uCUG* had any functional role in translation during basal and stress conditions by mutating the upstream *CUG* to a *CGG* in the reporter construct. There was no observable difference between wild-type and the mutant $\Delta uCUG$ luciferase expression values, indicating that this non-canonical start codon does not have a role in *IBTK α* translational control (Figure 9, construct 8). Together these studies suggest that uORF1 and uORF2 can serve as repressing elements in *IBTK α* translation, with uORF1 being predominant. Phosphorylation of eIF2 α is suggested to lead to a partial bypass of these repressing uORFs.

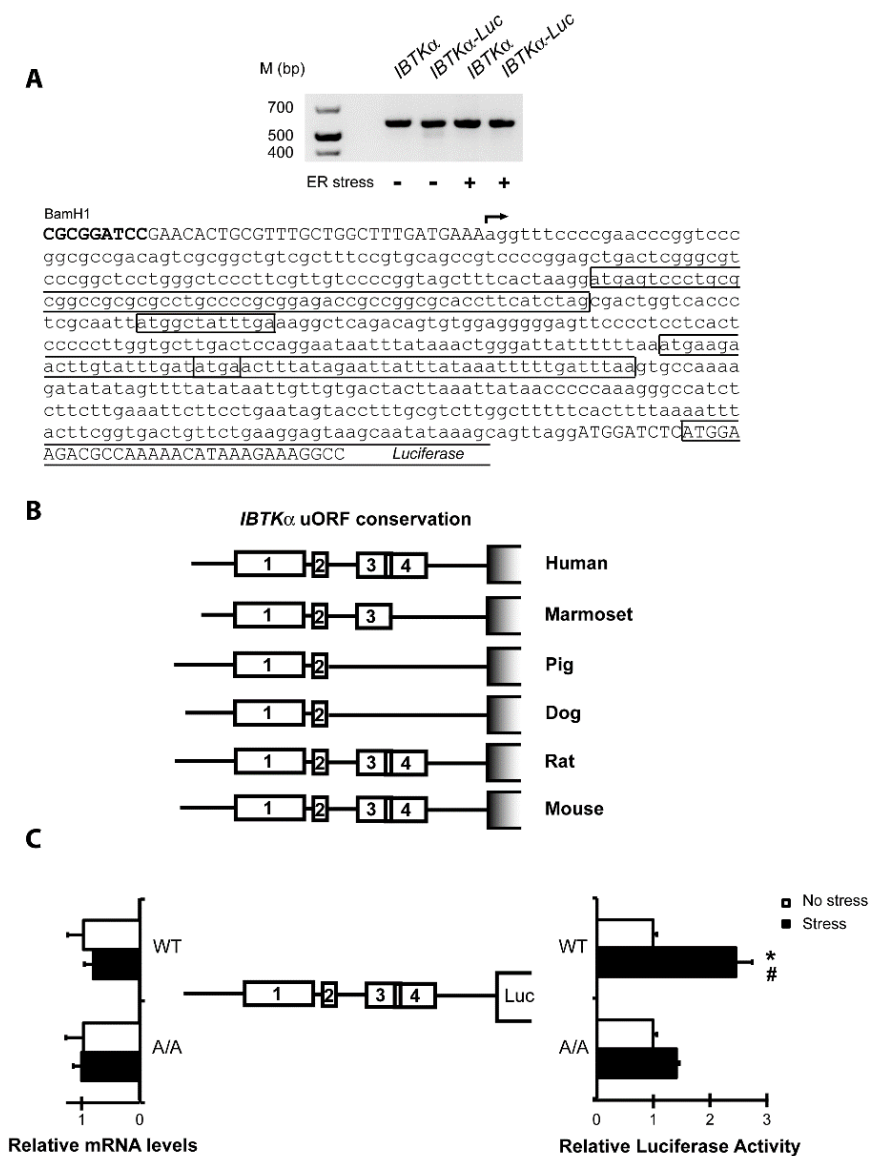


Figure 8. The 5'-leader of the *IBTK α* gene transcript confers preferential translation in response to eIF2 α ~P. (A) A 5'-RACE was performed to establish the transcriptional start site for *IBTK α* in the presence and absence of stress. The arrow indicates the transcriptional start site, and each of the four uORFs present in the *IBTK α* 5'-leader are boxed. 5'-RACE assays were performed using RNA containing endogenous transcript and the luciferase translational reporters prepared from cells treated with TG or no stress. The image of the cDNA products that were analyzed by

agarose gel electrophoresis is presented above the *IBTK α* sequence. (B) Schematic of phylogenetic conservation of uORFs in the 5'-leader of the *IBTK α* mRNA among different mammalian species. (C) *IBTK α* translational control was measured by a dual luciferase assay. The P_{TK}-*IBTK α* -*Luc* reporter, which contains the *IBTK α* leader sequence, and a control Renilla-luciferase plasmid, were introduced into wild-type or eIF2 α -S51A MEF cells, and treated with TG or no stress. Three independent experiments were conducted for each measurement, and relative values are represented, with the S.D. indicated. In parallel, the levels of the *IBTK α* -*Luc* mRNA were measured by qPCR, and relative values are presented with error bars representing the S.D. The “*” indicates a significant difference in wild-type MEF cells in response to ER stress, and “#” among wild-type and eIF2 α -S51A cells during TG treatment (p < 0.001).

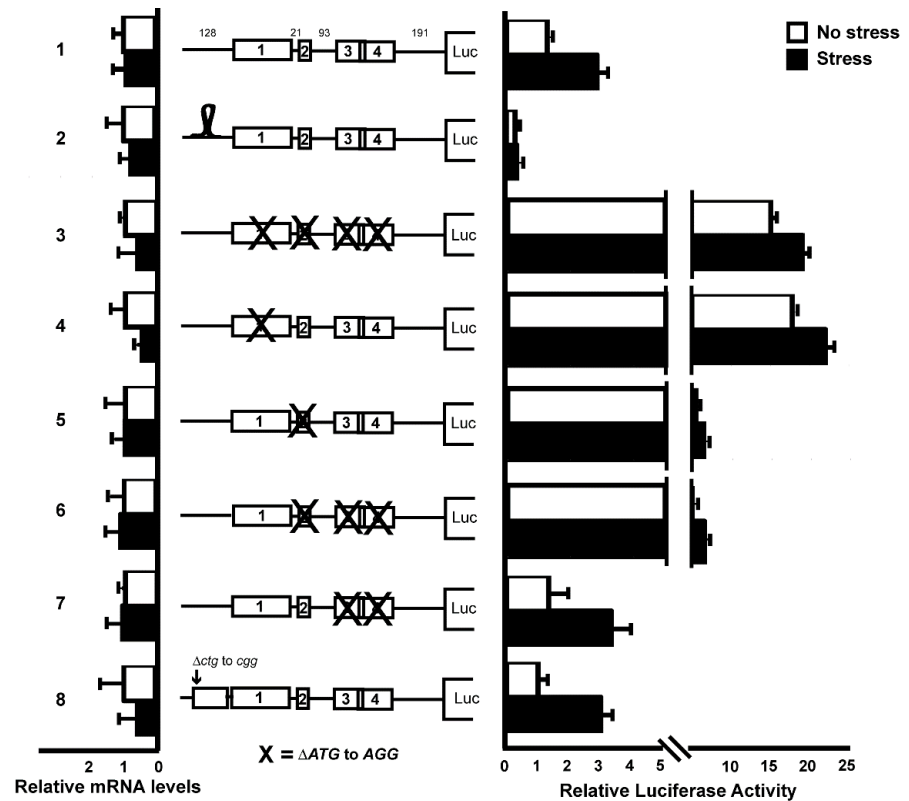


Figure 9. Translation of *IBTKα* mRNA is regulated by a scanning model involving two inhibitory upstream ORFs. Wild-type and the depicted mutant versions of the P_{TK} -*IBTKα*-Luc reporter were analyzed in MEF cells subject to TG or no stress treatment. The 5'-leader of the *IBTKα* mRNA is illustrated upstream of the firefly luciferase reporter. Boxes indicate the uORFs 1, 2, 3, and 4, and the numbers in the wild-type leader depiction represent the number of nucleotides separating the ORFs. Relative luciferase activities are shown following ER stress, or no stress treatment, with error bars indicating the S.D. On the left side of the panel are the relative levels of the reporter mRNAs as measured by qPCR. The stem-loop structure ($\Delta G = -41$ kcal/mol) adjacent to the 5'-end of the reporter is illustrated, and the X indicates mutations of the start codon for the indicated uORF.

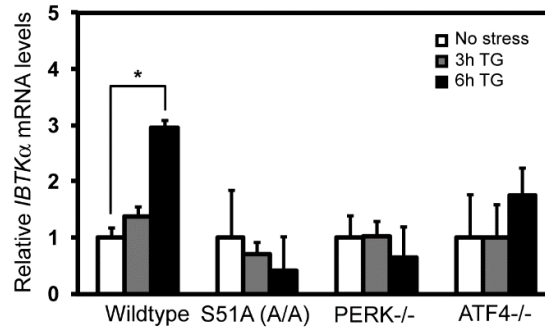
3.3 Induction of *IBTK α* gene expression requires PERK in both cultured cell and animal models of ER stress

Transcriptional induction is also central for expression of PERK targets *ATF4*, *CHOP* and *ATF5* in the UPR. To determine whether *IBTK α* mRNA is increased by PERK signaling, we measured *IBTK α* transcripts in wild-type and mutant MEF cells treated with TG, or not subjected to stress. There was a 3-fold increase in the amount of *IBTK α* mRNA ($p = 0.05$) in the wild-type cells in response to ER stress. Importantly, this stress-responsive increase in *IBTK α* mRNA was abrogated in eIF2 α -S51A, *PERK*^{-/-}, and *ATF4*^{-/-} mutant cell lines (Figure 10A). These results suggest that in addition to preferential translation, the PERK/eIF2 α -P/ATF4 pathway facilitates increased *IBTK α* mRNA levels in response to ER stress.

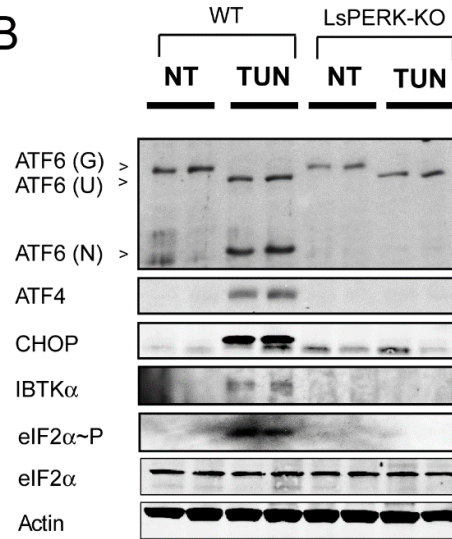
We further addressed the requirement of PERK for *IBTK α* induction during ER stress in a mouse model system. For this, liver-specific knockout (LsPERK-KO) mice and their wild-type counterparts were subjected to a single intraperitoneal injection of tunicamycin. Tunicamycin inhibits N-linked glycosylation and as a result acts as a potent inducer of ER stress. We previously reported that loss of PERK in livers exposed to tunicamycin disrupted liver homeostasis and increased apoptosis (97). There was a significant induction of eIF2 α -P, ATF4, CHOP and *IBTK α* protein 6 hours following treatment of the ER stress agent in the wild-type mice (Figure 10B). Furthermore, there was also a substantial increase in cleavage and release of ATF6 N-terminal protein, a hallmark of UPR activation. As expected, the LsPERK-KO mice failed to show an increase in expression of *ATF4* and *CHOP* or ATF6 activation in response to the tunicamycin treatment. Importantly, induction of the *IBTK α* protein following tunicamycin injection was also undetected upon loss of PERK (Figure 10B). We also measured *IBTK α* mRNA levels in livers of the wild-type and LsPERK-KO mice treated with

tunicamycin. There was a significant ~ 3 fold increase ($p = 0.005$) of *IBTK α* mRNA during ER stress that was completely abrogated in the LsPERK-KO samples (Figure 10C). Consistent with prior reports, PERK was also required for increased levels of *ATF4* mRNA in response to tunicamycin treatment. These results indicate that PERK signaling facilitates increased *IBTK α* expression in response to ER stress in both cultured cells and mouse model systems.

A



B



C

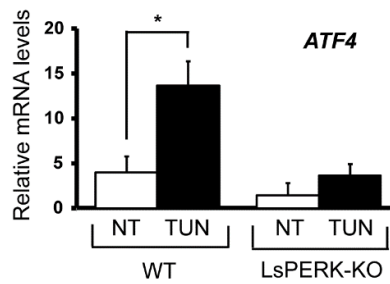
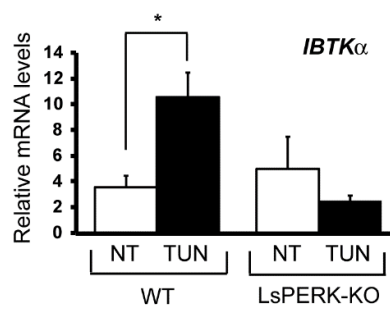


Figure 10. Enhanced *IBTK α* gene expression requires PERK in both cultured cell and animal models of ER stress. (A) *IBTK α* mRNA levels were measured by qPCR in wild-type and mutant MEF cells that were treated with TG for 3 or 6 hours, or no stress (0). The error bars indicate the S.D., and the “*” indicates a significant enhancement in transcript levels in response to the ER stress ($p < 0.05$). (B) Wild-type and liver specific PERK knock-out (LsPERK-KO) mice were subjected to a single i.p. injection of tunicamycin or saline control and sacrificed after 6 hours. Lysates were prepared and immunoblot analyses carried using antibodies against the indicated proteins (C). Alternatively, RNA was prepared from the LsPERK-KO livers and qPCR analyses were carried out to measure *IBTK α* or *ATF4* mRNA levels. The error bars indicate the S.D., and the “*” indicates a significant increase in transcript levels in response to the ER stress ($p < 0.005$).

3.4 Loss of *IBTK α* expression results in lowered cell viability

To address the importance of *IBTK α* in cell viability, we used shRNA and a lentiviral delivery system to knockdown expression of *IBTK α* in MEF cells. We present analysis using lentivirus targeted against *IBTK α* (Sigma TRCN0000088505), with a second shRNA (Sigma TRCN0000088503) showing similar results. There was a significant depletion of *IBTK α* mRNA in MEF cells compared to the control scrambled shRNA (Figure 11A). Knockdown of *IBTK α* led to a reduced number of cultured MEF cells compared to the control cells when plated at either high density or low density in the medium (Figure 11B). The lowered cell number was not the result of reduced cell division as measured by EdU incorporation (Figures 11C and D). Rather there was a sharp enhancement of cleaved caspase 3/7 that occurred in the absence of stress treatment (Figure 11E, left panel). There was also enhanced caspase 3/7 when *IBTK α* was reduced using shRNA in other cell types, including HepG2 human hepatocytes

(Figure 11E, right panel), supporting the idea that IBTK α performs pro-survival functions in both mouse and human cell types.

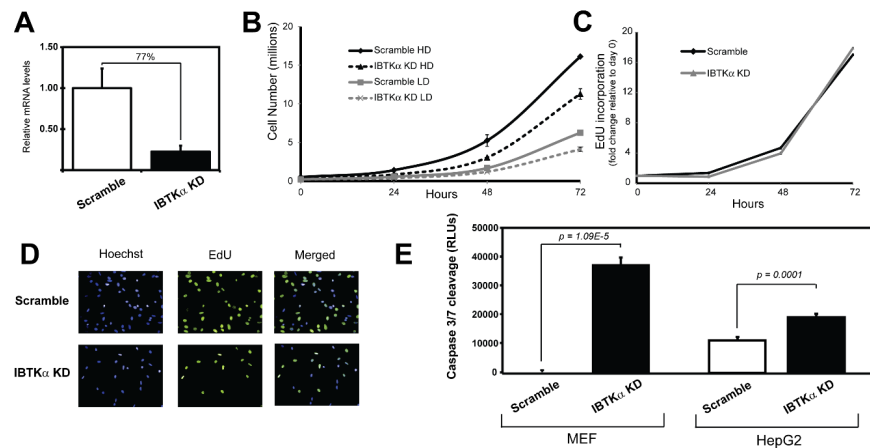


Figure 11. Knockdown of *IBTKα* lowers cell viability and increase caspase 3/7 cleavage.

shRNA against *IBTKα* and a lentiviral delivery system were used to knockdown *IBTKα* expression in wild-type MEF cells. (A) qPCR measurements of *IBTKα* mRNA in knockdown cells (KD) and control shRNA expressing cells (scrambled). (B) *IBTKα*-KD and control MEF cells expressing scrambled shRNA were plated in culture dishes at low density or high density. Cell numbers were determined upon culturing for up to 72 hours. (C) Measurements of cell proliferation by EdU incorporation during cell culture normalized to day 0. (D) Images of Hoeschst stained, EdU stained, and merged *IBTKα*-KD and scrambled control cells. (E) Measurements of caspase 3/7 cleavage in MEF cells and HepG2 cells expressing *IBTKα*-shRNA (*IBTKα*-KD) or scramble shRNA.

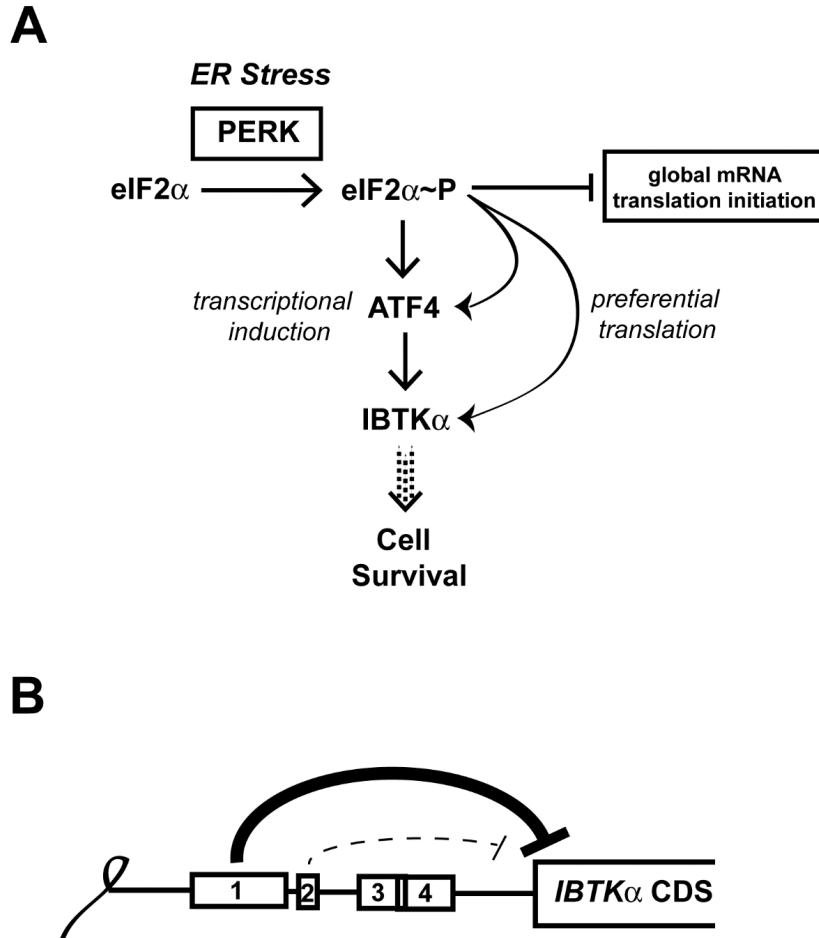


Figure 12. Model depicting *IBTK α* transcriptional and translational regulation during PERK induced *eIF2 α ~P*. (A) During ER stress, the PERK arm of the UPR directs phosphorylation of *eIF2 α* , resulting in a global dampening of translation initiation. During this decrease in global mRNA translation, ATF4 and its downstream target *IBTK α* are suggested to be both transcriptionally induced and subject to preferential translation, which collectively can determine cell viability during ER stress. (B) The inhibitory uORFs 1 and 2 serve to repress *IBTK α* translational expression. uORF1 is a major inhibitory element, with uORF2 serving a secondary role. In response to ER stress, *eIF2 α ~P* overcomes these inhibitory elements to translate the downstream *IBTK α* CDS.

CHAPTER 4. RESULTS: BYPASS OF A NONCANONICAL uORF REGULATES TRANSLATION OF *EPRS* mRNA

4.1 eIF2 α -P leads to translation expression of *EPRS* mRNA

The microarray study previously discussed in this thesis identified gene transcripts suggested to be preferentially translated in mouse embryonic fibroblast (MEF) cells following a 6 hour treatment with thapsigargin, a potent inducer of ER stress, which results in a global repression in translation initiation (Figure 9, 13A). A 6 hour treatment was selected as the optimum time for the transcriptional induction of UPR genes, many of which we proposed to be subject to preferential translation. The mRNAs were separated by sucrose gradient analyses to yield three fractions, those transcripts associated with large polysomes (≥ 4 ribosomes per mRNA), those associated with monosome, disomes, or trisomes, and those fractionated at the top of the gradient with free ribosomes. Transcripts showing significantly increased association with large polysomes upon ER stress ($>10\%$ increase to large polysomes) were categorized as being candidates for preferential translation. Note that these are measured as changes in the percent association with large polysomes for the total transcripts encoded for each gene, and would not include induced total mRNA levels that can occur during ER stress. Using this criteria, a gene suggested to have one of the highest levels of preferential translation upon ER stress (33% increase in large polysome association) was *EPRS*, which encodes the bifunctional Glutamyl-Prolyl tRNA Synthetase. We confirmed this finding by using qPCR measurements of mRNAs from multiple sucrose gradient analyses of multiple biological replicates. WT MEF cells were treated for 6 h with 1 μ M TG or no stress. Following the treatment, cells were cultured in the presence of cycloheximide for 10 mins, rinsed with ice cold PBS containing cycloheximide, lysed and subject to sucrose gradient ultracentrifugation. RNA was then isolated, cDNA generated,

and qPCR performed to quantify the amount of transcript in each fraction compared to an exogenous spike-in *Luciferase* mRNA control. During no stress conditions, the majority of *EPRS* mRNA resides in fractions 3-5, corresponding to monosomes, disomes and trisomes (Figure 13B). Conversely, during conditions of ER stress, the majority of *EPRS* transcript is associated with fractions 6 and 7 -- corresponding to the large polysomes (Figure 13B). Taken together these data suggest *EPRS* mRNA is preferentially translated during PERK activation of eIF2 α -P.

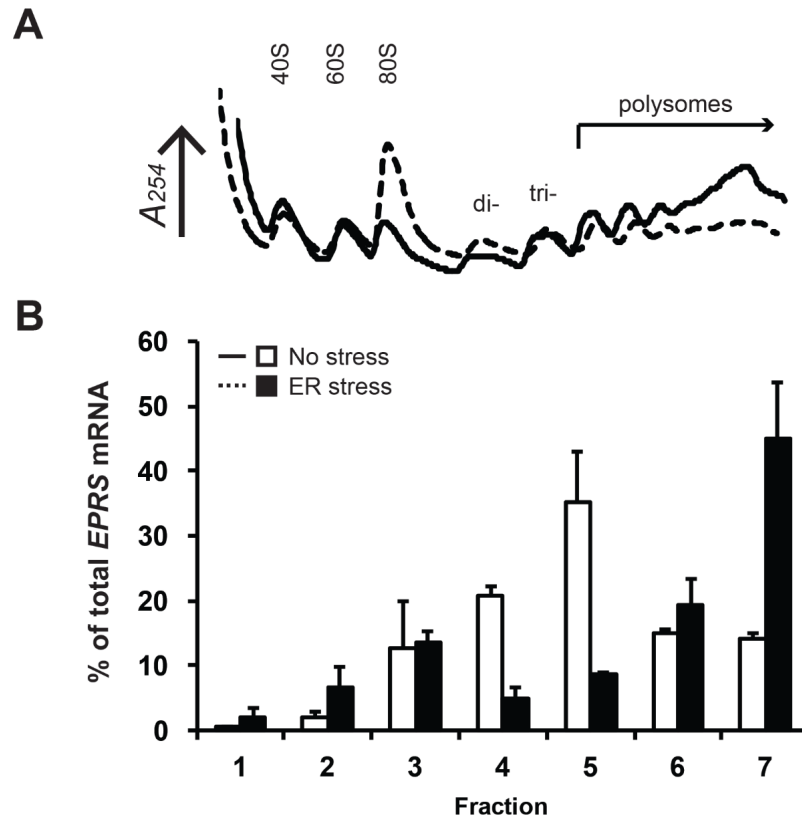


Figure 13. *EPRS* mRNA associates with large polysomes during ER stress. (A)

Polysome profiling was carried out using wild-type MEF cells treated with TG for 6 h or no stress treatment. (B) Changes in polysome association of *EPRS* mRNA during ER stress. Fractions were collected by sucrose gradient analyses of lysates prepared from wild-type MEF cells treated with TG for 6 h or no stress. For qPCR measurements, gene expression was normalized to an exogenous polyadenylated *Luciferase* spike-in mRNA control. Fractions 5-7 correspond to mRNA association with large polysomes.

4.2 A non-canonical *CUG* serves to initiate translation of an inhibitory uORF in the *EPRS* transcript

To define the 5'-leader of the mouse *EPRS* transcript, we performed a 5'-RACE to determine the transcription start site using RNA that was isolated from wild-type MEF cells in the absence and presence of ER stress. The 5'-leader of *EPRS* is 155

nucleotides in length and lacks any upstream *AUG* codons (Figure 14A). To determine whether the 5'-leader of *EPRS* confers preferential translation in response to eIF2 α -P, the cDNA segment encoding the 5'-leader of the mouse *EPRS* mRNA was inserted between a constitutive *TK* promoter and a firefly luciferase reporter gene. The resulting *P_{TK}-EPRS-Luc* plasmid was transfected into wild-type MEF cells, and these cells were exposed to TG or left untreated. In response to ER stress, there was a 2-fold induction of luciferase activity despite minimal changes in mRNA levels (Figure 14B). Importantly, when the same reporter construct was analyzed in MEF cells expressing eIF2 α -S51A, which cannot be phosphorylated by PERK, this induction of luciferase expression was abolished (Figure 14B). As expected, there were no significant changes in the levels of the reporter transcripts in these MEF cells and treatment conditions. Moreover, 5'-RACE assays were performed on the *EPRS-Luc* construct to rule out the possibility of truncation or alternative splicing events in the 5'-leader (Figure 14A). These results suggest that *EPRS* mRNA is preferentially translated in response to eIF2 α -P and ER stress.

To address the mechanism underlying preferential translation of *EPRS* in response to eIF2 α -P, we performed a phylogenetic analysis looking for conserved residues in the 5'-leader. From this analysis, we identified three upstream *CUG* codons conserved in mammals. *CUG* codons have been shown to serve as non-canonical start codons during translation initiation of mammalian mRNAs (14,210), and a previous ribosome footprinting study in mouse embryonic stem cells reported translation initiation at the *CUG* - 54 nucleotides upstream of the *EPRS* CDS start codon (208). To investigate if the reading frame containing these three u*CUG*s could facilitate translation initiation in our heterologous system, we generated fusion Luc constructs to the u*CUG* reading frame (denoted reading frame -1) such that the start *AUG* of the *Luciferase* CDS

has been deleted. We also generated a fusion Luc construct with the other alternate reading frame (denoted reading frame -2) to investigate any possible initiate event occurring in that frame as well. An illustration of these reporter constructs is depicted in Figure 15. As a result, any protein expression is presumed to arise from initiation of an uCUG which is now in frame with the CDS. When the uCUGs, containing the codon uCUG2 identified in earlier cited ribosome profiling study (208), was fused in frame with luciferase, we observed a 14 fold increase in luciferase expression as compared to the fusion construct with reading frame -2 (Figure 15A). To further validate if uCUG2 can facilitate translation initiation, we mutated the uCUG2 in the fusion construct to an AAA, which abolished the levels of luciferase protein expression (Figure 15B). Moreover, as expected, when the uCUG2 was mutated to a canonical AUG start codon in optimal Kozak context, expression levels increased ~5.5 fold as compared to the wild-type fusion construct (Figure 15B). These data indicate that uCUG2 is translated and suggests this uORF can serve to repress downstream *EPRS* expression by being both overlapping and being out-of-frame with the *EPRS* CDS. During stress conditions, these results suggest a bypass of this noncanonical CUG start codon and translation initiation at the downstream *EPRS* CDS start codon instead (see Figure 18).

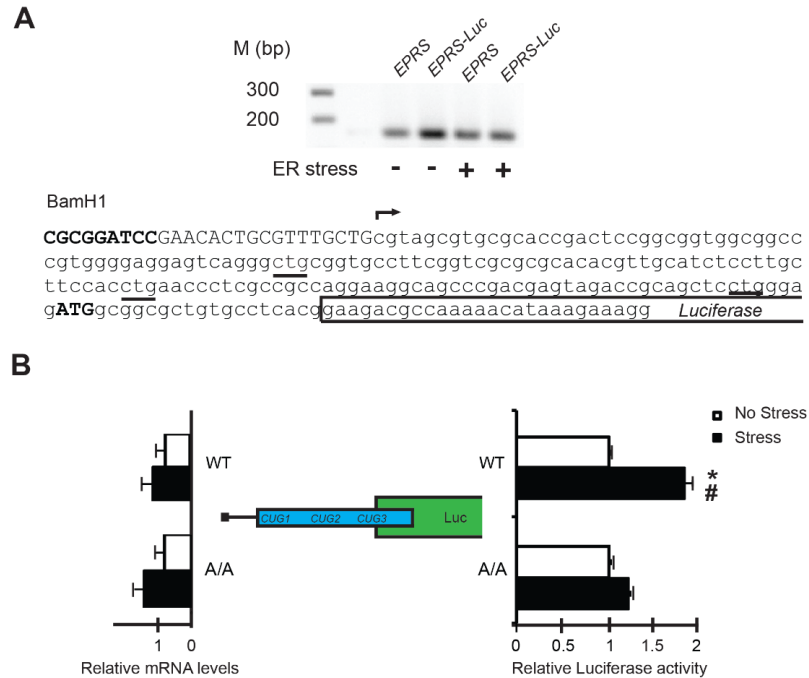


Figure 14. The 5'-leader of *EPRS* mRNA confers preferential translation during $eIF2\alpha\sim P$. (A) 5'-RACE was performed to establish the transcriptional start site for *EPRS* mRNA in the presence and absence of stress. The arrow indicates the transcriptional start site and the sequence of the 5'-leader of *EPRS*, which was fused to the firefly luciferase coding sequence (boxed) in the reporter construct. 5'-RACE assays were performed using RNA-containing endogenous transcript and the luciferase translational reporters prepared from cells treated with TG or no stress. The image of the cDNA products that were analyzed by agarose gel electrophoresis is presented above the *EPRS* sequence. (B) *EPRS* translational control was measured by a dual luciferase assay. The P_{TK} -*EPRS*-*Luc* reporter, which contains the murine *EPRS* leader sequence, and a control Renilla luciferase plasmid, were introduced into wild-type or $eIF2\alpha$ -S51A MEF cells and treated with TG or no stress. Three independent experiments were conducted for each measurement, and relative values are represented, with the SD indicated. The asterisk indicates a significant difference in wild-type MEF cells in

response to ER stress, and the pound sign (#) between wild-type and eIF2 α -S51A cells during TG treatment ($p < 0.001$).

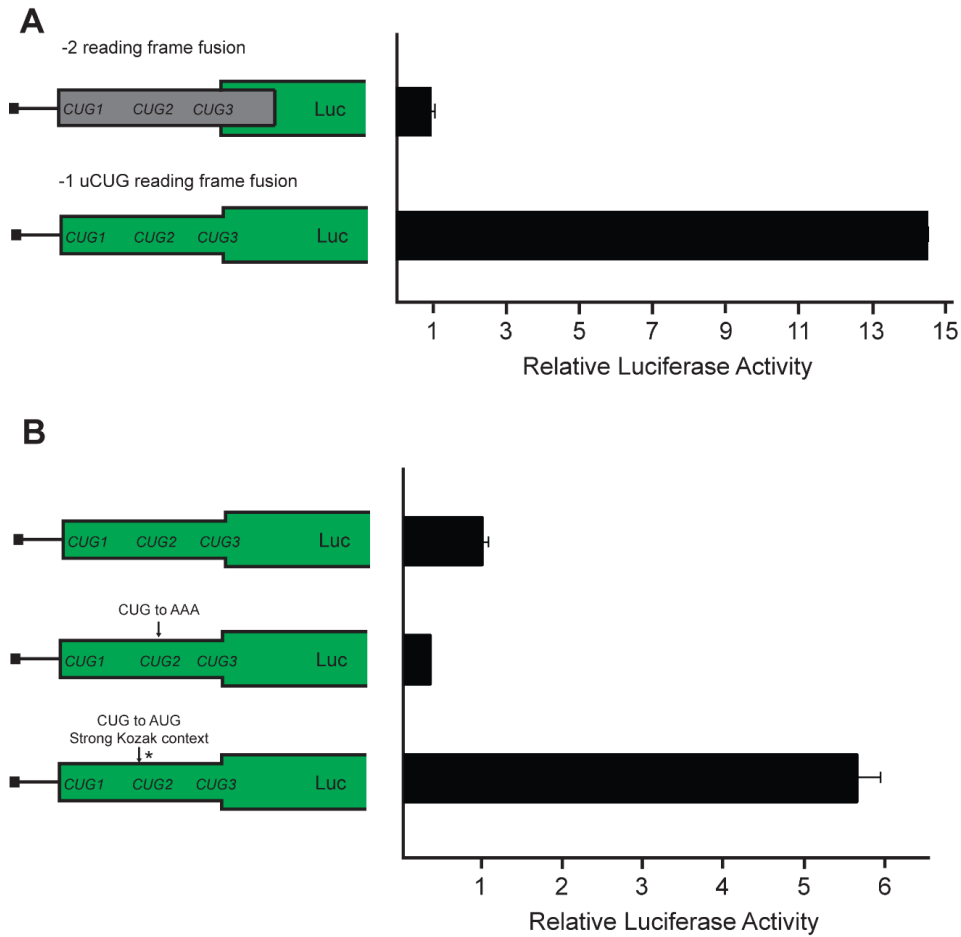


Figure 15. An upstream *CUG* in the *EPRS* 5'-leader serves as a non-canonical initiation codon for mRNA translation. (A) The two alternate reading frames with the *EPRS* ORF were fused in frame with a P_{TK} -*EPRS-Luc* reporter in which the *AUG* start codon for the *Luciferase* CDS was deleted. These constructs and a control *Renilla* luciferase plasmid were introduced into MEF cells to investigate levels of translation initiation and subsequent luciferase protein expression. (B) A P_{TK} -*EPRS-Luc* construct was designed in which upstream *CUG2* was fused in frame with the *Luciferase* CDS missing the *AUG* start codon. Site-directed mutagenesis was used to mutate the WT *CUG* fusion construct to an *AAA* (middle) and *ATG* in optimal Kozak context (bottom). Levels of protein expression were also monitored by a dual luciferase assay.

4.3 Translation control of *EPRS* during treatment with the drug Halofuginone

Halofuginone (HF), a drug currently in phase II clinical trials for the treatment of fibrotic disease and solid tumors (identified: NCT00064142), has recently been shown to confer surgical stress resistance in an animal model by a mechanism requiring the eIF2 α kinase GCN2 (211). HF competes with proline for the active site of EPRS, leading to an accumulation of uncharged tRNA and the activation of the GCN2/eIF2 α ~P/ATF4 pathway. Dietary restriction has been associated with an improved clinical outcome prior to an ischemic event in both animal and clinical models. The pharmacological induction of the GCN2/eIF2 α ~P/ATF4 pathway by HF offers the exciting potential of conferring pre-surgical stress resistance using a pharmaceutical. We determined that *EPRS* is preferentially associated with large polysomes upon ER stress and that the 5'-leader of the *EPRS* gene transcript confers translational control to a luciferase reporter genes, suggesting preferential translation of *EPRS* by eIF2 α ~P. As a result, we proposed that HF treatment would lead to the enhanced expression of its target substrate EPRS. To first examine the impact of HF treatment on eIF2 α ~P and global translation initiation, wild-type MEF cells were treated with 25 nM HF for 6 h or no treatment. HF treatment substantially reduced polysomes with an accumulation of the 80S monosome peak, indicative of eIF2 α ~P-induced defect in global translation initiation (Figure 16A). The biological implications of this during preconditioning is that, upon ischemic reperfusion, HF would induce eIF2 α ~P providing the benefits of target UPR genes important for stress remediation. Coincident with the induction of the UPR, the increase in EPRS protein levels would quickly alleviate the toxicity associated with the drug treatment.

To further address if *EPRS* mRNA is subject to translational control during HF treatment, wild-type and eIF2 α -S51A MEF cells were transfected with the *P_{TK}-EPRS-Luc* reporter for 24h, and treated with 25 nM HF for 12 hrs or left untreated. Both cell types

were also treated with 0.1 μ M TG or left untreated as a positive control for the 5'-mediated preferential translation during eIF2 α -P. In the wild-type MEF cells, both HF and TG treatment resulted in a 2.5 fold induction of EPRS-Luc expression (Figure 16B). Importantly, this increase in *EPRS-Luc* mRNA translation was absent in the alanine mutant (Figure 16B). We conclude that translation of *EPRS* is enhanced in response to different stress conditions, including that triggered by HF.

To examine the role of the ISR on cell fate, we treated WT and *GCN2*^{-/-} MEF cells with increasing doses of HF for 6 hrs, then allowed the cells to recover for 18 h in fresh media prior to measuring viability. From this analysis, we observed a sharp decrease in viability in the *GCN2*^{-/-} cells compared to their wild-type counterparts. This difference was most notable at the 12.5 nM treatment, at which we observed an over 20% decrease in viability in the *GCN2*^{-/-} cells compared to wild-type (Figure 17A). These results suggest that GCN2 and translational control are paramount to cell survival during HF treatment.

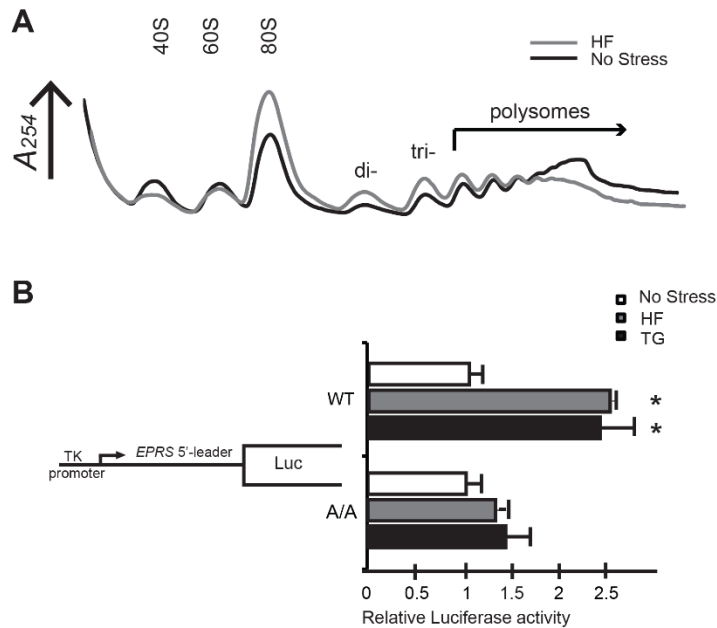


Figure 16. HF treatment reduces large polysomes and induces the 5'-mediated preferential translation of *EPRS* mRNA. (A) Polysome profiling was carried out using MEF cells treated with 25 nM HF for 6 hrs or untreated, (B) *EPRS* translational control was measured by a dual luciferase assay. The P_{TK} -*EPRS*-*Luc* reporter, which contains the murine *EPRS* leader sequence, and a control Renilla luciferase plasmid, were introduced into wild-type or eIF2 α -S51A MEF cells and treated with HF, TG or no stress. Three independent experiments were conducted for each measurement, and relative values are represented, with the SD indicated. The asterisk indicates a significant difference in wild-type MEF cells in response to ER stress ($p < 0.0001$)

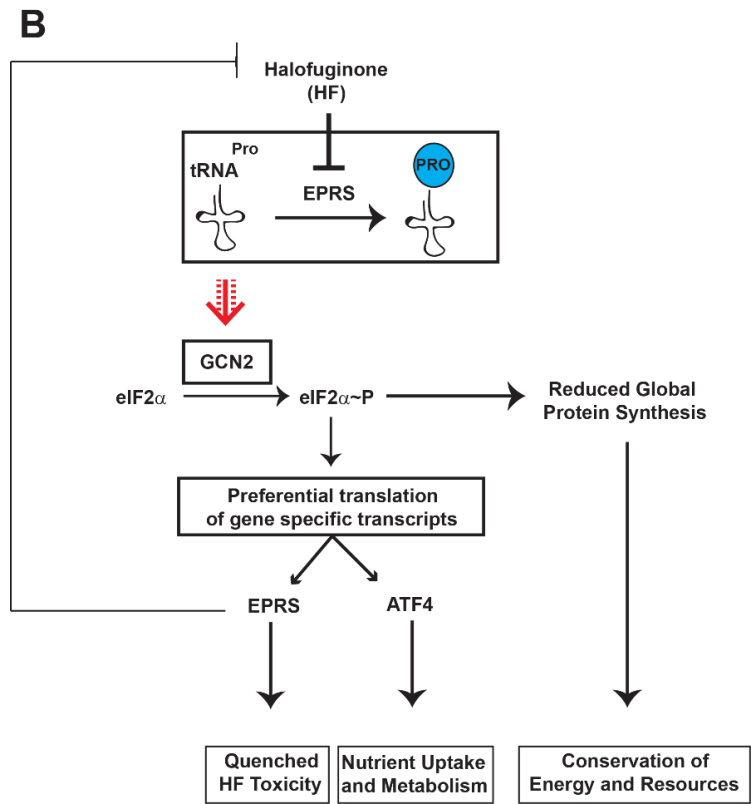
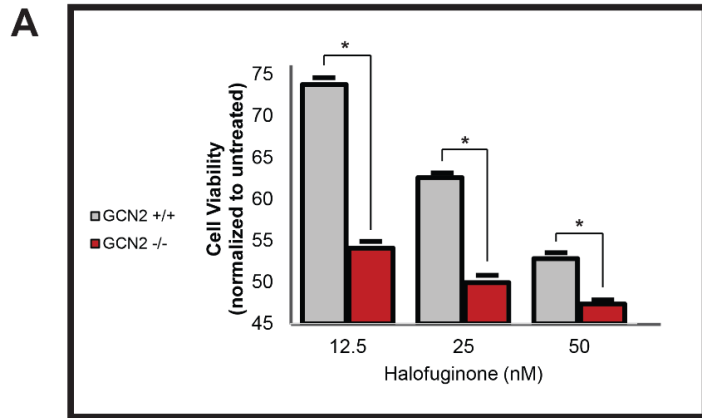


Figure 17. GCN2 confers protection against HF-induced toxicity through general and gene-specific translation control. (A) Cell viability of WT and *GCN2*^{-/-} MEF cells treated with HF for 6 hrs or untreated as measured by MTT assay. (B) Model depicting gene regulation downstream of the eIF2 kinase GCN2 during HF treatment. During the accumulation of uncharged prolyl-tRNA, activated GCN2 phosphorylates eIF2 α and decreases global mRNA translation initiation. Coincident with a decrease in overall translation, mRNA encoding ATF4 is subject to preferential translation, ultimately leading

to an increase in ATF4 downstream targets central to stress remediation. Also subject to preferential translation during eIF2 α -P is mRNA encoding EPRS. During HF treatment, *EPRS* is preferentially translated and the resulting increase in its expression is suggested to quench chronic drug toxicity.

CHAPTER 5. DISCUSSION

5.1 Selective regulation of the translome during ER stress

A genome-wide analysis was carried out to measure changes in mRNA association with large polysomes in response to ER stress. The majority of genes were either reduced or resistant to changes in polysome association, as exemplified by genes encoding eIF4e and Ppp1r15b, respectively (Figures 6A and 7). However, a significant subset of gene transcripts showed increased association with large polysomes in response to ER stress, suggestive of preferential translation (Figure 6B). These findings suggest there is a large collection of genes participating in cellular assembly and organization, gene expression, molecular transport, and post-transcriptional modifications, whose expression is subject to preferential translation (Figure 6C). We selected one of these genes, *IBTK α* , for further analysis. *IBTK α* translation is induced in response to eIF2 α ~P by PERK via a mechanism involving relief of two repressing uORFs in the *IBTK α* mRNA (Figures 8 and 9). Additionally, levels of *IBTK α* mRNA are increased in response to ER stress by the PERK/eIF2 α ~P/ATF4 pathway (Figure 10). These findings place *IBTK α* in the PERK pathway of the UPR (Figure 12A), which features key regulatory proteins that are each subject to enhanced transcription and translation during ER stress. These key regulators are each suggested to be critical for the efficacy of the UPR and, ultimately, cell fate. Indeed, we showed that knockdown of *IBTK α* in cultured cells substantially reduced their viability along with sharply enhancing caspase 3 activity (Figure 11).

5.2 Translation control of *IBTK α* by eIF2 α ~P

Measurements of *IBTK α* mRNA in the sucrose gradient fractions showed a 55% increase in transcript association with large polysomes in response to ER stress (Figure 7). This enhanced association with large polysomes was comparable to that measured

for the characterized UPR transcription factors *ATF4* and *ATF5*. However, it is noteworthy that there was a different pattern in the abundance of *IBTK α* transcripts in the sucrose gradient fractions compared with *ATF4* and *ATF5*. During ER stress, almost 85% of the *IBTK α* mRNA was present in the largest fraction 7, whereas *ATF4* and *ATF5* transcripts showed a broader distribution, with the median at fraction 5. The likely explanation for this difference is that *IBTK α* is a large transcript, with a CDS 4056 nucleotides in length that can accommodate a large number of elongating ribosomes. By comparison, the CDSs for *ATF4* and *ATF5* are 1047 and 849 nucleotides in length, respectively, and as a consequence each are expected to accommodate fewer translating ribosomes. Differences in CDS lengths are therefore likely to be an important feature when determining the changes in ribosome association for each gene transcript that occurs upon ER stress. We selected association with ~4 or more ribosomes as being a measure of efficient translation, which would also account for the ribosomes that are participating in the uORFs of transcripts which are potentially being subject to preferential translation.

Enhanced translation of *IBTK α* in response to eIF2 α -P centers around two uORFs that are well conserved among vertebrates (Figures 8 and 12B). The uORF1 is a major repressing element, whereas uORF2 appears to be less inhibitory. The presence of two repressing uORFs in the 5'-leader of the *IBTK α* mRNA suggests that the mechanism of translational control governing *IBTK α* is different from that described for *ATF4*. *ATF4* translational control features a positive-acting 5'-proximal uORF, which allows for ribosomes to scan through an inhibitory uORF due to delayed reinitiation that occurs as a consequence of eIF2 α -P and reduced eIF2/GTP levels required for ribosome acquisition of charged initiator tRNA. However, *IBTK α* does share features with the translational control mechanism described for *CHOP*. *CHOP* contains a single

inhibitory uORF that is suggested to be bypassed by scanning ribosomes in response to eIF2 α ~P. In the case of *IBTK α* , uORF1 is suggested to be a major inhibitory element that can be overcome by eIF2 α ~P. While uORF2 is also repressing, uORF2 appears to have an ancillary role to uORF1 in *IBTK α* translational control. A feature of the *CHOP* uORF that is thought to contribute to its bypass in response to eIF2 α ~P is a weak initiation codon context, a feature enriched in the preferential list of genes and shared with the major inhibitory uORF1 in the *IBTK α* transcript. The *CHOP* uORF is thought to thwart translation elongation, thus reducing reinitiation at the downstream CDS (10). It is not currently known whether translation of uORFs 1 and 2 of *IBTK α* also serve as elongation barriers. Furthermore, following translation of the *IBTK α* uORFs, there may be some regulated reinitiation at the downstream CDS in response to eIF2 α ~P and ER stress.

Translation of most mRNAs are suggested to be repressed or resistant to eIF2 α ~P. Among these, we showed that the gene transcript encoding the 5'-cap-binding protein, eIF4e, displayed lowered levels and was sharply shifted away from polysomes during ER stress. This finding suggests that translation of *eIF4e* mRNA is repressed during the UPR. It is noted that during ER stress, ATF4 is also suggested to increase expression of 4E-BP1 (165), a repressor of eIF4E association with eIF4G, suggesting there can be multiple mechanisms by which PERK/eIF2 α ~P/ATF4 can lower cap-dependent translation.

5.3 *IBTK α* facilitates cell survival

In response to acute ER stress, PERK and the UPR are thought to be critical for survival as cells expand their ER processing capacity to address increased demands on the secretory pathway. Knockdown of *IBTK α* by shRNA substantially reduces the number of MEF cells in culture (Figure 11). This is not due to lowered cell proliferation,

but rather is suggested to occur by enhanced cell death accompanied by increased activation of caspase 3. Increased caspase 3 activation also occurs with knockdown of *IBTK α* in human hepatoma HepG2 cells, emphasizing that *IBTK α* also enhances cell survival in cultured human cells. It is noteworthy that the reduced cell survival by lowered *IBTK α* expression occurs even without stress treatments.

In mice there are two isoforms of IBTK- the α isoform that is the focus of this study and a shorter form IBTK γ (207), a 26 kDa protein that is highly expressed in hematopoietic tissues, that was previously reported to bind to and repress Btk protein kinase, hence the IBTK acronym “Inhibitor of BTK.” IBTK γ suppression of Btk, lowers the BTK-mediated calcium mobilization and reduces activation of nuclear factor- κ B–targeted transcription in B cells (212,213). Subsequently it was determined that the *IBTK* gene encoded an additional larger product, *IBTK α* that is a result of an alternative upstream promoter. *IBTK α* is a 150 kDa multidomain protein that contains ankyrin repeats, RCC1 repeats, and two BTB/POZ segments (200). The BTB is a protein-protein interaction domain, and it was reported that *IBTK α* can associate with the ubiquitin ligase CUL3, suggesting that *IBTK α* may serve as a substrate adaptor in protein ubiquitylation. We currently do not know possible target proteins for the suggested *IBTK α* ubiquitylation adaptor function, but a related BTB containing protein KLHL12 was reported to facilitate monoubiquitylation of SEC31, contributing to the assembly of large COPII vesicle coats (201). An important question for the future is whether *IBTK α* also facilitates ubiquitylation of proteins that facilitate key secretory processes.

5.4 Translational control of *EPRS* by eIF2 α ~P

Our initial microarray data indicated *EPRS* mRNA is associated with large polysomes during ER stress. We further validated this finding by isolating RNA from sucrose fractions subjected to ultracentrifugation and looking at changes in mRNA

distribution by qPCR (Figure 13B). As previously discussed in Chapter 5.2, the distribution pattern of *EPRS* mRNA across sucrose gradient fractions is different from that seen for *ATF4* and *ATF5* transcripts. As explained for *IBTK α* , this is likely also due to the extended length of the *EPRS* CDS, which is 4539 nts in length, encoding a protein 163 kDa in weight. One important distinction in distribution from *IBTK α* , however, is the presence of *EPRS* mRNA in the fifth fraction during no stress conditions, corresponding to disomes and high levels of translation. This may be attributed to differences in the amount of repression each uORF has on the downstream CDS. Deletion of *IBTK α* uORF1 in the heterologous reporter resulted in a 20-fold increase in luciferase expression (Figure 9, construct 4), suggesting it is a major repressing element. Conversely, the non-canonical uCUG in the *EPRS* transcript appears to be a more modest inhibitor of downstream CDS expression. This translational mechanism of modest dampening during the basal state is likely necessary to maintain *EPRS* expression and consequentially tRNA charging under different stress conditions.

Whereas expression levels of the transcription factors CHOP and ATF4 are tightly coupled with stress conditions, *EPRS* protein appears to be relatively well expressed basally, but significantly enhanced during stress. Interestingly, the translational mechanism providing this more modest form of regulation shares two key features with that of the ATF4 “delayed reinitiation” and CHOP “bypass” mechanisms (see Figures 3 and 18). In the ATF4 delayed reinitiation model, the uORF2 element is repressive because it both overlaps and is out-of-frame with the CDS ORF (4). As a result, following termination at the stop codon of uORF2, the translating ribosome dissociates thereby missing the opportunity to initiate at the start codon of the CDS. This same feature holds true for the *EPRS* model (Figure 18). The uORF encoded by *CUG2* is inhibitory because it too overlaps and is out-of-frame with the *EPRS* CDS. A major

distinction between the *ATF4* and *EPRS* models, however, involves the positive acting uORF1 element present in *ATF4* delayed reinitiation. As discussed in the introduction, *ATF4* expression increases during stress as the result of low-levels of eIF2-GTP and the ternary complex. As a result, following translation termination at uORF1, the scanning 40S ribosomal subunit is unable to reacquire a new eIF2-TC before scanning past the start codon of uORF2. Consequently, translation initiation occurs at the downstream start codon for the *ATF4* CDS instead, leading to an increase in *ATF4* protein expression.

Like *CHOP*, the *EPRS* model of translation control lacks a positive-acting uORF. The *CHOP* bypass model involves a single inhibitory uORF, which is circumvented during stress conditions leading to enhanced expression of the downstream CDS (10). This bypass is suggested to occur as the result of a poor initiation consensus sequence flanking the *CHOP* uORF start codon. The *EPRS* model shares this fundamental feature, with the exception that rather than having an uORF with a start codon in poor context, the uORF of *EPRS* is in fact encoded by a non-canonical *CUG* start codon. This suggests a biochemical mechanism by which the scanning 43S PIC not only distinguishes initiation context of canonical start codons, but can further delineate non-canonical codons in favor of an *AUG* during eIF2 α -P. A final important distinction between the *CHOP* and *EPRS* model concerns the nature of uORF inhibitory properties on downstream CDS expression. In the *CHOP* model, the uORF is inhibitory as the result of a translational stall that the ribosome is suggested to encounter while translating the C-terminus of the encoded uORF polypeptide. Alternatively and as mentioned above, the *EPRS* uORF is inhibitory to downstream expression because it overlaps the CDS ORF in a different reading frame. These three models illustrate the dynamic nature by which uORFs have evolved to modulate downstream expression.

BYPASS of a non-canonical overlapping uORF

No stress: Low eIF2 α -P; High eIF2-GTP levels



Stress: High eIF2 α -P; Low eIF2-GTP levels

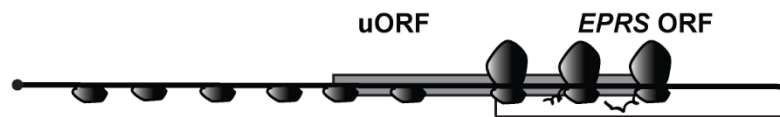


Figure 18. Proposed model of *EPRS* mRNA translation regulation. *EPRS* mRNA is preferentially translated during eIF2 α -P via a 'Bypass' model in which ribosomes leaky scan through a single inhibitory overlapping uORF with a non-canonical *CUG* initiation codon, resulting in enhanced translation of the downstream *EPRS* coding sequence.

5.5 HF preconditioning activates ISR gene expression

Halifuginone is the synthetic analogue of febrifugine, a natural alkaloid found in the Chinese quinine plant (*Dichroa febrifuga*) whose roots and leaves have been used for centuries in traditional east Asian medicine (214). Though used extensively as an antiprotozoal agent in the past (214), the molecular target of febrifugine and halofuginone remained elusive until recently. Halofuginone binds glutamyl-prolyl-tRNA synthetase (*EPRS*) inhibiting prolyl-tRNA synthetase charging activity (215). Consequently, halifuginone treatment results in an accumulation of uncharged prolyl-tRNA, activating GCN2 phosphorylation of eIF2 α and the Integrated Stress Response pathway (215). This finding has provided the alluring potential for the use of HF as a pharmacological agent for dietary preconditioning. Dietary restriction has been shown to be beneficial prior to acute stresses such as ischemia reperfusion in various mammalian models (216-221), and many of these benefits can be recapitulated by depletion of a

single amino acid from the diet (221,222). In a mouse model of ischemia reperfusion, dietary preconditioning by removal of both total protein and the single amino acid tryptophan for 6 to 14 days drastically reduced hepatic and renal ischemic injury (211). Interestingly, similar results were also noted when the animals were injected daily with HF for three days prior to surgery (211). Both nutritional and pharmacological activation of the preconditioning mechanism required GCN2, implicating the ISR as the major pathway facilitating protection.

To see if HF induced eIF2 α ~P and a translational defect in culture, we treated MEFs with 25 nM HF for 6 hrs and performed polysome profiling analysis. HF treatment did result in a decrease in polysomes coincident with an increase in the monosome peak, indicative of eIF2 α ~P (Figure 16A). We further show that GCN2-mediated translation control is critical to cell viability during HF treatment, as GCN2^{-/-} MEFs were hyper-sensitive to the drug at nanomolar concentrations (Figure 17A). These results further support that HF activates the ISR through the GCN2 kinase, and downstream regulators of eIF2 α ~P are critical for stress remediation.

In a dietary preconditioning model, HF treatment prior to surgical stress may provide protection by 'priming' gene expression to better handle a second insult. For instance, many gene targets of ATF4 are central to redox processes, amino acid uptake, and protein folding. Following HF treatment, these proteins would have already undergone synthesis and maturation prior to the acute stress, such as an ischemic event, enabling the tissue to better handle the oxidative damage, inflammation and energy depletion inherent to reperfusion. Furthermore, drastic reductions in ATP hydrolysis and nutrient consumption from the global decrease in protein synthesis conferred by eIF2 α ~P would conserve energy resources prior to the second insult (Figure 17B).

We showed earlier that *EPRS* mRNA is subject to preferential translation during PERK-induced eIF2 α -P (Figures 13 and 14). To see if the 5'-leader of *EPRS* confers preferential translation during HF treatment, we transiently transfected the *P_{TK}-EPRS-Luc* into WT and eIF2 α -S51A MEFs and treated the cells with 25 nM HF or no treatment for 12 hours. HF treatment resulted in a 2.5 fold induction of Luciferase activity, which is comparable to what we observed during 12h of 0.1 μ M TG treatment (Figure 16B). Importantly, this induction was completely abrogated in the alanine mutant cells, indicating that HF activation of GCN2/eIF2 α -P is required for *EPRS* translation control. In this current model, HF treatment confers stress resistance prior to a second insult in multiple facets. HF induces GCN2/eIF2 α -P, which as mentioned earlier not only conserves resources by dampening global protein synthesis, but further reprograms gene expression for stress remediation by the enhanced expression of ATF4 downstream targets. Following this burst of gene reprogramming, mRNA encoding the *EPRS* substrate of HF is subject to enhanced expression via translational control, and we propose this increase in *EPRS* protein expression may help quench drug toxicity, enabling the cell to resume prolyl-tRNA charging and global mRNA translation (Figure 17B). A more detailed understanding of downstream targets responsible for HF's protection against secondary stress could be leveraged to facilitate the future development of more selective and potent cytoprotective agents.

5.6 Concluding remarks

Translational regulation is dynamic, and the results of our genome-wide study indicate a broader range of eIF2 α -p translation control than has been suggested by previous models. A major goal of this undertaking was to establish predictive rules based on how a gene transcript would be gauged by the translational machinery during stress. While we present insight about the nature of uORFs and the consensus

sequence flanking upstream start codons, an encompassing rule book of translational efficiencies using transcript characteristics remains elusive. Based on the few known examples of mRNAs subject to preferential translation during eIF2 α ~P, we hypothesized an enrichment of uORFs in transcripts shifted towards the large polysomes during ER stress. Possible explanations why this was not the case are manifold. While it is generally assumed that the translating ribosome initiates at the first *AUG* codon it encounters while scanning, we did not establish that these uORFs predicted by the EST library were in fact translated. Additionally, there is evidence that ribosome reinitiation at a downstream coding sequence following termination at the uORF may be a common occurrence. Perhaps the gene transcripts encoding uORFs in the resistant and repressed groups are subject to constitutive reinitiation and are therefore not inducible. Furthermore, there is evidence stemming from ribosomal profiling that noncanonical initiation codons may be functional among uORFs. Therefore, our informatic analysis that was restricted to *AUG* initiation codons would not identify these putative regulatory coding sequences. Our informatics analysis also ignored potential contributions of the 3'-UTR, which as mentioned in the introduction can also play an important role in translation control. Lastly, alternative mRNA splicing is a major regulator of gene expression, and a limitation of our microarray based approach is the inability to detect splicing variants. The capacity to distinguish specific spliced transcripts for each gene is a major benefit of RNA seq. An increasingly popular method of detecting ribosomal occupancy in eukaryotic cells is the ribosome profiling, or 'riboseq,' technique. This method couples ribosomal occupancy with deep sequencing to monitor mRNA translation *in vivo* (223,224). A major benefit of this method is the capacity to identify specific splicing variants, and genome-wide translational analyses have been performed in both budding yeast and several mammalian cell types (208,209,225). This technology may prove very useful in studying global stress-regulation of translation control much like

the work we present here, with the caveat that the analyses must be rigorous in accounting for changes in transcript abundance when portraying an accurate picture of translation efficiency for a specific mRNA.

Another major goal of the global analysis was to identify novel members of the ISR and better understand unidentified gene regulation. We show that *IBTK α* is under the transcriptional control of ATF4, and is subject to preferential translation during PERK-induced eIF2 α -P. This multidomain protein is conserved in fission yeast, and the observation that *IBTK α* depletion leads to enhanced apoptosis in the absence of stress suggests a fundamental role for this gene in eukaryotic cell homeostasis. Preliminary work in the developing zebrafish embryo suggests that depletion of *IBTK α* by splicing morpholino microinjection leads to defects in the development of secretory tissues (data not shown), supporting the results of the work in tissue culture in a whole-animal developmental system. It is paramount to identify the ubiquitylation target substrate of *IBTK α* to elucidate its biological function. Improving our knowledge of the function and regulation of *IBTK α* and other members of the Integrated Stress Response will provide for a greater understanding of how stress signal integration and the dysregulation of this pathway impacts disease etiology.

Appendix 1. The bottom, middle, and top 200 gene transcripts representing the repressed, resistant, and preferentially translated groups during eIF2 α -P.

| gene | UTR length | uORFs | CDS context | regulation | % shift towards polysomes |
|-----------------|-------------------|--------------|--------------------|-------------------|----------------------------------|
| Atf5 | 373 | 2 | Adequate | preferential | 32.58 |
| Ibtk | 568 | 4 | Strong | preferential | 32.27 |
| Sf3b1 | 112 | 0 | Strong | preferential | 30.96 |
| Cdk5rap2 | 163 | 1 | Strong | preferential | 29.06 |
| Eprs | 103 | 0 | Strong | preferential | 28.77 |
| Myo1b | 320 | 0 | Adequate | preferential | 28.35 |
| Snd1 | 217 | 0 | Adequate | preferential | 27.35 |
| Safb | 171 | 0 | Adequate | preferential | 26.85 |
| Rbm25 | 290 | 0 | Adequate | preferential | 26.69 |
| Baz1a | 204 | 0 | Adequate | preferential | 26.53 |
| Prpf8 | 317 | 1 | Strong | preferential | 25.40 |
| Dnmt1 | 430 | 3 | Strong | preferential | 25.29 |
| Atad2 | 108 | 0 | Adequate | preferential | 25.13 |
| Mlit4 | 420 | 1 | Adequate | preferential | 25.11 |
| Spnb2 | 425 | 3 | Strong | preferential | 24.54 |
| Tpr | 214 | 2 | Strong | preferential | 24.31 |
| Ppp1r12a | 248 | 0 | Adequate | preferential | 23.90 |
| Rrbp1 | 286 | 0 | Strong | preferential | 23.39 |
| Hk1 | 346 | 2 | Adequate | preferential | 22.89 |
| Polr2a | 411 | 0 | Adequate | preferential | 22.83 |
| Pogz | 175 | 0 | Strong | preferential | 22.80 |
| Myof | 254 | 0 | Adequate | preferential | 22.77 |
| Glg1 | 365 | 5 | Strong | preferential | 22.59 |
| Gbf1 | 294 | 1 | Strong | preferential | 22.36 |
| Ncapg | 102 | 0 | Strong | preferential | 22.20 |
| Plcd3 | 239 | 0 | Strong | preferential | 21.77 |
| Npc1 | 99 | 0 | Strong | preferential | 21.76 |
| Aqr | 173 | 0 | Strong | preferential | 21.50 |
| Mybbp1a | 30 | 0 | Strong | preferential | 21.44 |
| Diap2 | 234 | 0 | Strong | preferential | 21.44 |
| Ckap5 | 177 | 0 | Strong | preferential | 21.29 |
| Vars | 250 | 0 | Adequate | preferential | 21.08 |
| Xpo5 | 169 | 1 | Strong | preferential | 21.06 |

| | | | | | |
|-----------------|-----|---|----------|--------------|-------|
| Uba6 | 62 | 0 | Strong | preferential | 21.04 |
| Cdca2 | 387 | 0 | Strong | preferential | 20.99 |
| Rnf160 | 139 | 0 | Strong | preferential | 20.73 |
| Cgn1 | 109 | 0 | Strong | preferential | 20.70 |
| Nup98 | 423 | 5 | Adequate | preferential | 20.66 |
| Dhx36 | 65 | 0 | Adequate | preferential | 20.59 |
| Iqgap1 | 136 | 1 | Adequate | preferential | 20.45 |
| Pcm1 | 224 | 1 | Strong | preferential | 20.43 |
| Ints4 | 141 | 0 | Strong | preferential | 20.36 |
| Mpdz | 54 | 1 | Adequate | preferential | 20.25 |
| Bms1 | 500 | 1 | Strong | preferential | 20.22 |
| Med12 | 170 | 0 | Strong | preferential | 20.11 |
| Kif11 | 283 | 1 | Strong | preferential | 20.09 |
| Polr3a | 130 | 0 | Strong | preferential | 20.00 |
| Eif5b | 280 | 2 | Strong | preferential | 19.96 |
| Eif3a | 184 | 0 | Adequate | preferential | 19.95 |
| Yeats2 | 192 | 0 | Adequate | preferential | 19.93 |
| Edc4 | 200 | 0 | Adequate | preferential | 19.91 |
| Ddit3 | 186 | 1 | Strong | preferential | 19.86 |
| Stat3 | 279 | 0 | Strong | preferential | 19.85 |
| Top2a | 423 | 6 | Strong | preferential | 19.68 |
| Cltc | 226 | 0 | Strong | preferential | 19.67 |
| Son | 84 | 1 | Strong | preferential | 19.65 |
| Diap3 | 76 | 0 | Strong | preferential | 19.59 |
| Usp9x | 505 | 5 | Adequate | preferential | 19.58 |
| Ddb1 | 119 | 0 | Adequate | preferential | 19.56 |
| Rad50 | 256 | 1 | Weak | preferential | 19.50 |
| Tpp2 | 82 | 0 | Adequate | preferential | 19.43 |
| Sfmbt2 | 203 | 2 | Strong | preferential | 19.38 |
| Nup133 | 105 | 0 | Adequate | preferential | 19.38 |
| Esf1 | 148 | 0 | Adequate | preferential | 19.23 |
| Aldh18a1 | 248 | 0 | Adequate | preferential | 19.20 |
| Ktn1 | 160 | 0 | Strong | preferential | 19.15 |
| Ttc21b | 83 | 0 | Strong | preferential | 19.13 |
| Ep400 | 389 | 4 | Adequate | preferential | 18.99 |
| Qars | | 2 | Strong | preferential | 18.96 |
| Lrpprc | 273 | 1 | Strong | preferential | 18.89 |
| Ubr2 | 313 | 0 | Strong | preferential | 18.83 |
| Filip1l | 141 | 0 | Strong | preferential | 18.69 |
| Ctr9 | 186 | 0 | Adequate | preferential | 18.56 |
| Rab3gap2 | 130 | 0 | Strong | preferential | 18.44 |

| | | | | | |
|--|-----|---|----------|--------------|-------|
| Senp7 | 130 | 0 | Strong | preferential | 18.37 |
| Sdccag1 | 67 | 0 | Adequate | preferential | 18.34 |
| Zfp318 | 73 | 0 | Adequate | preferential | 18.32 |
| Pop1 | 107 | 0 | Adequate | preferential | 18.29 |
| Cwf1912 /// LOC10004 4213 | 66 | 0 | Strong | preferential | 18.25 |
| Nbea | 466 | 1 | Adequate | preferential | 18.21 |
| Smc5 | 79 | 0 | Strong | preferential | 18.14 |
| Atf4 | 278 | 2 | Adequate | preferential | 18.12 |
| Aco2 | 145 | 2 | Strong | preferential | 18.11 |
| Arid4a | 909 | 6 | Strong | preferential | 18.08 |
| Pds5b | 146 | 1 | Strong | preferential | 18.08 |
| 4933407H 18Rik | 677 | 4 | Strong | preferential | 18.08 |
| Tcerg1 | | 1 | Strong | preferential | 18.07 |
| Hcfc1 | 312 | 1 | Strong | preferential | 18.04 |
| Chd4 | 258 | 1 | Strong | preferential | 18.03 |
| Ubr1 | 113 | 0 | Strong | preferential | 17.99 |
| Pgap1 | 102 | 0 | Adequate | preferential | 17.98 |
| Mthfd1 | 272 | 0 | Strong | preferential | 17.98 |
| Taf1 | 87 | 0 | Adequate | preferential | 17.96 |
| Crybg3 | 243 | 3 | Strong | preferential | 17.95 |
| Dennd4c | 375 | 1 | Adequate | preferential | 17.86 |
| Ganab | 22 | 0 | Strong | preferential | 17.83 |
| Dlgap5 | 300 | 1 | Adequate | preferential | 17.75 |
| Jak1 | 316 | 1 | Weak | preferential | 17.70 |
| Rbm39 | 450 | 2 | Weak | preferential | 17.60 |
| Ttc17 | 438 | 6 | Weak | preferential | 17.51 |
| Gemin5 | 751 | 5 | Strong | preferential | 17.50 |
| Prpf3 | 483 | 3 | Strong | preferential | 17.50 |
| 1110037F0 2Rik | 85 | 0 | Strong | preferential | 17.48 |
| Smarca4 | 260 | 0 | Adequate | preferential | 17.47 |
| Helb | 103 | 0 | Strong | preferential | 17.46 |
| Rbm28 | 116 | 0 | Adequate | preferential | 17.41 |
| Nup160 | 651 | 5 | Strong | preferential | 17.41 |
| Ipo5 | 101 | 0 | Strong | preferential | 17.39 |
| Asph | 252 | 0 | Strong | preferential | 17.30 |
| Trp53bp2 | 257 | 0 | Weak | preferential | 17.24 |
| Pi4ka | 78 | 0 | Weak | preferential | 17.23 |
| Uhrf1 | 253 | 0 | Adequate | preferential | 17.21 |

| | | | | | |
|----------------------------|-----|---|----------|--------------|-------|
| Zfr | 69 | 0 | Weak | preferential | 17.14 |
| Peg3 | 362 | 1 | Adequate | preferential | 17.13 |
| Ptprd | 455 | 7 | Adequate | preferential | 17.12 |
| Trip12 | 125 | 1 | Weak | preferential | 17.10 |
| Msln | 157 | 0 | Strong | preferential | 17.03 |
| Atrx | 253 | | Adequate | preferential | 17.02 |
| C230096C 10Rik | 27 | 0 | Strong | preferential | 16.98 |
| Tjp1 | 408 | 1 | Adequate | preferential | 16.97 |
| BC037112 | 255 | 0 | Adequate | preferential | 16.94 |
| Hltf | 184 | 0 | Adequate | preferential | 16.87 |
| Nup155 | 254 | 3 | Adequate | preferential | 16.84 |
| Nup107 | 392 | 2 | Adequate | preferential | 16.83 |
| Lamb1-1 | 365 | 5 | Weak | preferential | 16.82 |
| Slk | 175 | 0 | Adequate | preferential | 16.79 |
| Wdr7 | 238 | 1 | Strong | preferential | 16.75 |
| ORF34 | 71 | 0 | Strong | preferential | 16.71 |
| Npepps | 180 | 0 | Weak | preferential | 16.67 |
| Cpsf1 | 113 | 0 | Adequate | preferential | 16.65 |
| Ltbp1 | 414 | 0 | Strong | preferential | 16.65 |
| Baz1b | 388 | 1 | Strong | preferential | 16.64 |
| Cdc5l | 304 | 0 | Adequate | preferential | 16.62 |
| Ap3b1 | 144 | 0 | Adequate | preferential | 16.62 |
| Atr | 128 | 0 | Strong | preferential | 16.57 |
| Ankrd17 | 138 | 0 | Strong | preferential | 16.56 |
| Lrch2 | 31 | 0 | Strong | preferential | 16.55 |
| Arid4b | 290 | 0 | Adequate | preferential | 16.54 |
| Hsph1 | 260 | 1 | Adequate | preferential | 16.54 |
| Acot1 /// Acot2 | 29 | 0 | Strong | preferential | 16.53 |
| Dhx9 | 150 | 1 | Strong | preferential | 16.45 |
| Acly | 229 | 1 | Adequate | preferential | 16.45 |
| Smc4 | 124 | 0 | Adequate | preferential | 16.41 |
| Wdr19 | 59 | 0 | Adequate | preferential | 16.41 |
| Smc3 | 188 | 1 | Adequate | preferential | 16.39 |
| Mical1 | 274 | 0 | Adequate | preferential | 16.30 |
| Ube2o | 40 | 0 | Strong | preferential | 16.27 |
| 2810474O 19Rik | 743 | 3 | Adequate | preferential | 16.26 |
| Col11a1 | 361 | 2 | Strong | preferential | 16.24 |
| Hectd1 | 390 | 1 | Strong | preferential | 16.20 |
| Cyfip1 | 238 | 0 | Strong | preferential | 16.19 |

| | | | | | |
|--|-----|---|----------|--------------|-------|
| Spna2 | 229 | 0 | Strong | preferential | 16.19 |
| Tanc2 | 314 | 0 | Adequate | preferential | 16.15 |
| Lrrcc1 | 146 | 0 | Strong | preferential | 16.13 |
| Larp4 | 193 | 3 | Strong | preferential | 16.12 |
| Nfkb2 | 158 | 0 | Strong | preferential | 16.10 |
| Flii | 51 | 0 | Strong | preferential | 16.10 |
| LOC64044 1 /// Thbs1 | 250 | 1 | Strong | preferential | 16.04 |
| Hdac6 | 59 | 1 | Strong | preferential | 16.04 |
| Akap8l | 109 | 0 | Adequate | preferential | 16.02 |
| Setdb1 | 147 | 0 | Adequate | preferential | 16.00 |
| Aars | 392 | 0 | Weak | preferential | 15.96 |
| Sec23ip | 152 | 0 | Strong | preferential | 15.93 |
| Ubr3 | 49 | 0 | Strong | preferential | 15.90 |
| Rbm5 | 382 | 3 | Weak | preferential | 15.89 |
| Phip | 219 | 2 | Weak | preferential | 15.89 |
| Gpd2 | 319 | 0 | Strong | preferential | 15.87 |
| Ddr2 | 287 | 1 | Adequate | preferential | 15.80 |
| Med23 | 113 | 0 | Adequate | preferential | 15.80 |
| 4930402E1 6Rik /// PDPR | 223 | 1 | Adequate | preferential | 15.80 |
| Afap1 | 224 | 1 | Strong | preferential | 15.80 |
| Mym1 | 35 | 0 | Strong | preferential | 15.74 |
| Mtap4 | 186 | 0 | Strong | preferential | 15.70 |
| Smg6 | 61 | 0 | Strong | preferential | 15.69 |
| Atp8a1 | 221 | 0 | Adequate | preferential | 15.69 |
| LOC10004 5677 /// Mcm3 | 104 | 0 | Strong | preferential | 15.67 |
| 4832420A 03Rik /// Rsf1 | 8 | 0 | Strong | preferential | 15.64 |
| Slc4a7 | 208 | 0 | Strong | preferential | 15.61 |
| Exoc4 | 33 | 0 | Strong | preferential | 15.59 |
| Dock7 | 386 | 3 | Adequate | preferential | 15.57 |
| Bclaf1 | 250 | 1 | Strong | preferential | 15.56 |
| Vcl | 123 | 0 | Adequate | preferential | 15.54 |
| Hook3 | 210 | 0 | Adequate | preferential | 15.54 |
| Cep290 | 193 | 1 | Adequate | preferential | 15.46 |
| Hadha | 69 | 0 | Strong | preferential | 15.43 |
| Col5a2 | 368 | 3 | Adequate | preferential | 15.39 |
| Egfr | 280 | 0 | Adequate | preferential | 15.37 |

| | | | | | |
|---|-----|---|----------|--------------|-------|
| EG384954 /// Tuba3a /// Tuba3b | 124 | 1 | Adequate | preferential | 15.36 |
| Spg11 | 41 | 0 | Strong | preferential | 15.32 |
| Prkca | 221 | 0 | Strong | preferential | 15.30 |
| Ylpm1 | 169 | 0 | Weak | preferential | 15.29 |
| Blm | 343 | 2 | Weak | preferential | 15.28 |
| Ints6 | 478 | 0 | Adequate | preferential | 15.25 |
| Usp33 | 210 | 0 | Adequate | preferential | 15.24 |
| Vps16 | 75 | 0 | Strong | preferential | 15.21 |
| Incenp | 184 | 0 | Strong | preferential | 15.20 |
| Zfp521 | 234 | 1 | Adequate | resistant | 0.20 |
| Polr1c | 82 | 0 | Strong | resistant | 0.20 |
| Usp4 | 87 | 0 | Strong | resistant | 0.20 |
| Ik | 117 | 0 | Adequate | resistant | 0.20 |
| BC023744 | 936 | 7 | Strong | resistant | 0.20 |
| Pja1 | 307 | 1 | Strong | resistant | 0.20 |
| Igf2bp3 | 483 | 0 | Adequate | resistant | 0.20 |
| Khdrbs1 | 144 | 0 | Weak | resistant | 0.19 |
| Agfg1 | 240 | 0 | Strong | resistant | 0.19 |
| 5730437N 04Rik | 43 | 0 | Strong | resistant | 0.19 |
| Traip | 112 | 0 | Adequate | resistant | 0.19 |
| D10Wsu52 e | 110 | 0 | Adequate | resistant | 0.19 |
| Klhdc5 | 457 | 2 | Adequate | resistant | 0.19 |
| Matn2 | 251 | 1 | Strong | resistant | 0.18 |
| Atp1a1 | 290 | 0 | Strong | resistant | 0.18 |
| Senp1 | 310 | 1 | Strong | resistant | 0.18 |
| Gosr1 | 14 | 0 | Strong | resistant | 0.18 |
| Cnot4 | 328 | 2 | Adequate | resistant | 0.18 |
| BC027231 | 226 | 3 | Weak | resistant | 0.17 |
| Pggt1b | 127 | 1 | Strong | resistant | 0.17 |
| Polr1c | 82 | 0 | Strong | resistant | 0.17 |
| Spg20 | 375 | 1 | Strong | resistant | 0.17 |
| Prkacb | 270 | 0 | Strong | resistant | 0.17 |
| Fntb | 68 | 2 | Strong | resistant | 0.17 |
| Pcdh9 | 194 | 4 | Strong | resistant | 0.17 |
| Pigo | 37 | 0 | Adequate | resistant | 0.17 |
| Stau1 | 304 | 1 | Weak | resistant | 0.16 |
| 1110008P1 4Rik | 145 | 0 | Adequate | resistant | 0.16 |
| Pibf1 | 88 | 0 | Adequate | resistant | 0.16 |

| | | | | | |
|---------------------------------------|-----|---|----------|-----------|------|
| Cxadr | 241 | 0 | Strong | resistant | 0.16 |
| Adnp2 | 130 | 0 | Adequate | resistant | 0.15 |
| Arid5a | 100 | 0 | Strong | resistant | 0.15 |
| Hnrnpd | 314 | 0 | Adequate | resistant | 0.15 |
| Atf7 | 123 | 0 | Strong | resistant | 0.15 |
| Tmod3 | 199 | 0 | Strong | resistant | 0.15 |
| Cct3 | 114 | 0 | Adequate | resistant | 0.15 |
| Akap9 | 257 | 1 | Strong | resistant | 0.14 |
| Cln4-2 | 915 | 9 | Adequate | resistant | 0.14 |
| Sec61a1 | 97 | 1 | Weak | resistant | 0.14 |
| OTTMUSG 000000106 57 | 399 | 6 | Adequate | resistant | 0.13 |
| LOC63990 5 /// Sap30bp | 42 | 0 | Strong | resistant | 0.13 |
| Cep152 | 245 | 0 | Adequate | resistant | 0.13 |
| Sfrs18 | 568 | 5 | Adequate | resistant | 0.13 |
| Osbpl7 | 538 | 2 | Adequate | resistant | 0.13 |
| Kti12 | 44 | 0 | Adequate | resistant | 0.13 |
| Gtf3c2 /// Mpv17 | 284 | 1 | Adequate | resistant | 0.12 |
| Smg5 | 383 | 3 | Adequate | resistant | 0.12 |
| Prr14 | 572 | 1 | Adequate | resistant | 0.12 |
| Atpif1 | 367 | 2 | Strong | resistant | 0.12 |
| Eif2a | 296 | 0 | Adequate | resistant | 0.11 |
| Atox1 | 145 | 0 | Adequate | resistant | 0.11 |
| Trp53 | 569 | 1 | Adequate | resistant | 0.11 |
| Usp34 | 293 | 4 | Adequate | resistant | 0.11 |
| 9130227C 08Rik | 609 | 4 | Weak | resistant | 0.11 |
| D4Wsu53e | 181 | 0 | Adequate | resistant | 0.11 |
| Rtn4 | 291 | 0 | Strong | resistant | 0.11 |
| Znrf2 | 280 | 1 | Strong | resistant | 0.11 |
| 2310061C 15Rik | 132 | 1 | Adequate | resistant | 0.10 |
| Tob2 | 497 | 2 | Adequate | resistant | 0.10 |
| Tusc2 | 132 | 2 | Strong | resistant | 0.10 |
| C2cd2l | 398 | 1 | Strong | resistant | 0.10 |
| Zfp182 | 180 | 2 | Adequate | resistant | 0.09 |
| G6pdx | 393 | 4 | Strong | resistant | 0.09 |
| Fam120b | 376 | 0 | Strong | resistant | 0.09 |
| Timp2 | 417 | 0 | Strong | resistant | 0.09 |

| | | | | | |
|---|------|---|----------|-----------|------|
| Add1 | 270 | 1 | Adequate | resistant | 0.09 |
| Vps37d | 67 | 0 | Adequate | resistant | 0.08 |
| Lman1 | 24 | 0 | Strong | resistant | 0.08 |
| Acad8 | 53 | 0 | Adequate | resistant | 0.07 |
| Nudcd1 | 531 | 3 | Strong | resistant | 0.07 |
| Serinc1 | 134 | 0 | Strong | resistant | 0.07 |
| Tmem131 | 272 | 1 | Strong | resistant | 0.06 |
| Pgk1 | 152 | 0 | Adequate | resistant | 0.06 |
| Pkm2 | 127 | 0 | Adequate | resistant | 0.06 |
| Rala | 261 | 0 | Strong | resistant | 0.06 |
| G3bp1 | 118 | 0 | Strong | resistant | 0.06 |
| Zfp518b | 639 | 5 | Adequate | resistant | 0.06 |
| Pde10a | 245 | 3 | Strong | resistant | 0.06 |
| Yy1 | 386 | 0 | Strong | resistant | 0.05 |
| AI415730 | 117 | 1 | Weak | resistant | 0.05 |
| Nab2 | 270 | 0 | Weak | resistant | 0.05 |
| Trim2 | 297 | 6 | Strong | resistant | 0.05 |
| Dstyk | 153 | 0 | Strong | resistant | 0.04 |
| NoI9 | 39 | 0 | Strong | resistant | 0.04 |
| Fads1 | 164 | 0 | Strong | resistant | 0.04 |
| Fdx1l /// Glp1 | 26 | 0 | Strong | resistant | 0.04 |
| Fam175b | 37 | 0 | Strong | resistant | 0.04 |
| Wsb2 | 50 | 0 | Adequate | resistant | 0.04 |
| Oxct1 | 552 | 1 | Adequate | resistant | 0.03 |
| Zfp37 | 185 | 2 | Strong | resistant | 0.03 |
| Xpr1 | 210 | 2 | Adequate | resistant | 0.02 |
| Birc2 | 777 | 9 | Adequate | resistant | 0.02 |
| Elk4 | 345 | 1 | Strong | resistant | 0.02 |
| Prkdc | 23 | 1 | Strong | resistant | 0.01 |
| Zfp790 | 284 | 2 | Strong | resistant | 0.01 |
| LOC10004 5958 /// Pura | 583 | 0 | Strong | resistant | 0.01 |
| Exoc8 | 139 | 0 | Adequate | resistant | 0.00 |
| Tgfb2 | 1218 | 2 | Adequate | resistant | 0.00 |
| Pxmp2 | 179 | 1 | Strong | resistant | 0.00 |
| Plk1 | 106 | 0 | Adequate | resistant | 0.00 |
| Zfp397 | 275 | 1 | Strong | resistant | 0.00 |
| 2700094K 13Rik | 184 | 0 | Strong | resistant | 0.00 |
| Kihl22 | 114 | 0 | Strong | resistant | 0.00 |

| | | | | | |
|--|------|----|----------|-----------|-------|
| Sirt1 | 65 | 0 | Strong | resistant | 0.00 |
| Ercc3 | 63 | 0 | Strong | resistant | 0.00 |
| Gm672 | 331 | 0 | Strong | resistant | -0.01 |
| Dhrs11 | 113 | 0 | Adequate | resistant | -0.01 |
| ENSMUSG 000000643 17 /// Lsm7 | 78 | 0 | Strong | resistant | -0.01 |
| Abcf1 | 64 | 0 | Adequate | resistant | -0.01 |
| Qk | 488 | 0 | Strong | resistant | -0.01 |
| Arih1 | 270 | 0 | Strong | resistant | -0.01 |
| Mapkbp1 | 354 | 2 | Strong | resistant | -0.02 |
| 2310016E0 2Rik///Ost 4 | 202 | 0 | Adequate | resistant | -0.02 |
| Eif5 /// LOC10004 7658 | 705 | 6 | Adequate | resistant | -0.02 |
| Fus | 109 | 0 | Strong | resistant | -0.03 |
| Dtx4 | 155 | 4 | Strong | resistant | -0.03 |
| Tmcc1 | 1173 | 12 | Adequate | resistant | -0.03 |
| Rin1 | 59 | 0 | Strong | resistant | -0.03 |
| 6720475J1 9Rik | 1054 | 7 | Weak | resistant | -0.04 |
| Mrp63 | 98 | 0 | Adequate | resistant | -0.04 |
| Zfp697 | 135 | 0 | Adequate | resistant | -0.04 |
| Pnrc1 | 390 | 1 | Adequate | resistant | -0.04 |
| 2300009A 05Rik | 22 | 0 | Strong | resistant | -0.04 |
| Pdia6 | 58 | 0 | Adequate | resistant | -0.04 |
| Dnm1l | 165 | 1 | Strong | resistant | -0.04 |
| Mid1 | 267 | 0 | Strong | resistant | -0.04 |
| Tmem49 | 122 | 1 | Strong | resistant | -0.05 |
| Usp14 | 221 | 1 | Adequate | resistant | -0.05 |
| Sfrs2ip | 263 | 1 | Adequate | resistant | -0.05 |
| 4933424B 01Rik | 546 | 4 | Adequate | resistant | -0.05 |
| Csnk2a2 | 373 | 0 | Adequate | resistant | -0.06 |
| Exod1///Er i2 | 118 | 0 | Strong | resistant | -0.06 |
| Ankrd1 | 99 | 0 | Adequate | resistant | -0.06 |
| Pus10 | 489 | 0 | Adequate | resistant | -0.06 |
| Tmem87b | 258 | 0 | Strong | resistant | -0.06 |
| EG245305 | 183 | 2 | Strong | resistant | -0.06 |
| Zbtb12 | 231 | 0 | Strong | resistant | -0.07 |

| | | | | | |
|--|-----|---|----------|-----------|-------|
| Wdr21 | 199 | 4 | Strong | resistant | -0.07 |
| 2610528E2 | 371 | 1 | Strong | resistant | -0.07 |
| 3Rik /// Frag1///At ad5 | | | | | |
| 2010309E2 | 88 | 0 | Strong | resistant | -0.08 |
| 1Rik | | | | | |
| Hnrnpa1 | 200 | 1 | Adequate | resistant | -0.08 |
| 6030408C | 219 | 1 | Adequate | resistant | -0.08 |
| 04Rik///G2 e3 | | | | | |
| Arfgap2 | 371 | 2 | Strong | resistant | -0.08 |
| Acbd3 | 68 | 0 | Strong | resistant | -0.08 |
| Tmcc3 | 186 | 2 | Adequate | resistant | -0.08 |
| Map4k5 | 440 | 1 | Strong | resistant | -0.08 |
| Actb | 136 | 0 | Strong | resistant | -0.08 |
| Aldh3a2 | 178 | 0 | Strong | resistant | -0.08 |
| Oma1 | 94 | 0 | Adequate | resistant | -0.08 |
| Sord | 83 | 0 | Strong | resistant | -0.08 |
| Txnrd3 | 256 | 0 | Weak | resistant | -0.09 |
| Cish | 359 | 1 | Strong | resistant | -0.09 |
| Ncdn | 140 | 0 | Weak | resistant | -0.09 |
| Rnf19a | 318 | 3 | Weak | resistant | -0.09 |
| Rpl12 | 125 | 0 | Adequate | resistant | -0.09 |
| Traf6 | 215 | 0 | Adequate | resistant | -0.09 |
| Tbl3 | 96 | 0 | Strong | resistant | -0.09 |
| Myo5a | 124 | 0 | Adequate | resistant | -0.09 |
| Slc39a6 | 540 | 1 | Strong | resistant | -0.09 |
| Fam60a | 177 | 0 | Strong | resistant | -0.09 |
| G430022H | 163 | 0 | Strong | resistant | -0.09 |
| 21Rik///Me ttl14 | | | | | |
| Atp5a1 | 322 | 1 | Adequate | resistant | -0.10 |
| Ndufa6 | 95 | 0 | Strong | resistant | -0.10 |
| Slc9a1 | 772 | 2 | Adequate | resistant | -0.10 |
| Rbbp8 | 230 | 3 | Adequate | resistant | -0.10 |
| Zfand3 | 199 | 0 | Strong | resistant | -0.10 |
| Nr4a2 | 299 | 0 | Adequate | resistant | -0.10 |
| Klhl24 | 242 | 2 | Strong | resistant | -0.11 |
| Rpusd1 | 323 | 4 | Adequate | resistant | -0.11 |
| Rbpj | 372 | 3 | Adequate | resistant | -0.11 |
| Zfp354a | 372 | 4 | Adequate | resistant | -0.11 |
| Hdlbp | 210 | 0 | Adequate | resistant | -0.12 |

| | | | | | |
|---|-----|---|----------|-----------|--------|
| Txndc9 | 227 | 1 | Strong | resistant | -0.12 |
| Nsfl1c | 40 | 0 | Strong | resistant | -0.12 |
| Capn7 | 218 | 0 | Strong | resistant | -0.12 |
| Ccdc76 | 808 | 6 | Strong | resistant | -0.13 |
| Pitrm1 | 25 | 0 | Adequate | resistant | -0.13 |
| Zfp687 | 145 | 0 | Strong | resistant | -0.13 |
| Rrp1b | 300 | 2 | Adequate | resistant | -0.13 |
| Cnih4 | 63 | 1 | Strong | resistant | -0.13 |
| Zeb2 | 526 | 2 | Adequate | resistant | -0.13 |
| Arl4c /// LOC63243 3 | 527 | 1 | Strong | resistant | -0.13 |
| Atl3 | 291 | 2 | Adequate | resistant | -0.14 |
| Eny2 | 327 | 1 | Weak | resistant | -0.14 |
| Rfwd3 | 65 | 1 | Strong | resistant | -0.14 |
| 2010111I0 1Rik | 270 | 1 | Strong | resistant | -0.14 |
| Pdlim5 | 100 | 0 | Adequate | resistant | -0.14 |
| Plekha8 | 361 | 4 | Adequate | resistant | -0.14 |
| Cnot6 | 359 | 3 | Adequate | resistant | -0.15 |
| Tes | 138 | 1 | Strong | resistant | -0.15 |
| Rnpep | 208 | 1 | Strong | resistant | -0.15 |
| Ankrd1 | 99 | 0 | Adequate | resistant | -0.15 |
| Cnm3 | 45 | 0 | Strong | resistant | -0.16 |
| Camk2g /// LOC10004 5547 | 123 | 0 | Strong | resistant | -0.16 |
| Zxda | 106 | 0 | Strong | resistant | -0.17 |
| Kctd7 | 195 | 1 | Strong | resistant | -0.17 |
| Zfp82 | 762 | 6 | Strong | resistant | -0.17 |
| Cldn1 | 217 | 0 | Strong | resistant | -0.17 |
| Zc3h8 | 153 | 1 | Strong | resistant | -0.18 |
| Brwd1 | 254 | 1 | Strong | resistant | -0.18 |
| Dym | 26 | 0 | Adequate | repressed | -21.66 |
| Rab3ip | 203 | 1 | Strong | repressed | -21.69 |
| Eya1 | 579 | 4 | Weak | repressed | -21.71 |
| 2810021B 07Rik | 72 | 0 | Adequate | repressed | -21.71 |
| Fam125a | 53 | 0 | Strong | repressed | -21.71 |
| Mpzi1 | 165 | 0 | Strong | repressed | -21.71 |
| Reps1 | 23 | 0 | Strong | repressed | -21.73 |
| Rpia | 47 | 0 | Adequate | repressed | -21.74 |
| 100039707 | 146 | 0 | Adequate | repressed | -21.74 |

| | | | | | |
|---|-----|---|----------|-----------|--------|
| /// Mthfs | | | | | |
| Mlec | 142 | 1 | Adequate | repressed | -21.76 |
| 1300012G 16Rik | 35 | 0 | Strong | repressed | -21.76 |
| Fnta /// LOC10004 6996 | 63 | 0 | Strong | repressed | -21.77 |
| Pgrmc1 | 76 | 0 | Strong | repressed | -21.77 |
| Cops7a | 191 | 0 | Adequate | repressed | -21.80 |
| Prdx6 | 105 | 0 | Adequate | repressed | -21.81 |
| Ext2 | 212 | 0 | Adequate | repressed | -21.82 |
| Prelid2 | 51 | 0 | Weak | repressed | -21.84 |
| Kctd3 | 228 | 1 | Strong | repressed | -21.87 |
| Med31 | 604 | 3 | Strong | repressed | -21.93 |
| Ptpa | 287 | 1 | Strong | repressed | -21.98 |
| Dnajc10 /// LOC10004 7007 | 487 | 5 | Adequate | repressed | -21.98 |
| LOC10004 7604 /// Psmg2 | 441 | 3 | Adequate | repressed | -22.01 |
| Snx12 | 137 | 0 | Adequate | repressed | -22.02 |
| Pofut2 | 23 | 0 | Strong | repressed | -22.06 |
| F2rl1 | 113 | 0 | Adequate | repressed | -22.07 |
| BC023829 /// LOC10004 5774 | 139 | 1 | Adequate | repressed | -22.09 |
| Pgls | 43 | 0 | Strong | repressed | -22.11 |
| Rab32 | 146 | 0 | Adequate | repressed | -22.11 |
| Ripk2 | 254 | 1 | Adequate | repressed | -22.14 |
| Nudt16l1 | 38 | 0 | Adequate | repressed | -22.16 |
| LOC10004 1230 | 38 | 0 | Adequate | repressed | -22.17 |
| Hist1h4a /// Hist1h4b | 24 | 0 | Adequate | repressed | -22.21 |
| Bcas2 | 298 | 3 | Adequate | repressed | -22.23 |
| Ethe1 | 569 | 3 | Strong | repressed | -22.25 |
| LOC10004 6081 /// Otub1 | 57 | 0 | Strong | repressed | -22.29 |
| Chchd7 | 190 | 0 | Adequate | repressed | -22.31 |
| Atg10 | 60 | 0 | Strong | repressed | -22.34 |
| Scap | 310 | 4 | Adequate | repressed | -22.38 |

| | | | | | |
|---|------|---|----------|-----------|--------|
| Colec12 | 142 | 1 | Adequate | repressed | -22.44 |
| I7Rn6 | 259 | 2 | Adequate | repressed | -22.45 |
| Fam118b | 195 | 2 | Adequate | repressed | -22.45 |
| Fam107b | 235 | 0 | Strong | repressed | -22.49 |
| Cdk7 | 105 | 0 | Adequate | repressed | -22.51 |
| Glr3 | 78 | 0 | Strong | repressed | -22.52 |
| Ndufb10 | 163 | 1 | Adequate | repressed | -22.52 |
| Zzz3 | 95 | 2 | Weak | repressed | -22.57 |
| Rfc5 | 69 | 0 | Adequate | repressed | -22.58 |
| Nudt21 | 152 | 1 | Adequate | repressed | -22.59 |
| Cyb561d2 | 139 | 0 | Strong | repressed | -22.60 |
| Tatdn2 | 126 | 0 | Adequate | repressed | -22.60 |
| Ndufs8 | 99 | 0 | Adequate | repressed | -22.62 |
| Rhobtb3 | 394 | 1 | Adequate | repressed | -22.71 |
| Chchd6 | 107 | 0 | Strong | repressed | -22.71 |
| Cotl1 | 191 | 0 | Strong | repressed | -22.72 |
| Entpd4 /// LOC10004 8085 | 239 | 2 | Strong | repressed | -22.73 |
| Mrpl41 | 234 | 0 | Strong | repressed | -22.74 |
| Cacna2d1 | 323 | 1 | Strong | repressed | -22.76 |
| Tmbim4 | 81 | 0 | Strong | repressed | -22.79 |
| Map2k4 | 70 | 0 | Strong | repressed | -22.82 |
| Tm2d3 | 417 | 4 | Strong | repressed | -22.82 |
| Smad7 | 1591 | 3 | Weak | repressed | -22.86 |
| 1810009O 10Rik | 67 | 0 | Adequate | repressed | -22.87 |
| Tapbp | 256 | 1 | Adequate | repressed | -22.88 |
| Adi1 | 70 | 0 | Strong | repressed | -22.89 |
| Tor2a | 57 | 0 | Adequate | repressed | -22.89 |
| Rbac1 | 172 | 1 | Strong | repressed | -22.90 |
| Ptk2 | 312 | 1 | Strong | repressed | -22.94 |
| Rnf181 | 50 | 0 | Strong | repressed | -22.96 |
| Sap18 | 37 | 0 | Weak | repressed | -22.96 |
| Dut | 31 | 0 | Adequate | repressed | -23.00 |
| Mlx | 36 | 0 | Adequate | repressed | -23.01 |
| Wipi1 | 121 | 0 | Adequate | repressed | -23.02 |
| Rnpc3 | 95 | 0 | Adequate | repressed | -23.03 |
| Entpd5 | 90 | 0 | Strong | repressed | -23.06 |
| C77080 | 108 | 1 | Strong | repressed | -23.08 |
| Ptprk | 261 | 1 | Strong | repressed | -23.10 |
| Klc1 | 195 | 1 | Weak | repressed | -23.11 |

| | | | | | |
|-----------------|-----|---|----------|-----------|--------|
| Blnk | 737 | 5 | Adequate | repressed | -23.11 |
| Bckdk | 271 | 2 | Adequate | repressed | -23.14 |
| Ap2m1 | 151 | 0 | Adequate | repressed | -23.17 |
| Fkbp3 | 52 | 0 | Strong | repressed | -23.18 |
| Tdrkh | 116 | 1 | Adequate | repressed | -23.19 |
| Kif24 | 164 | 1 | Strong | repressed | -23.20 |
| Isoc1 | 33 | 0 | Strong | repressed | -23.22 |
| Timm17b | 98 | 1 | Strong | repressed | -23.22 |
| Itgb5 | 296 | 2 | Adequate | repressed | -23.22 |
| Polr3e | 201 | 1 | Strong | repressed | -23.30 |
| Aktip | 275 | 3 | Adequate | repressed | -23.35 |
| Eif4e | 133 | 0 | Strong | repressed | -23.36 |
| Cdipt | 458 | 2 | Adequate | repressed | -23.37 |
| Ly6e | 467 | 5 | Weak | repressed | -23.40 |
| Prdx1 | 116 | 0 | Adequate | repressed | -23.42 |
| Polb | 78 | 0 | Adequate | repressed | -23.47 |
| Kat2a | 66 | 1 | Strong | repressed | -23.53 |
| BC016495 | 95 | 1 | Adequate | repressed | -23.54 |
| Efr3a | 222 | 1 | Adequate | repressed | -23.55 |
| Fundc2 | 34 | 0 | Strong | repressed | -23.58 |
| Ubl4 | 259 | 1 | Adequate | repressed | -23.60 |
| Sar1b | 153 | 0 | Adequate | repressed | -23.61 |
| Ifitm2 | 122 | 1 | Adequate | repressed | -23.66 |
| 25100390 | 139 | 0 | Weak | repressed | -23.68 |
| 18Rik | | | | | |
| Sssca1 | 41 | 0 | Strong | repressed | -23.68 |
| LOC10004 | 430 | 2 | Adequate | repressed | -23.69 |
| 8247 /// | | | | | |
| Pcgf5 | | | | | |
| Sbf1 | 195 | 1 | Strong | repressed | -23.72 |
| Tmem85 | 128 | 1 | Adequate | repressed | -23.72 |
| Prkrip1 | 66 | 0 | Strong | repressed | -23.75 |
| LOC10004 | 69 | 0 | Strong | repressed | -23.77 |
| 1546 /// | | | | | |
| LOC10004 | | | | | |
| Mylc2b | 130 | 0 | Adequate | repressed | -23.82 |
| Stx8 | 43 | 0 | Strong | repressed | -23.83 |
| LOC67752 | 92 | 0 | Adequate | repressed | -23.84 |
| 4 /// | | | | | |
| Rbbp9 | | | | | |
| Mif1 | 156 | 0 | Adequate | repressed | -23.84 |
| Scit1 | 486 | 2 | Strong | repressed | -23.84 |
| Cln8 | 699 | 6 | Adequate | repressed | -23.98 |
| Lypla1 | 92 | 0 | Weak | repressed | -24.03 |

| | | | | | |
|-------------------------------------|-----|---|----------|-----------|--------|
| Papola | 205 | 2 | Adequate | repressed | -24.03 |
| Ggct | 114 | 0 | Strong | repressed | -24.08 |
| Rnase4 | 191 | 0 | Adequate | repressed | -24.11 |
| Hmbs | 179 | 0 | Adequate | repressed | -24.13 |
| N6amt2 | 59 | 0 | Weak | repressed | -24.15 |
| Slc25a14 | 419 | 3 | Adequate | repressed | -24.15 |
| Sgk3 | 346 | 1 | Weak | repressed | -24.21 |
| Slc35f5 | 229 | 1 | Adequate | repressed | -24.23 |
| Kctd20 | 141 | 0 | Adequate | repressed | -24.24 |
| Paip1 | 112 | 0 | Strong | repressed | -24.28 |
| Smn1 | 44 | 0 | Strong | repressed | -24.29 |
| Psmg2 | 108 | 0 | Adequate | repressed | -24.30 |
| Dse | 525 | 2 | Adequate | repressed | -24.31 |
| Creg1 | 53 | 0 | Strong | repressed | -24.34 |
| Pcbp3 | 861 | 7 | Adequate | repressed | -24.40 |
| Casp6 | 95 | 0 | Adequate | repressed | -24.48 |
| Oaf | 287 | 2 | Adequate | repressed | -24.55 |
| Hn1 | 114 | 0 | Adequate | repressed | -24.64 |
| Mapkap1 | 144 | 1 | Strong | repressed | -24.69 |
| Unc50 | 326 | 0 | Adequate | repressed | -24.79 |
| Pxmp3 | 567 | 5 | Adequate | repressed | -24.80 |
| 1200003C 05Rik | 294 | 2 | Strong | repressed | -24.84 |
| Utp23 | 94 | 0 | Adequate | repressed | -25.08 |
| Hist1h1e | 99 | 0 | Adequate | repressed | -25.16 |
| Bnip3 | 113 | 0 | Adequate | repressed | -25.21 |
| Mrpl13 | 178 | 0 | Adequate | repressed | -25.38 |
| Pcolce2 | 194 | 1 | Strong | repressed | -25.41 |
| EG623818 /// Hmbs | 179 | 0 | Adequate | repressed | -25.41 |
| Creld2 | 122 | 0 | Adequate | repressed | -25.43 |
| Plekho2 | 716 | 6 | Weak | repressed | -25.49 |
| Mitd1 | 101 | 0 | Strong | repressed | -25.51 |
| Jmjd4 | 198 | 1 | Adequate | repressed | -25.78 |
| OTTMUSG 000000044 61 | 273 | 2 | Strong | repressed | -25.92 |
| Med29 | 27 | 0 | Strong | repressed | -25.93 |
| Fam120a | 442 | 2 | Strong | repressed | -25.99 |
| Ppm1a | 441 | | Strong | repressed | -26.09 |
| Akirin1 | 203 | 0 | Strong | repressed | -26.09 |
| Rad23a | 100 | 1 | Strong | repressed | -26.21 |

| | | | | | |
|--|-----|---|----------|-----------|--------|
| Acp1 /// LOC63128 6 | 80 | 1 | Strong | repressed | -26.26 |
| Prss23 | 151 | 1 | Strong | repressed | -26.36 |
| Rad17 | 172 | 1 | Adequate | repressed | -26.44 |
| Rgl1 | 142 | 1 | Adequate | repressed | -26.44 |
| Gprc5b | 173 | 1 | Weak | repressed | -26.47 |
| Cetn2 | 128 | 1 | Strong | repressed | -26.48 |
| Bmp2k | 239 | 0 | Adequate | repressed | -26.52 |
| Tbc1d7 | 188 | 3 | Adequate | repressed | -26.57 |
| Rab5c | 206 | 0 | Strong | repressed | -26.57 |
| Slc25a16 | 119 | 1 | Adequate | repressed | -26.72 |
| Rnaseh2c | 36 | 0 | Adequate | repressed | -26.73 |
| Glo1 | 108 | 0 | Strong | repressed | -26.84 |
| Rad23b | 320 | 1 | Adequate | repressed | -26.86 |
| Surf4 | 189 | 0 | Strong | repressed | -26.88 |
| Itfg3 | 168 | 2 | Adequate | repressed | -26.89 |
| Rfc2 | 99 | 0 | Strong | repressed | -26.91 |
| Chid1 | 120 | 2 | Adequate | repressed | -27.12 |
| Orc2l | 399 | 3 | Adequate | repressed | -27.30 |
| Nubp1 | 39 | 0 | Strong | repressed | -27.37 |
| Taf6 | 306 | 2 | Strong | repressed | -27.39 |
| 0610009D 07Rik | 258 | 1 | Strong | repressed | -27.54 |
| Psmc9 | 117 | 0 | Adequate | repressed | -27.55 |
| Igfbp4 | 237 | 1 | Adequate | repressed | -27.56 |
| Rnf13 | 147 | 1 | Adequate | repressed | -27.65 |
| Stim2 | 361 | 0 | Adequate | repressed | -27.66 |
| Tcfe2a | 391 | 3 | Weak | repressed | -27.72 |
| Rab38 | 129 | 0 | Adequate | repressed | -27.88 |
| Cbx3 /// LOC63301 6 | 153 | 1 | Strong | repressed | -28.08 |
| EG623112 /// Stmn1 | 173 | 1 | Strong | repressed | -28.10 |
| Sgcb | 38 | 0 | Strong | repressed | -28.49 |
| Rhod | 81 | 0 | Adequate | repressed | -28.53 |
| Mtmr6 | 129 | 1 | Strong | repressed | -28.65 |
| LOC10004 6080 /// Spin1 | 261 | 1 | Weak | repressed | -28.89 |
| Hgsnat | 33 | 0 | Adequate | repressed | -28.91 |
| Tm7sf3 | 131 | 1 | Adequate | repressed | -29.03 |

| | | | | | |
|---------------------------|-----|---|----------|-----------|--------|
| Rap1a | 170 | 0 | Adequate | repressed | -29.44 |
| Htatip2 | 41 | 0 | Adequate | repressed | -29.64 |
| Vapb | 122 | 0 | Strong | repressed | -29.79 |
| 1110036O 03Rik | 180 | 0 | Strong | repressed | -29.79 |
| Fam134c | 405 | 4 | Weak | repressed | -29.91 |
| Ces7 | 156 | 1 | Strong | repressed | -29.98 |
| Hist1h1c | 79 | 0 | Adequate | repressed | -30.10 |
| Rpgr /// SrpX | 381 | 4 | | repressed | -30.18 |
| Pttg1 | 311 | 3 | Strong | repressed | -30.24 |
| Asb5 | 114 | 0 | Adequate | repressed | -30.26 |
| MtMr14 | 123 | 1 | Adequate | repressed | -30.95 |
| Scara3 | 431 | 1 | Adequate | repressed | -31.76 |
| Ppp3cb | 133 | 1 | Strong | repressed | -33.19 |
| Angptl2 | 534 | 3 | Adequate | repressed | -33.40 |
| Gas1 | 594 | 6 | Adequate | repressed | -36.12 |

REFERENCES

1. Schwanhausser, B., Busse, D., Li, N., Dittmar, G., Schuchhardt, J., Wolf, J., Chen, W., and Selbach, M. (2011) Global quantification of mammalian gene expression control. *Nature* **473**, 337-342
2. Harding, H. P., Novoa, I., Zhang, Y., Zeng, H., Wek, R., Schapira, M., and Ron, D. (2000) Regulated translation initiation controls stress-induced gene expression in mammalian cells. *Mol Cell* **6**, 1099-1108
3. Lu, P. D., Jousse, C., Marciniak, S. J., Zhang, Y., Novoa, I., Scheuner, D., Kaufman, R. J., Ron, D., and Harding, H. P. (2004) Cytoprotection by preemptive conditional phosphorylation of translation initiation factor 2. *The EMBO journal* **23**, 169-179
4. Vatter, K. M., and Wek, R. C. (2004) Reinitiation involving upstream open reading frames regulates *ATF4* mRNA translation in mammalian cells. *Proc Natl Acad Sci U.S.A.* **101**, 11269-11274
5. Harding, H. P., Zhang, Y., Zeng, H., Novoa, I., Lu, P. D., Calton, M., Sadri, N., Yun, C., Popko, B., Paules, R., Stojdl, D. F., Bell, J. C., Hettmann, T., Leiden, J. M., and Ron, D. (2003) An integrated stress response regulates amino acid metabolism and resistance to oxidative stress. *Mol Cell* **11**, 619-633
6. Hinnebusch, A. G. (2005) Translational regulation of GCN4 and the general amino acid control of yeast. *Annu Rev Microbiol* **59**, 407-450
7. Hinnebusch, A. G. (2011) Molecular mechanism of scanning and start codon selection in eukaryotes. *Microbiology and molecular biology reviews : MMBR* **75**, 434-467, first page of table of contents

8. Dang Do, A. N., Kimball, S. R., Cavener, D. R., and Jefferson, L. S. (2009) eIF2alpha kinases GCN2 and PERK modulate transcription and translation of distinct sets of mRNAs in mouse liver. *Physiol Genomics* **38**, 328-341
9. Fernandez, J., Yaman, I., Sarnow, P., Snider, M. D., and Hatzoglou, M. (2002) Regulation of internal ribosomal entry site-mediated translation by phosphorylation of the translation initiation factor eIF2alpha. *The Journal of biological chemistry* **277**, 19198-19205
10. Palam, L. R., Baird, T. D., and Wek, R. C. (2011) Phosphorylation of eIF2 facilitates ribosomal bypass of an inhibitory upstream ORF to enhance CHOP translation. *The Journal of biological chemistry* **286**, 10939-10949
11. Powley, I. R., Kondrashov, A., Young, L. A., Dobbyn, H. C., Hill, K., Cannell, I. G., Stoneley, M., Kong, Y. W., Cotes, J. A., Smith, G. C., Wek, R., Hayes, C., Gant, T. W., Spriggs, K. A., Bushell, M., and Willis, A. E. (2009) Translational reprogramming following UVB irradiation is mediated by DNA-PKcs and allows selective recruitment to the polysomes of mRNAs encoding DNA repair enzymes. *Genes & development* **23**, 1207-1220
12. Dey, S., Baird, T. D., Spandau, D. F., and Wek, R. C. (2010) Coupled transcriptional and translational regulation of ATF4 is central to the Integrated Stress Response. *Manuscript in preparation*
13. Jackson, R. J., Hellen, C. U., and Pestova, T. V. (2010) The mechanism of eukaryotic translation initiation and principles of its regulation. *Nature reviews. Molecular cell biology* **11**, 113-127
14. Sonenberg, N., and Hinnebusch, A. G. (2009) Regulation of translation initiation in eukaryotes: mechanisms and biological targets. *Cell* **136**, 731-745
15. Carthew, R. W., and Sontheimer, E. J. (2009) Origins and Mechanisms of miRNAs and siRNAs. *Cell* **136**, 642-655

16. Wilkie, G. S., Dickson, K. S., and Gray, N. K. (2003) Regulation of mRNA translation by 5'- and 3'-UTR-binding factors. *Trends Biochem Sci* **28**, 182-188
17. Shyu, A. B., Wilkinson, M. F., and van Hoof, A. (2008) Messenger RNA regulation: to translate or to degrade. *The EMBO journal* **27**, 471-481
18. Algire, M. A., Maag, D., and Lorsch, J. R. (2005) Pi release from eIF2, not GTP hydrolysis, is the step controlled by start-site selection during eukaryotic translation initiation. *Mol Cell* **20**, 251-262
19. Pavitt, G. D., Ramaiah, K. V., Kimball, S. R., and Hinnebusch, A. G. (1998) eIF2 independently binds two distinct eIF2B subcomplexes that catalyze and regulate guanine-nucleotide exchange. *Genes & development* **12**, 514-526
20. Gomez, E., Mohammad, S. S., and Pavitt, G. D. (2002) Characterization of the minimal catalytic domain within eIF2B: the guanine-nucleotide exchange factor for translation initiation. *The EMBO journal* **21**, 5292-5301
21. Krishnamoorthy, T., Pavitt, G. D., Zhang, F., Dever, T. E., and Hinnebusch, A. G. (2001) Tight binding of the phosphorylated α subunit of initiation factor 2 (eIF2 α) to the regulatory subunits of guanine nucleotide exchange factor eIF2B is required for inhibition of translation initiation. *Molecular and cellular biology* **21**, 5018-5030
22. Kimball, S. R., Fabian, J. R., Pavitt, G. D., Hinnebusch, A. G., and Jefferson, L. S. (1998) Regulation of guanine nucleotide exchange through phosphorylation of eukaryotic initiation factor eIF2 α . Role of the α - and δ -subunits of eIF2b. *The Journal of biological chemistry* **273**, 12841-12845
23. Zoncu, R., Efeyan, A., and Sabatini, D. M. (2011) mTOR: from growth signal integration to cancer, diabetes and ageing. *Nature reviews. Molecular cell biology* **12**, 21-35

24. Ma, X. M., and Blenis, J. (2009) Molecular mechanisms of mTOR-mediated translational control. *Nature reviews. Molecular cell biology* **10**, 307-318
25. Mamane, Y., Petroulakis, E., LeBacquer, O., and Sonenberg, N. (2006) mTOR, translation initiation and cancer. *Oncogene* **25**, 6416-6422
26. Thoreen, C. C., Chantranupong, L., Keys, H. R., Wang, T., Gray, N. S., and Sabatini, D. M. (2012) A unifying model for mTORC1-mediated regulation of mRNA translation. *Nature* **485**, 109-113
27. Shahbazian, D., Parsyan, A., Petroulakis, E., Hershey, J., and Sonenberg, N. (2010) eIF4B controls survival and proliferation and is regulated by proto-oncogenic signaling pathways. *Cell cycle* **9**, 4106-4109
28. Shahbazian, D., Roux, P. P., Mieulet, V., Cohen, M. S., Raught, B., Taunton, J., Hershey, J. W., Blenis, J., Pende, M., and Sonenberg, N. (2006) The mTOR/PI3K and MAPK pathways converge on eIF4B to control its phosphorylation and activity. *The EMBO journal* **25**, 2781-2791
29. Wek, R. C., Jiang, H. Y., and Anthony, T. G. (2006) Coping with stress: eIF2 kinases and translational control. *Biochem Soc Trans* **34**, 7-11
30. Walter, P., and Ron, D. (2011) The unfolded protein response: from stress pathway to homeostatic regulation. *Science* **334**, 1081-1086
31. Schroder, M., and Kaufman, R. J. (2005) The mammalian unfolded protein response. *Annu Rev Biochem* **74**, 739-789
32. Han, A., Yu, C., Lu, L., Fujiwara, Y., Browne, C., Chin, G., Fleming, P., Leboulch, P., Orkin, S. H., and Chen, J.-J. (2001) Heme-regulated eIF2 α kinase (HRI) is required for translational regulation and survival of erythroid precursors in iron deficiency. *The EMBO journal* **20**, 6909-6918
33. Chen, J. J. (2007) Regulation of protein synthesis by the heme-regulated eIF2 α kinase: relevance to anemias. *Blood* **109(7):2693-9**.

34. Dey, M., Cao, C., Dar, A. C., Tamura, T., Ozato, K., Sicheri, F., and Dever, T. E. (2005) Mechanistic link between PKR dimerization, autophosphorylation, and eIF2alpha substrate recognition. *Cell* **122**, 901-913
35. García MA, M. E., Esteban M. (2007) The dsRNA protein kinase PKR: virus and cell control. *Biochimie*. **89(6-7):799-811**.
36. Pindel, A., and Sadler, A. (2011) The role of protein kinase R in the interferon response. *Journal of interferon & cytokine research : the official journal of the International Society for Interferon and Cytokine Research* **31**, 59-70
37. Rothenburg, S., Seo, E. J., Gibbs, J. S., Dever, T. E., and Dittmar, K. (2009) Rapid evolution of protein kinase PKR alters sensitivity to viral inhibitors. *Nature structural & molecular biology* **16**, 63-70
38. Wek, S. A., Zhu, S., and Wek, R. C. (1995) The histidyl-tRNA synthetase-related sequence in eIF-2 alpha protein kinase GCN2 interacts with tRNA and is required for activation in response to starvation for different amino acids. *Molecular and cellular biology* **15**, 4497-4506
39. Dong, J., Qiu, H., Garcia-Barrio, M., Anderson, J., and Hinnebusch, A. G. (2000) Uncharged tRNA activates GCN2 by displacing the protein kinase moiety from a bipartite tRNA-binding domain. *Mol Cell* **6**, 269-279
40. Wek, R. C., Jackson, B. M., and Hinnebusch, A. G. (1989) Juxtaposition of domains homologous to protein kinases and histidyl-tRNA synthetases in GCN2 protein suggests a mechanism for coupling *GCN4* expression to amino acid availability. *Proc Natl Acad Sci U.S.A.* **86**, 4579-4583
41. Garriz, A., Qiu, H., Dey, M., Seo, E. J., Dever, T. E., and Hinnebusch, A. G. (2009) A network of hydrophobic residues impeding helix alphaC rotation maintains latency of kinase Gcn2, which phosphorylates the alpha subunit of translation initiation factor 2. *Molecular and cellular biology* **29**, 1592-1607

42. Padyana, A. K., Qiu, H., Roll-Mecak, A., Hinnebusch, A. G., and Burley, S. K. (2005) Structural basis for autoinhibition and mutational activation of eukaryotic initiation factor 2alpha protein kinase GCN2. *The Journal of biological chemistry* **280**, 29289-29299
43. Qiu, H., Hu, C., Dong, J., and Hinnebusch, A. G. (2002) Mutations that bypass tRNA binding activate the intrinsically defective kinase domain in GCN2. *Genes & development* **16**, 1271-1280
44. Pali, S. S., Kays, C. E., Deval, C., Bruhat, A., Fafournoux, P., and Kilberg, M. S. (2008) Specificity of amino acid regulated gene expression: analysis of genes subjected to either complete or single amino acid deprivation. *Amino Acids*
45. Reinert, R. B., Oberle, L. M., Wek, S. A., Bunpo, P., Wang, X. P., Mileva, I., Goodwin, L. O., Aldrich, C. J., Durden, D. L., McNurlan, M. A., Wek, R. C., and Anthony, T. G. (2006) Role of glutamine depletion in directing tissue-specific nutrient stress responses to L-asparaginase. *The Journal of biological chemistry* **281**, 31222-31233
46. Anthony, T. G., McDaniel, B. J., Byerley, R. L., McGrath, B. C., Cavener, D. R., McNurlan, M. A., and Wek, R. C. (2004) Preservation of liver protein synthesis during dietary leucine deprivation occurs at the expense of skeletal muscle mass in mice deleted for eIF2 kinase GCN2. *The Journal of biological chemistry* **279**, 36553-36561
47. Bunpo, P., Dudley, A., Cundiff, J. K., Cavener, D. R., Wek, R. C., and Anthony, T. G. (2009) GCN2 protein kinase is required to activate amino acid deprivation responses in mice treated with the anti-cancer agent L-asparaginase. *The Journal of biological chemistry* **284**, 32742-32749
48. Habibi, D., Ogloff, N., Jalili, R. B., Yost, A., Weng, A. P., Ghahary, A., and Ong, C. J. (2012) Borrelidin, a small molecule nitrile-containing macrolide inhibitor of

- threonyl-tRNA synthetase, is a potent inducer of apoptosis in acute lymphoblastic leukemia. *Investigational new drugs* **30**, 1361-1370
49. Usui, T., Nagumo, Y., Watanabe, A., Kubota, T., Komatsu, K., Kobayashi, J., and Osada, H. (2006) Brasilicardin A, a natural immunosuppressant, targets amino Acid transport system L. *Chemistry & biology* **13**, 1153-1160
 50. Broer, A., Juelich, T., Vanslambrouck, J. M., Tietze, N., Solomon, P. S., Holst, J., Bailey, C. G., Rasko, J. E., and Broer, S. (2011) Impaired nutrient signaling and body weight control in a Na⁺ neutral amino acid cotransporter (Slc6a19)-deficient mouse. *The Journal of biological chemistry* **286**, 26638-26651
 51. Marion, V., Sankaranarayanan, S., de Theije, C., van Dijk, P., Lindsey, P., Lamers, M. C., Harding, H. P., Ron, D., Lamers, W. H., and Kohler, S. E. (2011) Arginine deficiency causes runting in the suckling period by selectively activating the stress kinase GCN2. *The Journal of biological chemistry* **286**, 8866-8874
 52. Lanker, S., Bushman, J. L., Hinnebusch, A. G., Trachsel, H., and Mueller, P. P. (1992) Autoregulation of the yeast lysyl-tRNA synthetase gene GCD5/KRS1 by translational and transcriptional control mechanisms. *Cell* **70**, pp. 647-657
 53. Guo, F., and Cavener, D. R. (2007) The GCN2 eIF2alpha kinase regulates fatty-acid homeostasis in the liver during deprivation of an essential amino acid. *Cell Metab* **5**, 103-114
 54. Eyries, M., Montani, D., Girerd, B., Perret, C., Leroy, A., Lonjou, C., Chelghoum, N., Coulet, F., Bonnet, D., Dorfmueller, P., Fadel, E., Sitbon, O., Simonneau, G., Tregouet, D. A., Humbert, M., and Soubrier, F. (2014) EIF2AK4 mutations cause pulmonary veno-occlusive disease, a recessive form of pulmonary hypertension. *Nature genetics* **46**, 65-69

55. Deng, J., Harding, H., Raught, B., Gingras, A., Berlanga, J., Scheuner, D., Kaufman, R., Ron, D., and Sonenberg, N. (2002) Activation of GCN2 in UV-irradiated cells inhibits translation. *Curr Biol* **12**, 1279-1286
56. Jiang, H. Y., and Wek, R. C. (2005) Gcn2 phosphorylation of eIF2a activates NF- κ B in response to UV irradiation. *Biochem J* **385**, 371-380
57. Jiang, H. Y., and Wek, R. C. (2005) Phosphorylation of the α -subunit of the eukaryotic initiation factor -2 (eIF2a) reduces protein synthesis and enhances apoptosis in response to proteasome inhibition. *The Journal of biological chemistry* **280**, 14189-14202
58. Peidis, P., Papadakis, A. I., Rajesh, K., and Koromilas, A. E. (2010) HDAC pharmacological inhibition promotes cell death through the eIF2 α kinases PKR and GCN2. *Aging* **2**, 669-677
59. Neznanov, N., Dragunsky, E. M., Chumakov, K. M., Neznanova, L., Wek, R. C., Gudkov, A. V., and Banerjee, A. K. (2008) Different effect of proteasome inhibition on vesicular stomatitis virus and poliovirus replication. *PloS one* **3**, e1887
60. Yang, R., Wek, S. A., and Wek, R. C. (2000) Glucose limitation induces GCN4 translation by activation of Gcn2 protein kinase. *Molecular and cellular biology* **20**, 2706-2717
61. Ye, J., Kumanova, M., Hart, L. S., Sloane, K., Zhang, H., De Panis, D. N., Bobrovnikova-Marjon, E., Diehl, J. A., Ron, D., and Koumenis, C. (2010) The GCN2-ATF4 pathway is critical for tumour cell survival and proliferation in response to nutrient deprivation. *The EMBO journal* **29**, 2082-2096
62. Cai, Q., and Brooks, H. L. (2011) Phosphorylation of eIF2 α via the general control kinase, GCN2, modulates the ability of renal medullary cells to survive

- high urea stress. *American journal of physiology. Renal physiology* **301**, F1202-1207
63. Zhu, S., Sobolev, A. Y., and Wek, R. C. (1996) Histidyl-tRNA synthetase-related sequences in GCN2 protein kinase regulate in vitro phosphorylation of eIF-2. *The Journal of biological chemistry* **271**, 24989-24994
64. Narasimhan, J., Staschke, K. A., and Wek, R. C. (2004) Dimerization is required for activation of eIF2 kinase Gcn2 in response to diverse environmental stress conditions. *The Journal of biological chemistry* **279**, 22820-22832
65. Zaborske, J. M., Narasimhan, J., Jiang, L., Wek, S. A., Dittmar, K. A., Freimoser, F., Pan, T., and Wek, R. C. (2009) Genome-wide analysis of tRNA charging and activation of the eIF2 kinase Gcn2p. *The Journal of biological chemistry* **284**, 25254-25267
66. Garcia-Barrio, M., Dong, J., Ulfano, S., and Hinnebusch, A. G. (2000) Association of GCN1-GCN20 regulatory complex with the N-terminus of eIF2alpha kinase GCN2 is required for GCN2 activation. *The EMBO journal* **19**, 1887-1899
67. Kubota, H., Sakaki, Y., and Ito, T. (2000) GI domain-mediated association of the eukaryotic initiation factor 2alpha kinase GCN2 with its activator GCN1 is required for general amino acid control in budding yeast. *Journal of Biological Chemistry* **275**, 20243-20246
68. Kubota, H., Ota, K., Sakaki, Y., and Ito, T. (2001) Budding yeast GCN1 binds the GI domain to activate the eIF2alpha kinase GCN2. *The Journal of biological chemistry* **276**, 17591-17596
69. Marton, M. J., Crouch, D., and Hinnebusch, A. G. (1993) GCN1, a translational activator of GCN4 in *Saccharomyces cerevisiae*, is required for phosphorylation

- of eukaryotic translation initiation factor 2 by protein kinase GCN2. *Molecular and cellular biology* **13**, 3541-3556
70. Marton, M. J., Vazquez de Aldana, C. R., Qui, H., Chakraborty, K., and Hinnebusch, A. G. (1997) Evidence that GCN1 and GCN20, translational regulators of GCN4, function on elongating ribosomes in activation of eIF-2alpha kinase GCN2. *Molecular and cellular biology* **17**, 4474-4489
71. Sattlegger, E., and Hinnebusch, A. G. (2000) Separate domains in GCN1 for binding protein kinase GCN2 and ribosome are required for GCN2 activation in amino acid-starved cells. *EMBO Journal* **19**, 6622-6633
72. Bittencourt, S., Pereira, C. M., Avedissian, M., Delamano, A., Mello, L. E., and Castilho, B. A. (2008) Distribution of the protein IMPACT, an inhibitor of GCN2, in the mouse, rat, and marmoset brain. *The Journal of comparative neurology* **507**, 1811-1830
73. Pereira, C. M., Sattlegger, E., Jiang, H. Y., Longo, B. M., Jaqueta, C. B., Hinnebusch, A. G., Wek, R. C., Mello, L. E., and Castilho, B. A. (2005) IMPACT, a protein preferentially expressed in the mouse brain, binds GCN1 and inhibits GCN2 activation. *Journal of Biological Chemistry* **280**, 28316-28323
74. Sattlegger, E., Swanson, M. J., Ashcraft, E. A., Jennings, J. L., Fekete, R. A., Link, A. J., and Hinnebusch, A. G. (2004) YIH1 is an actin-binding protein that inhibits protein kinase GCN2 and impairs general amino acid control when overexpressed. *The Journal of biological chemistry* **279**, 29952-29962
75. Harding, H. P., Zhang, Y., and Ron, D. (1999) Protein translation and folding are coupled by an endoplasmic-reticulum-resident kinase. *Nature* **397**, 271-274
76. Shi, Y., Vattam, K. M., Sood, R., An, J., Liang, J., Stramm, L., and Wek, R. C. (1998) Identification and characterization of pancreatic eukaryotic initiation factor

- 2 a-subunit kinase, PEK, involved in translation control. *Molecular and cellular biology* **18**, 7499-7509
77. Ma, K., Vatter, K. M., and Wek, R. C. (2002) Dimerization and release of molecular chaperone inhibition facilitate activation of eukaryotic initiation factor-2 kinase in response to endoplasmic reticulum stress. *The Journal of biological chemistry* **277**, 18728-18735
78. Bertolotti, A., Zhang, Y., Hendershot, L. M., Harding, H. P., and Ron, D. (2000) Dynamic interaction of BiP and ER stress transducers in the unfolded protein response. *Nature cell biology* **2**, 326-332
79. Malhi, H., and Kaufman, R. J. (2011) Endoplasmic reticulum stress in liver disease. *Journal of hepatology* **54**, 795-809
80. Scheuner, D., and Kaufman, R. J. (2008) The unfolded protein response: a pathway that links insulin demand with beta-cell failure and diabetes. *Endocr Rev* **29**, 317-333
81. Hotamisligil, G. S. (2010) Endoplasmic reticulum stress and the inflammatory basis of metabolic disease. *Cell* **140**, 900-917
82. Osowski, C. M., and Urano, F. (2010) A switch from life to death in endoplasmic reticulum stressed beta-cells. *Diabetes, obesity & metabolism* **12 Suppl 2**, 58-65
83. Marciniak, S. J., and Ron, D. (2006) Endoplasmic reticulum stress signaling in disease. *Physiol Rev* **86**, 1133-1149
84. Delepine, M., Nicolino, M., Barrett, T., Golamaully, M., Lathrop, G. M., and Julier, C. (2000) EIF2AK3, encoding translation initiation factor 2-a kinase 3, is mutated in patients with Wolcott-Rallison syndrome. *Nature genetics* **25**, 406-409
85. Julier, C., and Nicolino, M. (2010) Wolcott-Rallison syndrome. *Orphanet J Rare Dis* **5**, 29

86. Senee, V., Vатtem, K. M., Delepine, M., Rainbow, L. A., Haton, C., Lecoq, A., Shaw, N. J., Robert, J. J., Rоoman, R., Diatloff-Zito, C., Michaud, J. L., Bin-Abbas, B., Taha, D., Zabel, B., Franceschini, P., Topaloglu, A. K., Lathrop, G. M., Barrett, T. G., Nicolino, M., Wek, R. C., and Julier, C. (2004) Wolcott-Rallison Syndrome: clinical, genetic, and functional study of EIF2AK3 mutations and suggestion of genetic heterogeneity. *Diabetes* **53**, 1876-1883
87. Wolcott, C. D., and Rallison, M. L. (1972) Infancy-onset diabetes mellitus and multiple epiphyseal dysplasia. *The Journal of pediatrics* **80**, 292-297
88. Ron, D., and Walter, P. (2007) Signal integration in the endoplasmic reticulum unfolded protein response. *Nature reviews. Molecular cell biology* **8**, 519-529
89. Credle, J. J., Finer-Moore, J. S., Papa, F. R., Stroud, R. M., and Walter, P. (2005) On the mechanism of sensing unfolded protein in the endoplasmic reticulum. *Proc Natl Acad Sci U S A* **102**, 18773-18784
90. Gardner, B. M., and Walter, P. (2011) Unfolded proteins are Ire1-activating ligands that directly induce the unfolded protein response. *Science* **333**, 1891-1894
91. Li, H., Korennykh, A. V., Behrman, S. L., and Walter, P. (2010) Mammalian endoplasmic reticulum stress sensor IRE1 signals by dynamic clustering. *Proc Natl Acad Sci U S A* **107**, 16113-16118
92. Korennykh, A. V., Egea, P. F., Korostelev, A. A., Finer-Moore, J., Zhang, C., Shokat, K. M., Stroud, R. M., and Walter, P. (2009) The unfolded protein response signals through high-order assembly of Ire1. *Nature* **457**, 687-693
93. Munzarova, V., Panek, J., Gunisova, S., Danyi, I., Szamecz, B., and Valasek, L. S. (2011) Translation reinitiation relies on the interaction between eIF3a/TIF32 and progressively folded cis-acting mRNA elements preceding short uORFs. *PLoS genetics* **7**, e1002137

94. Szamecz, B., Rutkai, E., Cuchalova, L., Munzarova, V., Herrmannova, A., Nielsen, K. H., Burela, L., Hinnebusch, A. G., and Valasek, L. (2008) eIF3a cooperates with sequences 5' of uORF1 to promote resumption of scanning by post-termination ribosomes for reinitiation on GCN4 mRNA. *Genes & development* **22**, 2414-2425
95. Kilberg, M. S., Shan, J., and Su, N. (2009) ATF4-dependent transcription mediates signaling of amino acid limitation. *Trends in endocrinology and metabolism: TEM* **20**, 436-443
96. Fawcett, T. W., Martindale, J. L., Guyton, K. Z., Hai, T., and Holbrook, N. J. (1999) Complexes containing activating transcription factor (ATF)/cAMP-responsive-element-binding-protein (CREB) interact with the CCAAT/enhancer-binding protein (C/EBP)-ATF composite site to regulate Gadd153 expression during the stress response. *Biochemical Journal* **339**, 135-141
97. Teske, B. F., Wek, S. A., Bunpo, P., Cundiff, J. K., McClintick, J. N., Anthony, T. G., and Wek, R. C. (2011) The eIF2 kinase PERK and the integrated stress response facilitate activation of ATF6 during endoplasmic reticulum stress. *Molecular biology of the cell* **22**, 4390-4405
98. Rouschop, K. M., van den Beucken, T., Dubois, L., Niessen, H., Bussink, J., Savelkoul, K., Keulers, T., Mujcic, H., Landuyt, W., Voncken, J. W., Lambin, P., van der Kogel, A. J., Koritzinsky, M., and Wouters, B. G. (2010) The unfolded protein response protects human tumor cells during hypoxia through regulation of the autophagy genes MAP1LC3B and ATG5. *The Journal of clinical investigation* **120**, 127-141
99. Rzymiski, T., Milani, M., Pike, L., Buffa, F., Mellor, H. R., Winchester, L., Pires, I., Hammond, E., Ragoussis, I., and Harris, A. L. (2010) Regulation of autophagy by ATF4 in response to severe hypoxia. *Oncogene* **29**, 4424-4435

100. Jiang, H. Y., Wek, S. A., McGrath, B. C., Lu, D., Hai, T., Harding, H. P., Wang, X., Ron, D., Cavener, D. R., and Wek, R. C. (2004) Activating transcription factor 3 is integral to the eukaryotic initiation factor 2 kinase stress response. *Molecular and cellular biology* **24**, 1365-1377
101. Kilberg, M. S., Pan, Y. X., Chen, H., and Leung-Pineda, V. (2005) Nutritional control of gene expression: how mammalian cells respond to amino acid limitation. *Annual review of nutrition* **25**, 59-85
102. Chen, H., Pan, Y. X., Dudenhausen, E. E., and Kilberg, M. S. (2004) Amino acid deprivation induces the transcription rate of the human asparagine synthetase gene through a timed program of expression and promoter binding of nutrient-responsive basic region/leucine zipper transcription factors as well as localized histone acetylation. *The Journal of biological chemistry* **279**, 50829-50839
103. Marciniak, S. J., Yun, C. Y., Oyadomari, S., Novoa, I., Zhang, Y., Jungreis, R., Nagata, K., Harding, H. P., and Ron, D. (2004) CHOP induces death by promoting protein synthesis and oxidation in the stressed endoplasmic reticulum. *Genes & development* **18**, 3066-3077
104. Kojima, E., Takeuchi, A., Haneda, M., Yagi, A., Hasegawa, T., Yamaki, K., Takeda, K., Akira, S., Shimokata, K., and Isobe, K. (2003) The function of GADD34 is a recovery from a shutoff of protein synthesis induced by ER stress: elucidation by GADD34-deficient mice. *FASEB journal : official publication of the Federation of American Societies for Experimental Biology* **17**, 1573-1575
105. Novoa, I., Zeng, H., Harding, H. P., and Ron, D. (2001) Feedback inhibition of the unfolded protein response by GADD34-mediated dephosphorylation of eIF2alpha. *J Cell Biol* **153**, 1011-1022

106. Novoa, I., Zhang, Y., Zeng, H., Jungreis, R., Harding, H. P., and Ron, D. (2003) Stress-induced gene expression requires programmed recovery from translational repression. *The EMBO journal* **22**, 1180-1187
107. Brush, M. H., Weiser, D. C., and Shenolikar, S. (2003) Growth arrest and DNA damage-inducible protein GADD34 targets protein phosphatase 1 alpha to the endoplasmic reticulum and promotes dephosphorylation of the alpha subunit of eukaryotic translation initiation factor 2. *Molecular and cellular biology* **23**, 1292-1303
108. Ma, Y., and Hendershot, L. M. (2003) Delineation of a negative feedback regulatory loop that controls protein translation during endoplasmic reticulum stress. *The Journal of biological chemistry* **278**, 34864-34873
109. Masuoka, H. C., and Townes, T. M. (2002) Targeted disruption of the activating transcription factor 4 gene results in severe fetal anemia in mice. *Blood* **99**, 736-745
110. Hettmann, T., Barton, K., and Leiden, J. M. (2000) Microphthalmia due to p53-mediated apoptosis of anterior lens epithelial cells in mice lacking the CREB-2 transcription factor. *Developmental Biology* **222**, 110-123
111. Firtina, Z., and Duncan, M. K. (2011) Unfolded Protein Response (UPR) is activated during normal lens development. *Gene expression patterns : GEP* **11**, 135-143
112. Yang, X., Matsuda, K., Bialek, P., Jacquot, S., Masuoka, H. C., Schinke, T., Li, L., Brancorsini, S., Sassone-Corsi, P., Townes, T. M., Hanauer, A., and Karsenty, G. (2004) ATF4 is a substrate of RSK2 and an essential regulator of osteoblast biology; implication for Coffin-Lowry Syndrome. *Cell* **117**, 387-398
113. Eleftheriou, F., Benson, M. D., Sowa, H., Starbuck, M., Liu, X., Ron, D., Parada, L. F., and Karsenty, G. (2006) ATF4 mediation of NF1 functions in osteoblast

- reveals a nutritional basis for congenital skeletal dysplasias. *Cell Metab* **4**, 441-451
114. Seo, J., Fortuno, E. S., 3rd, Suh, J. M., Stenesen, D., Tang, W., Parks, E. J., Adams, C. M., Townes, T., and Graff, J. M. (2009) Atf4 regulates obesity, glucose homeostasis, and energy expenditure. *Diabetes* **58**, 2565-2573
115. Back, S. H., Scheuner, D., Han, J., Song, B., Ribick, M., Wang, J., Gildersleeve, R., Subramaniam, P., and Kaufman, R. J. (2009) Translation attenuation through eIF2a phosphorylation preserves ER integrity, prevents oxidative stress, and maintains insulin production in beta cells. *Cell Metab* **in press**
116. Oyadomari, S., Harding, H. P., Zhang, Y., Oyadomari, M., and Ron, D. (2008) Dephosphorylation of translation initiation factor 2alpha enhances glucose tolerance and attenuates hepatosteatosis in mice. *Cell Metab* **7**, 520-532
117. Rutkowski, D. T., Wu, J., Back, S. H., Callaghan, M. U., Ferris, S. P., Iqbal, J., Clark, R., Miao, H., Hassler, J. R., Fornek, J., Katze, M. G., Hussain, M. M., Song, B., Swathirajan, J., Wang, J., Yau, G. D., and Kaufman, R. J. (2008) UPR pathways combine to prevent hepatic steatosis caused by ER stress-mediated suppression of transcriptional master regulators. *Dev Cell* **15**, 829-840
118. Song, B., Scheuner, D., Ron, D., Pennathur, S., and Kaufman, R. J. (2008) Chop deletion reduces oxidative stress, improves beta cell function, and promotes cell survival in multiple mouse models of diabetes. *The Journal of clinical investigation* **118**, 3378-3389
119. Hansen, M. B., Mitchelmore, C., Kjaerulff, K. M., Rasmussen, T. E., Pedersen, K. M., and Jensen, N. A. (2002) Mouse *ATF5*: Molecular cloning of two novel mRNAs, genomic organization, and odorant sensory neuron localization. *Genomics* **80**, 344-350

120. Zhou, D., Palam, L. R., Jiang, L., Narasimhan, J., Staschke, K. A., and Wek, R. C. (2008) Phosphorylation of eIF2 directs ATF5 translational control in response to diverse stress conditions. *The Journal of biological chemistry* **283**, 7064-7073
121. Watatani, Y., Ichikawa, K., Nakanishi, N., Fujimoto, M., Takeda, H., Kimura, N., Hirose, H., Takahashi, S., and Takahashi, Y. (2007) Stress-induced translation of ATF5 mRNA is regulated by the 5' untranslated region. *The Journal of biological chemistry*
122. Arias, A., Lame, M. W., Santarelli, L., Hen, R., Greene, L. A., and Angelastro, J. M. (2012) Regulated ATF5 loss-of-function in adult mice blocks formation and causes regression/eradication of gliomas. *Oncogene* **31**, 739-751
123. Greene, L. A., Lee, H. Y., and Angelastro, J. M. (2009) The transcription factor ATF5: role in neurodevelopment and neural tumors. *Journal of neurochemistry* **108**, 11-22
124. Ma, Y., Brewer, J. W., Diehl, J. A., and Hendershot, L. M. (2002) Two distinct stress signaling pathways converge upon the CHOP promoter during the mammalian unfolded protein response. *J Mol Biol* **318**, 1351-1365
125. Averous, J., Bruhat, A., Jousse, C., Carraro, V., Thiel, G., and Fafournoux, P. (2004) Induction of CHOP expression by amino acid limitation requires both ATF4 expression and ATF2 phosphorylation. *Journal of Biological Chemistry* **279**, 5288-5297
126. Jousse, C., Bruhat, A., Carraro, V., Urano, F., Ferrara, M., Ron, D., and Fafournoux, P. (2001) Inhibition of CHOP translation by a peptide encoded by an open reading frame localized in the chop 5'UTR. *Nucleic acids research* **29**, 4341-4351
127. Lee, H. C., Chen, Y. J., Liu, Y. W., Lin, K. Y., Chen, S. W., Lin, C. Y., Lu, Y. C., Hsu, P. C., Lee, S. C., and Tsai, H. J. (2011) Transgenic zebrafish model to

- study translational control mediated by upstream open reading frame of human chop gene. *Nucleic acids research* **39**, e139
128. Chen, Y. J., Tan, B. C., Cheng, Y. Y., Chen, J. S., and Lee, S. C. (2009) Differential regulation of CHOP translation by phosphorylated eIF4E under stress conditions. *Nucleic acids research*
129. Kozak, M. (1987) An analysis of 5'-noncoding sequences from 699 vertebrate messenger RNAs. *Nucleic acids research* **15**, 8125-8148
130. Lee, Y. Y., Cevallos, R. C., and Jan, E. (2009) An upstream open reading frame regulates translation of GADD34 during cellular stresses that induce eIF2alpha phosphorylation. *The Journal of biological chemistry* **284**, 6661-6673
131. Sherrill, K. W., Byrd, M. P., Van Eden, M. E., and Lloyd, R. E. (2004) BCL-2 translation is mediated via internal ribosome entry during cell stress. *The Journal of biological chemistry* **279**, 29066-29074
132. Riley, A., Jordan, L. E., and Holcik, M. (2010) Distinct 5' UTRs regulate XIAP expression under normal growth conditions and during cellular stress. *Nucleic acids research* **38**, 4665-4674
133. Lang, K. J., Kappel, A., and Goodall, G. J. (2002) Hypoxia-inducible factor-1alpha mRNA contains an internal ribosome entry site that allows efficient translation during normoxia and hypoxia. *Molecular biology of the cell* **13**, 1792-1801
134. Fernandez, J., Yaman, I., Huang, C., Liu, H., Lopez, A. B., Komar, A. A., Caprara, M. G., Merrick, W. C., Snider, M. D., Kaufman, R. J., Lamers, W. H., and Hatzoglou, M. (2005) Ribosome stalling regulates IRES-mediated translation in eukaryotes, a parallel to prokaryotic attenuation. *Mol Cell* **17**, 405-416
135. Wilson, J. E., Pestova, T. V., Hellen, C. U., and Sarnow, P. (2000) Initiation of protein synthesis from the A site of the ribosome. *Cell* **102**, 511-520

136. Dey, S., Baird, T. D., Zhou, D., Palam, L. R., Spandau, D. F., and Wek, R. C. (2010) Both transcriptional regulation and translational control of ATF4 is central to the Integrated Stress Response. *The Journal of biological chemistry*
137. Rutkowski DT, A. S., Miller CN, Wu J, Li J, Gunnison KM, Mori K, Sadighi Akha AA, Raden D, Kaufman RJ. (2006) Adaptation to ER stress is mediated by differential stabilities of pro-survival and pro-apoptotic mRNAs and proteins. *PLoS Biol.* **4(11):e374.**
138. Kumar, R., Krause, G. S., Yoshida, H., Mori, K., and DeGracia, D. J. (2003) Dysfunction of the unfolded protein response during global brain ischemia and reperfusion. *J Cereb Blood Flow Metab* **23**, 462-471
139. Puri, P., Mirshahi, F., Cheung, O., Natarajan, R., Maher, J. W., Kellum, J. M., and Sanyal, A. J. (2008) Activation and dysregulation of the unfolded protein response in nonalcoholic fatty liver disease. *Gastroenterology* **134**, 568-576
140. Dey, S., Savant, S., Teske, B. F., Hatzoglou, M., Calkhoven, C. F., and Wek, R. C. (2012) Transcriptional repression of ATF4 gene by CCAAT/enhancer-binding protein beta (C/EBPbeta) differentially regulates integrated stress response. *The Journal of biological chemistry* **287**, 21936-21949
141. Adachi, Y., Yamamoto, K., Okada, T., Yoshida, H., Harada, A., and Mori, K. (2008) ATF6 is a transcription factor specializing in the regulation of quality control proteins in the endoplasmic reticulum. *Cell Struct Funct* **33**, 75-89
142. Armstrong, J. L., Flockhart, R., Veal, G. J., Lovat, P. E., and Redfern, C. P. (2010) Regulation of endoplasmic reticulum stress-induced cell death by ATF4 in neuroectodermal tumor cells. *The Journal of biological chemistry* **285**, 6091-6100
143. Siu, F., Blain, P. J., LeBlanc-Chaffin, R., Chen, H., and Kilberg, M. S. (2002) ATF4 is a mediator of the nutrient-sensing response pathway that activates the

- human asparagine synthetase gene. *The Journal of biological chemistry* **277**, 24120-24127
144. Afonyushkin, T., Oskolkova, O. V., Philippova, M., Resink, T. J., Erne, P., Binder, B. R., and Bochkov, V. N. (2010) Oxidized phospholipids regulate expression of ATF4 and VEGF in endothelial cells via NRF2-dependent mechanism: novel point of convergence between electrophilic and unfolded protein stress pathways. *Arteriosclerosis, thrombosis, and vascular biology* **30**, 1007-1013
145. Miyamoto, N., Izumi, H., Miyamoto, R., Bin, H., Kondo, H., Tawara, A., Sasaguri, Y., and Kohno, K. (2011) Transcriptional regulation of activating transcription factor 4 under oxidative stress in retinal pigment epithelial ARPE-19/HPV-16 cells. *Investigative ophthalmology & visual science* **52**, 1226-1234
146. Levenson, V. V., Davidovich, I. A., and Roninson, I. B. (2000) Pleiotropic resistance to DNA-interactive drugs is associated with increased expression of genes involved in DNA replication, repair, and stress response. *Cancer Res* **60**, 5027-5030
147. Tanabe, M., Izumi, H., Ise, T., Higuchi, S., Yamori, T., Yasumoto, K., and Kohno, K. (2003) Activating transcription factor 4 increases the cisplatin resistance of human cancer cell lines. *Cancer Res* **63**, 8592-8595
148. Igarashi, T., Izumi, H., Uchiumi, T., Nishio, K., Arao, T., Tanabe, M., Uramoto, H., Sugio, K., Yasumoto, K., Sasaguri, Y., Wang, K. Y., Otsuji, Y., and Kohno, K. (2007) Clock and ATF4 transcription system regulates drug resistance in human cancer cell lines. *Oncogene* **26**, 4749-4760
149. Sachdeva, M. M., Claiborn, K. C., Khoo, C., Yang, J., Groff, D. N., Mirmira, R. G., and Stoffers, D. A. (2009) Pdx1 (MODY4) regulates pancreatic beta cell susceptibility to ER stress. *Proc Natl Acad Sci U S A* **106**, 19090-19095

150. DeBose-Boyd, R. A., Brown, M. S., Li, W. P., Nohturfft, A., Goldstein, J. L., and Espenshade, P. J. (1999) Transport-dependent proteolysis of SREBP: relocation of site-1 protease from Golgi to ER obviates the need for SREBP transport to Golgi. *Cell* **99**, 703-712
151. Shen, J., and Prywes, R. (2004) Dependence of site-2 protease cleavage of ATF6 on prior site-1 protease digestion is determined by the size of the luminal domain of ATF6. *The Journal of biological chemistry* **279**, 43046-43051
152. Calfon, M., Zeng, H., Urano, F., Till, J. H., Hubbard, S. R., Harding, H. P., Clark, S. G., and Ron, D. (2002) IRE1 couples endoplasmic reticulum load to secretory capacity by processing the XBP-1 mRNA. *Nature* **415**, 92-96
153. Yoshida, H., Matsui, T., Yamamoto, A., Okada, T., and Mori, K. (2001) XBP1 mRNA is induced by ATF6 and spliced by IRE1 in response to ER stress to produce a highly active transcription factor. *Cell* **107**, 881-891
154. Ozcan, U., Ozcan, L., Yilmaz, E., Duvel, K., Sahin, M., Manning, B. D., and Hotamisligil, G. S. (2008) Loss of the tuberous sclerosis complex tumor suppressors triggers the unfolded protein response to regulate insulin signaling and apoptosis. *Mol Cell* **29**, 541-551
155. Babcock, J. T., Nguyen, H. B., He, Y., Hendricks, J. W., Wek, R. C., and Quilliam, L. A. (2013) Mammalian target of rapamycin complex 1 (mTORC1) enhances bortezomib-induced death in tuberous sclerosis complex (TSC)-null cells by a c-MYC-dependent induction of the unfolded protein response. *The Journal of biological chemistry* **288**, 15687-15698
156. Ozcan, U., Cao, Q., Yilmaz, E., Lee, A. H., Iwakoshi, N. N., Ozdelen, E., Tuncman, G., Gorgun, C., Glimcher, L. H., and Hotamisligil, G. S. (2004) Endoplasmic reticulum stress links obesity, insulin action, and type 2 diabetes. *Science* **306**, 457-461

157. Urano, F., Wang, X., Bertolotti, A., Zhang, Y., Chung, P., Harding, H. P., and Ron, D. (2000) Coupling of stress in the ER to activation of JNK protein kinases by transmembrane protein kinase IRE1. *Science* **287**, 664-666
158. Kane, R. C., Bross, P. F., Farrell, A. T., and Pazdur, R. (2003) Velcade: U.S. FDA approval for the treatment of multiple myeloma progressing on prior therapy. *The oncologist* **8**, 508-513
159. Kang, Y. J., Lu, M. K., and Guan, K. L. (2011) The TSC1 and TSC2 tumor suppressors are required for proper ER stress response and protect cells from ER stress-induced apoptosis. *Cell death and differentiation* **18**, 133-144
160. Rutkowski, D. T., and Hegde, R. S. (2010) Regulation of basal cellular physiology by the homeostatic unfolded protein response. *J Cell Biol* **189**, 783-794
161. Tabas, I., and Ron, D. (2011) Integrating the mechanisms of apoptosis induced by endoplasmic reticulum stress. *Nature cell biology* **13**, 184-190
162. Jin, H. O., Seo, S. K., Woo, S. H., Kim, E. S., Lee, H. C., Yoo, D. H., An, S., Choe, T. B., Lee, S. J., Hong, S. I., Rhee, C. H., Kim, J. I., and Park, I. C. (2009) Activating transcription factor 4 and CCAAT/enhancer-binding protein-beta negatively regulate the mammalian target of rapamycin via Redd1 expression in response to oxidative and endoplasmic reticulum stress. *Free radical biology & medicine* **46**, 1158-1167
163. Sofer, A., Lei, K., Johannessen, C. M., and Ellisen, L. W. (2005) Regulation of mTOR and cell growth in response to energy stress by REDD1. *Molecular and cellular biology* **25**, 5834-5845
164. Whitney, M. L., Jefferson, L. S., and Kimball, S. R. (2009) ATF4 is necessary and sufficient for ER stress-induced upregulation of REDD1 expression. *Biochemical and biophysical research communications* **379**, 451-455

165. Yamaguchi, S., Ishihara, H., Yamada, T., Tamura, A., Usui, M., Tominaga, R., Munakata, Y., Satake, C., Katagiri, H., Tashiro, F., Aburatani, H., Tsukiyama-Kohara, K., Miyazaki, J., Sonenberg, N., and Oka, Y. (2008) ATF4-mediated induction of 4E-BP1 contributes to pancreatic beta cell survival under endoplasmic reticulum stress. *Cell Metab* **7**, 269-276
166. Harding, H., Zeng, H., Zhang, Y., Jungreis, R., Chung, P., Plesken, H., Sabatini, D. D., and Ron, D. (2001) Diabetes mellitus and exocrine pancreatic dysfunction in *Perk* *-/-* mice reveals a role for translational control in secretory cell survival. *Mol Cell* **7**, 1153-1163
167. Zhang, P., McGrath, B., Li, S., Frank, A., Zambito, F., Reinert, J., Gannon, M., Ma, K., McNaughton, K., and Cavener, D. R. (2002) The PERK eukaryotic initiation factor 2 alpha kinase is required for the development of the skeletal system, postnatal growth, and the function and viability of the pancreas. *Molecular and cellular biology* **22**, 3864-3874
168. Zhang, W., Feng, D., Li, Y., Iida, K., McGrath, B., and Cavener, D. R. (2006) PERK EIF2AK3 control of pancreatic beta cell differentiation and proliferation is required for postnatal glucose homeostasis. *Cell Metab* **4**, 491-497
169. Iida, K., Li, Y., McGrath, B. C., Frank, A., and Cavener, D. R. (2007) PERK eIF2 alpha kinase is required to regulate the viability of the exocrine pancreas in mice. *BMC Cell Biol* **8**, 38
170. Izumi, T., Yokota-Hashimoto, H., Zhao, S., Wang, J., Halban, P. A., and Takeuchi, T. (2003) Dominant negative pathogenesis by mutant proinsulin in the Akita diabetic mouse. *Diabetes* **52**, 409-416
171. Wang, J., Takeuchi, T., Tanaka, S., Kubo, S. K., Kayo, T., Lu, D., Takata, K., Koizumi, A., and Izumi, T. (1999) A mutation in the insulin 2 gene induces

- diabetes with severe pancreatic beta-cell dysfunction in the Mody mouse. *The Journal of clinical investigation* **103**, 27-37
172. Stoy, J., Edghill, E. L., Flanagan, S. E., Ye, H., Paz, V. P., Pluzhnikov, A., Below, J. E., Hayes, M. G., Cox, N. J., Lipkind, G. M., Lipton, R. B., Greeley, S. A., Patch, A. M., Ellard, S., Steiner, D. F., Hattersley, A. T., Philipson, L. H., Bell, G. I., and Neonatal Diabetes International Collaborative, G. (2007) Insulin gene mutations as a cause of permanent neonatal diabetes. *Proc Natl Acad Sci U S A* **104**, 15040-15044
173. Cardozo, A. K., Ortis, F., Storling, J., Feng, Y. M., Rasschaert, J., Tonnesen, M., Van Eylen, F., Mandrup-Poulsen, T., Herchuelz, A., and Eizirik, D. L. (2005) Cytokines downregulate the sarcoendoplasmic reticulum pump Ca²⁺ ATPase 2b and deplete endoplasmic reticulum Ca²⁺, leading to induction of endoplasmic reticulum stress in pancreatic beta-cells. *Diabetes* **54**, 452-461
174. Karaskov, E., Scott, C., Zhang, L., Teodoro, T., Ravazzola, M., and Volchuk, A. (2006) Chronic palmitate but not oleate exposure induces endoplasmic reticulum stress, which may contribute to INS-1 pancreatic beta-cell apoptosis. *Endocrinology* **147**, 3398-3407
175. Kharroubi, I., Ladriere, L., Cardozo, A. K., Dogusan, Z., Cnop, M., and Eizirik, D. L. (2004) Free fatty acids and cytokines induce pancreatic beta-cell apoptosis by different mechanisms: role of nuclear factor-kappaB and endoplasmic reticulum stress. *Endocrinology* **145**, 5087-5096
176. Oyadomari, S., Takeda, K., Takiguchi, M., Gotoh, T., Matsumoto, M., Wada, I., Akira, S., Araki, E., and Mori, M. (2001) Nitric oxide-induced apoptosis in pancreatic beta cells is mediated by the endoplasmic reticulum stress pathway. *Proc Natl Acad Sci U S A* **98**, 10845-10850

177. Oyadomari, S., Koizumi, A., Takeda, K., Gotoh, T., Akira, S., Araki, E., and Mori, M. (2002) Targeted disruption of the Chop gene delays endoplasmic reticulum stress-mediated diabetes. *The Journal of clinical investigation* **109**, 525-532
178. Avivar-Valderas, A., Salas, E., Bobrovnikova-Marjon, E., Diehl, J. A., Nagi, C., Debnath, J., and Aguirre-Ghiso, J. A. (2011) PERK integrates autophagy and oxidative stress responses to promote survival during extracellular matrix detachment. *Molecular and cellular biology* **31**, 3616-3629
179. Ohoka, N., Yoshii, S., Hattori, T., Onozaki, K., and Hayashi, H. (2005) TRB3, a novel ER stress-inducible gene, is induced via ATF4-CHOP pathway and is involved in cell death. *The EMBO journal* **24**, 1243-1255
180. Puthalakath, H., O'Reilly, L. A., Gunn, P., Lee, L., Kelly, P. N., Huntington, N. D., Hughes, P. D., Michalak, E. M., McKimm-Breschkin, J., Motoyama, N., Gotoh, T., Akira, S., Bouillet, P., and Strasser, A. (2007) ER stress triggers apoptosis by activating BH3-only protein Bim. *Cell* **129**, 1337-1349
181. Yamaguchi, H., and Wang, H. G. (2004) CHOP is involved in endoplasmic reticulum stress-induced apoptosis by enhancing DR5 expression in human carcinoma cells. *Journal of Biological Chemistry* **279**, 45495-45502
182. Yoshida, T., Shiraishi, T., Nakata, S., Horinaka, M., Wakada, M., Mizutani, Y., Miki, T., and Sakai, T. (2005) Proteasome inhibitor MG132 induces death receptor 5 through CCAAT/enhancer-binding protein homologous protein. *Cancer Res* **65**, 5662-5667
183. Inoue, H., Tanizawa, Y., Wasson, J., Behn, P., Kalidas, K., Bernal-Mizrachi, E., Mueckler, M., Marshall, H., Donis-Keller, H., Crock, P., Rogers, D., Mikuni, M., Kumashiro, H., Higashi, K., Sobue, G., Oka, Y., and Permutt, M. A. (1998) A gene encoding a transmembrane protein is mutated in patients with diabetes mellitus and optic atrophy (Wolfram syndrome). *Nature genetics* **20**, 143-148

184. Strom, T. M., Hortnagel, K., Hofmann, S., Gekeler, F., Scharfe, C., Rabl, W., Gerbitz, K. D., and Meitinger, T. (1998) Diabetes insipidus, diabetes mellitus, optic atrophy and deafness (DIDMOAD) caused by mutations in a novel gene (wolframin) coding for a predicted transmembrane protein. *Human molecular genetics* **7**, 2021-2028
185. Osman, A. A., Saito, M., Makepeace, C., Permutt, M. A., Schlesinger, P., and Mueckler, M. (2003) Wolframin expression induces novel ion channel activity in endoplasmic reticulum membranes and increases intracellular calcium. *The Journal of biological chemistry* **278**, 52755-52762
186. Hofmann, S., Philbrook, C., Gerbitz, K. D., and Bauer, M. F. (2003) Wolfram syndrome: structural and functional analyses of mutant and wild-type wolframin, the WFS1 gene product. *Human molecular genetics* **12**, 2003-2012
187. Fonseca, S. G., Gromada, J., and Urano, F. (2011) Endoplasmic reticulum stress and pancreatic beta-cell death. *Trends in endocrinology and metabolism: TEM* **22**, 266-274
188. Gietzen, D. W., Hao, S., and Anthony, T. G. (2007) Mechanisms of food intake repression in indispensable amino acid deficiency. *Annual review of nutrition* **27**, 63-78
189. Hao, S., Sharp, J. W., Ross-Inta, C. M., McDaniel, B. J., Anthony, T. G., Wek, R. C., Cavener, D. R., McGrath, B. C., Rudell, J. B., Koehnle, T. J., and Gietzen, D. W. (2005) Uncharged tRNA and sensing of amino acid deficiency in mammalian piriform cortex. *Science* **307**, 1776-1778
190. Maurin, A. C., Jousse, C., Averous, J., Parry, L., Bruhat, A., Cherasse, Y., Zeng, H., Zhang, Y., Harding, H. P., Ron, D., and Fafournoux, P. (2005) The GCN2 kinase biases feeding behavior to maintain amino acid homeostasis in omnivores. *Cell Metab* **1**, 273-277

191. Costa-Mattioli, M., Gobert, D., Harding, H., Herdy, B., Azzi, M., Bruno, M., Bidinosti, M., Ben Mamou, C., Marcinkiewicz, E., Yoshida, M., Imataka, H., Cuello, A. C., Seidah, N., Sossin, W., Lacaille, J. C., Ron, D., Nader, K., and Sonenberg, N. (2005) Translational control of hippocampal synaptic plasticity and memory by the eIF2alpha kinase GCN2. *Nature* **436**, 1166-1173
192. Hanefeld, F., Holzbach, U., Kruse, B., Wilichowski, E., Christen, H. J., and Frahm, J. (1993) Diffuse white matter disease in three children: an encephalopathy with unique features on magnetic resonance imaging and proton magnetic resonance spectroscopy. *Neuropediatrics* **24**, 244-248
193. Schiffmann, R., Moller, J. R., Trapp, B. D., Shih, H. H., Farrer, R. G., Katz, D. A., Alger, J. R., Parker, C. C., Hauer, P. E., Kaneski, C. R., and et al. (1994) Childhood ataxia with diffuse central nervous system hypomyelination. *Annals of neurology* **35**, 331-340
194. Bugiani, M., Boor, I., Powers, J. M., Scheper, G. C., and van der Knaap, M. S. (2010) Leukoencephalopathy with vanishing white matter: a review. *Journal of neuropathology and experimental neurology* **69**, 987-996
195. Li, W., Wang, X., Van Der Knaap, M. S., and Proud, C. G. (2004) Mutations linked to leukoencephalopathy with vanishing white matter impair the function of the eukaryotic initiation factor 2B complex in diverse ways. *Molecular and Cellular Biology* **24**, 3295-3306
196. Leegwater, P. A., Vermeulen, G., Konst, A. A., Naidu, S., Mulders, J., Visser, A., Kersbergen, P., Mobach, D., Fonds, D., van Berkel, C. G., Lemmers, R. J., Frants, R. R., Oudejans, C. B., Schutgens, R. B., Pronk, J. C., and van der Knaap, M. S. (2001) Subunits of the translation initiation factor eIF2B are mutant in leukoencephalopathy with vanishing white matter. *Nature genetics* **29**, 383-388

197. Richardson, J. P., Mohammad, S. S., and Pavitt, G. D. (2004) Mutations causing childhood ataxia with central nervous system hypomyelination reduce eukaryotic initiation factor 2B complex formation and activity. *Molecular and cellular biology* **24**, 2352-2363
198. Richards, N. G., and Kilberg, M. S. (2006) Asparagine synthetase chemotherapy. *Annu Rev Biochem* **75**, 629-654
199. Blais, J. D., Addison, C. L., Edge, R., Falls, T., Zhao, H., Wary, K., Koumenis, C., Harding, H. P., Ron, D., Holcik, M., and Bell, J. C. (2006) Perk-dependent translational regulation promotes tumor cell adaptation and angiogenesis in response to hypoxic stress. *Molecular and cellular biology* **26**, 9517-9532
200. Hadjebi, O., Casas-Terradellas, E., Garcia-Gonzalo, F. R., and Rosa, J. L. (2008) The RCC1 superfamily: from genes, to function, to disease. *Biochimica et biophysica acta* **1783**, 1467-1479
201. Jin, L., Pahuja, K. B., Wickliffe, K. E., Gorur, A., Baumgartel, C., Schekman, R., and Rape, M. (2012) Ubiquitin-dependent regulation of COPII coat size and function. *Nature* **482**, 495-500
202. Teske, B. F., Fusakio, M. E., Zhou, D., Shan, J., McClintick, J. N., Kilberg, M. S., and Wek, R. C. (2013) CHOP induces activating transcription factor 5 (ATF5) to trigger apoptosis in response to perturbations in protein homeostasis. *Molecular biology of the cell* **24**, 2477-2490
203. Teske, B. F., Baird, T. D., and Wek, R. C. (2011) Methods for analyzing eIF2 kinases and translational control in the unfolded protein response. *Methods in enzymology* **490**, 333-356
204. Sampath, P., Pritchard, D. K., Pabon, L., Reinecke, H., Schwartz, S. M., Morris, D. R., and Murry, C. E. (2008) A hierarchical network controls protein translation

- during murine embryonic stem cell self-renewal and differentiation. *Cell stem cell* **2**, 448-460
205. Iacono, M., Mignone, F., and Pesole, G. (2005) uAUG and uORFs in human and rodent 5'untranslated mRNAs. *Gene* **349**, 97-105
206. Matsui, M., Yachie, N., Okada, Y., Saito, R., and Tomita, M. (2007) Bioinformatic analysis of post-transcriptional regulation by uORF in human and mouse. *FEBS letters* **581**, 4184-4188
207. Spatuzza, C., Schiavone, M., Di Salle, E., Janda, E., Sardiello, M., Fiume, G., Fierro, O., Simonetta, M., Argiriou, N., Faraonio, R., Capparelli, R., Quinto, I., and Scala, G. (2008) Physical and functional characterization of the genetic locus of IBtk, an inhibitor of Bruton's tyrosine kinase: evidence for three protein isoforms of IBtk. *Nucleic acids research* **36**, 4402-4416
208. Ingolia, N. T., Lareau, L. F., and Weissman, J. S. (2011) Ribosome profiling of mouse embryonic stem cells reveals the complexity and dynamics of mammalian proteomes. *Cell* **147**, 789-802
209. Lee, S., Liu, B., Lee, S., Huang, S. X., Shen, B., and Qian, S. B. (2012) Global mapping of translation initiation sites in mammalian cells at single-nucleotide resolution. *Proc Natl Acad Sci U S A* **109**, E2424-2432
210. Gerashchenko, M. V., Su, D., and Gladyshev, V. N. (2010) CUG start codon generates thioredoxin/glutathione reductase isoforms in mouse testes. *The Journal of biological chemistry* **285**, 4595-4602
211. Peng, W., Robertson, L., Gallinetti, J., Mejia, P., Vose, S., Charlip, A., Chu, T., and Mitchell, J. R. (2012) Surgical stress resistance induced by single amino acid deprivation requires Gcn2 in mice. *Science translational medicine* **4**, 118ra111

212. Liu, W., Quinto, I., Chen, X., Palmieri, C., Rabin, R. L., Schwartz, O. M., Nelson, D. L., and Scala, G. (2001) Direct inhibition of Bruton's tyrosine kinase by IBtk, a Btk-binding protein. *Nature immunology* **2**, 939-946
213. Janda, E., Palmieri, C., Pisano, A., Pontoriero, M., Iaccino, E., Falcone, C., Fiume, G., Gaspari, M., Nevolo, M., Di Salle, E., Rossi, A., De Laurentiis, A., Greco, A., Di Napoli, D., Verheij, E., Britti, D., Lavecchia, L., Quinto, I., and Scala, G. (2011) Btk regulation in human and mouse B cells via protein kinase C phosphorylation of IBtkgamma. *Blood* **117**, 6520-6531
214. Koepfli, J. B., Mead, J. F., and Brockman, J. A., Jr. (1947) An alkaloid with high antimalarial activity from *Dichroa febrifuga*. *Journal of the American Chemical Society* **69**, 1837
215. Keller, T. L., Zocco, D., Sundrud, M. S., Hendrick, M., Edenius, M., Yum, J., Kim, Y. J., Lee, H. K., Cortese, J. F., Wirth, D. F., Dignam, J. D., Rao, A., Yeo, C. Y., Mazitschek, R., and Whitman, M. (2012) Halofuginone and other febrifugine derivatives inhibit prolyl-tRNA synthetase. *Nature chemical biology* **8**, 311-317
216. Shinmura, K., Tamaki, K., and Bolli, R. (2008) Impact of 6-mo caloric restriction on myocardial ischemic tolerance: possible involvement of nitric oxide-dependent increase in nuclear Sirt1. *American journal of physiology. Heart and circulatory physiology* **295**, H2348-2355
217. Shinmura, K., Tamaki, K., Saito, K., Nakano, Y., Tobe, T., and Bolli, R. (2007) Cardioprotective effects of short-term caloric restriction are mediated by adiponectin via activation of AMP-activated protein kinase. *Circulation* **116**, 2809-2817
218. Chandrasekar, B., Nelson, J. F., Colston, J. T., and Freeman, G. L. (2001) Calorie restriction attenuates inflammatory responses to myocardial ischemia-

- reperfusion injury. *American journal of physiology. Heart and circulatory physiology* **280**, H2094-2102
219. Yu, Z. F., and Mattson, M. P. (1999) Dietary restriction and 2-deoxyglucose administration reduce focal ischemic brain damage and improve behavioral outcome: evidence for a preconditioning mechanism. *Journal of neuroscience research* **57**, 830-839
220. Ahmet, I., Wan, R., Mattson, M. P., Lakatta, E. G., and Talan, M. (2005) Cardioprotection by intermittent fasting in rats. *Circulation* **112**, 3115-3121
221. Mitchell, J. R., Verweij, M., Brand, K., van de Ven, M., Goemaere, N., van den Engel, S., Chu, T., Forrer, F., Muller, C., de Jong, M., van, I. W., JN, I. J., Hoeijmakers, J. H., and de Bruin, R. W. (2010) Short-term dietary restriction and fasting precondition against ischemia reperfusion injury in mice. *Aging cell* **9**, 40-53
222. Miller, R. A., Buehner, G., Chang, Y., Harper, J. M., Sigler, R., and Smith-Wheelock, M. (2005) Methionine-deficient diet extends mouse lifespan, slows immune and lens aging, alters glucose, T4, IGF-I and insulin levels, and increases hepatocyte MIF levels and stress resistance. *Aging cell* **4**, 119-125
223. Ingolia, N. T. (2014) Ribosome profiling: new views of translation, from single codons to genome scale. *Nature reviews. Genetics* **15**, 205-213
224. Ingolia, N. T., Brar, G. A., Rouskin, S., McGeachy, A. M., and Weissman, J. S. (2012) The ribosome profiling strategy for monitoring translation in vivo by deep sequencing of ribosome-protected mRNA fragments. *Nature protocols* **7**, 1534-1550
225. Ingolia, N. T., Ghaemmaghami, S., Newman, J. R., and Weissman, J. S. (2009) Genome-wide analysis in vivo of translation with nucleotide resolution using ribosome profiling. *Science* **324**, 218-223

CURRICULUM VITAE

Thomas David Baird

Education

Indiana University, Ph.D., biochemistry and molecular biology, 2014

College of Charleston, M.S., marine biology, 2008

Franklin College, B.A. *summa cum laude*, biology, 2004

Honors, Awards, Fellowships

- 2012-2014 Predoctoral Research Training Grant in Diabetes and Obesity
(NIH T32 DK064466)
- 2009-2010 I.U. School of Medicine University Fellowship
- 2008 Best Graduate Student Presentation, SEERS Conference
- 2008 Sigma Xi Award - Best Oral Presentation, GPMB Annual Colloquium
- 2007-2008 Presidential Summer Research Award, College of Charleston
- 2004 Naomi Hougham Award in Biology, Franklin College
- 2003 Outstanding Performance by an Upperclassman Award in Biology,
Franklin College
- 2003 NSF REU Fort Johnson Undergraduate Summer Research Program
Fellow, College of Charleston

Research and Training Experience

- 2009-2014 Graduate Fellow, I.U. School of Medicine, Indianapolis, IN
- 2007-2008 Sea Grant Fellow, Center for Coastal Environmental Health &
Biomolecular Research, National Oceanic & Atmospheric Administration,
Charleston, SC

2006 Research Assistant, CORSACS Research Cruise, Ross Sea, Antarctica
2002 Research Assistant, Dept of Anatomy, I.U. School of Medicine
2000-2004 Lab Assistant, Dept of Biology, Franklin College, Franklin, IN

Teaching Experience

2010 Graduate Teaching Assistant, G716 Molecular Biology and Genetics, I.U.
 School of Medicine
2007 Graduate Teaching Assistant, Dept of Biology, College of Charleston
2004-2006 Assistant Language Teacher, Kuji City Board of Education, Kuji, Japan

Publications

Hongzhen H., Singh I., Wek S.A., Dey S., **Baird T.D.**, Wek R.C. and M.M. Georgiadis.

2014. Crystal structures of GCN2 C-terminal domain suggest regulatory differences in yeast and mammals. *J. Biol. Chem.* 289: 15023-15034.

Baird T.D., Palam L.R., Fusakio M.E., Willy J.A., Davis C.M., McClintick J.N., Anthony

T.G. and R.C. Wek. 2014. Selective mRNA translation during eIF2 phosphorylation induces expression of IBTK α . *Mol. Biol. Cell.* 25: 1686-1697.

DeLorenzo M.E., Danese L.E. and **T.D. Baird**. 2013. Influence of increasing temperature

and salinity on herbicide toxicity in estuarine phytoplankton. *Environ. Toxicol.* 28: 359-371.

Baird T.D. and R.C. Wek. 2012. Eukaryotic initiation factor 2 phosphorylation and

translational control in metabolism. *Adv. Nutr.* 3: 307-321.

Palam L.R., **Baird T.D.** and R.C. Wek. 2011. Phosphorylation of eIF2 facilitates

ribosomal bypass of an inhibitory upstream ORF to enhance *CHOP* translation. *J. Biol. Chem.* 286: 10939-10949.

- Baird T.D.**, Henson C.A., Daily N.M., Baccari G.V. and C.J. Murren. 2011. Differential patterns of plasticity to water along native and naturalized latitudinal gradients. *Evol. Ecol. Res.* 13: 55-73.
- Teske B.F., **Baird T.D.** and R.C. Wek. 2011. Methods for analyzing eIF2 kinases and translational control in metabolism. *Method. Enzymol.* 490: 333-356.
- Dey S., **Baird T.D.**, Zhou D., Palam L.R., Spandau D.F. and R.C. Wek. 2010. Both transcriptional regulation and translation control of *ATF4* are central to the integrated stress response. *J. Biol. Chem.* 285: 33165-33174.
- Baird T.D.** and M.E. DeLorenzo. 2009. Descriptive and mechanistic toxicity of conazole fungicides using the model test alga *Dunaliella tertiolecta* (Chlorophyceae). *Environ. Toxicol.* 25: 213-220.
- DeLorenzo M.E., Wallace S.C., Danese L. and **T.D. Baird**. 2009. Temperature and salinity effects on the toxicity of common pesticides to the grass shrimp, *Palaemonetes pugio*. *J. Environ. Sci. Health, Part B.* 44: 455-460.